

$B \rightarrow D^*$ zero-recoil formfactor and the heavy quark expansion in QCD: a systematic study

PAOLO GAMBINO

Università di Torino, Dipartimento di Fisica
and
INFN Torino, I-10125 Torino, Italy

THOMAS MANNEL, NIKOLAI URALTSEV^{a,*}

Theoretische Physik 1, Fachbereich Physik, Universität Siegen, D-57068 Siegen, Germany

^a also Department of Physics, University of Notre Dame du Lac, Notre Dame, IN 46556, U.S.A.

Abstract

We present a QCD analysis of heavy quark mesons focussing on the $B \rightarrow D^*$ formfactor at zero recoil, $\mathcal{F}_{D^*}(1)$. An advanced treatment of the perturbative corrections in the Wilsonian approach is presented. We estimate the higher-order power corrections to the OPE sum rule and describe a refined analysis of the nonresonant continuum contribution. In the framework of a model-independent approach, we show that the inelastic contribution in the phenomenological part of the OPE is related to the m_Q -dependence of the hyperfine splitting and conclude that the former is large, lowering the prediction for $\mathcal{F}_{D^*}(1)$ down to about 0.86. This likewise implies an enhanced yield of radial and D -wave charm excitations in semileptonic B decays and alleviates the problem with the inclusive yield of the wide excited states. We also apply the approach to the expectation values of dimension 7 and 8 local operators and to a few other issues in the heavy quark expansion.

* On leave of absence from Petersburg Nuclear Physics Institute, Gatchina, St. Petersburg 188300, Russia

Contents

1	Introduction	2
2	The framework	4
3	Perturbative corrections	5
3.1	Numerical analysis	10
4	Power corrections to I_0	11
5	Estimates of I_{inel}	14
5.1	Numerical estimate of I_{inel}	16
5.2	Continuum $D^{(*)}\pi$ contribution	18
6	A closer look at the heavy quark excited states	21
6.1	Model-independent spectral representation	22
6.1.1	Intermediate state contributions	24
6.2	Hyperfine splitting and the estimate of the correlators	27
6.3	The hyperfine constraint and the excited states	33
6.3.1	Estimate of I_1	34
6.3.2	The inclusive $\frac{1}{2}^+$ and $\frac{3}{2}^+$ yield	35
6.3.3	The radial and D -wave excited states	38
6.4	Nonresonant $D^{(*)}\pi$ in the spectral representation	39
6.5	Nonfactorizable contributions to higher-dimensional local expectation values	45
6.5.1	Ground-state factorization and N_c	49
6.5.2	Perturbative normalization point dependence	50
7	Discussion	51
7.1	On a resummation of the $1/m_c^k$ corrections	51
7.2	Vector formfactor in $B \rightarrow D$ transitions	52
7.3	Lattice determination of \mathcal{F}_{D^*}	53
8	Conclusions	55
9	Appendices	58
A	BLM corrections and summation	58
B	One-loop perturbative calculation with a Wilsonian cutoff	58
C	Details of the perturbative calculation	62
D	Transitions to the ‘radial’ states and the inclusive yield	65

1 Introduction

A precision determination of the parameters of the Standard Model (SM) is mandatory for a stringent test of the theory and eventually to identify the effects of new physics. Decades of large-scale experimental efforts have been devoted to testing the SM. At high energies LEP has examined the gauge structure of the SM with great precision without any serious hint of effects beyond the SM. The flavor structure of the SM has been verified in many ways, and in particular at the B factories of SLAC and KEK. In both respects, the flavor and the gauge structure, the SM has so far passed all the tests.

A sound theoretical foundation is needed to perform such tests along with precise data. Methods have been developed in heavy flavor physics over the last two decades that allow systematic and controllable calculations. As an example, the determination of the CKM matrix element V_{cb} employing the heavy mass expansion has reached a relative theoretical uncertainty of about two percent; its extraction from inclusive semileptonic decays is presently believed to be most precise.

The determination of V_{cb} from the exclusive decay $B \rightarrow D^* \ell \bar{\nu}$ requires the knowledge of the form factor at the zero-recoil point where the velocities of the initial and final states are equal, $v \cdot v' = 1$. In the heavy quark limit the form factor is normalized to unity owing to the heavy quark symmetries; the precision determination of V_{cb} requires to control the deviation from the symmetry limit.

The zero-recoil version of the heavy quark sum rules was proposed back in the 1990s to estimate the scale of the nonperturbative corrections, which turned out significant, even considering that the effects are driven by the moderate charm mass. As soon as the first experimental $B \rightarrow D^* \ell \bar{\nu}$ data were available, these early analyses suggested a value of V_{cb} in agreement with the inclusive value, but were unable to make precise predictions because of the poor knowledge of the important heavy quark hadronic parameters.

A model-independent accurate calculation of the formfactor may be expected from QCD lattice simulations provided they measure directly its deviation from unity. The value for the form factor $\mathcal{F}(1)$ obtained in existing lattice calculations leads to smaller V_{cb} compared to the values from the inclusive determination. The latter meanwhile has become quite mature both experimentally and theoretically.

The significant progress in our understanding of heavy mesons brought about by all the precision data in the B sector calls for a reappraisal of the heavy quark expansion for $\mathcal{F}(1)$. In particular, it allows us to obtain a prediction for $\mathcal{F}(1)$ with an informative and defendable error estimate.

In the present paper we discuss the technical details of the analysis that led to the results reported in Ref. [1]. Our estimate for the central value of the formfactor at $v \cdot v' = 1$ is appreciably lower than lattice estimates, which in turn appear marginally compatible with the unitarity bound. Consequently, the value of V_{cb} extracted using our formfactor is larger and happens to be close to the inclusive one, although it still suffers from larger theory uncertainty.

In the course of the analysis of the zero-recoil sum rule we have found a fruitful link among three apparently unrelated topics in heavy meson phenomenology: the value of $\mathcal{F}(1)$,

the hyperfine splitting in B and D , and the ‘ $\frac{1}{2} > \frac{3}{2}$ ’ puzzle. In all three cases the experimental data are naturally described if the transition amplitudes into the ‘radial’ and/or D -wave states are more significant than in the naive quark models.

The paper is divided in two parts. The first part describes the principal ingredients required for the evaluation of $\mathcal{F}(1)$. Our general approach, outlined in Sect. 2, is essentially an implementation of the Heavy Quark sum rules laid down in Ref. [2]. Technically, we formulate it in a somewhat different way which has several advantages. To eventually sharpen the estimate, a number of points had to be improved.

First, the perturbative corrections should be calculated with the hard cutoff consistent with the Wilsonian ‘kinetic’ renormalization scheme. This is a nontrivial point which caused confusion in the past literature. We present a method to obtain the leading α_s -corrections together with all BLM-improvement terms as a function of the cutoff scale μ , avoiding an expansion in μ/m_Q . This is the subject of Sect. 3 where the numeric results are also presented, including known second-order non-BLM terms.

Section 4 discusses power corrections in the short-distance expansion of the scattering amplitude off the heavy quark; these correspond to the power corrections in the sum rules. We find a noticeable impact of the $1/m_c^3$ corrections lowering $\mathcal{F}(1)$, and estimate higher-order effects in the framework of the recent analysis [3] of $1/m_Q^4$ and $1/m_Q^5$ corrections in the inclusive decays.

Section 5 presents the novel evaluation of the inelastic contributions to the unitarity relation, which uses as an input the hyperfine splitting of B and D mesons. We found that the usual nonlocal $D=3$ correlators for heavy quark mesons are rather large, and this yields a large inelastic contribution which significantly exceeds the naive estimates of the past. This in turn lowers the expected central value of $\mathcal{F}(1)$ down to about 0.86. We have also refined the estimate of the $D^{(*)}\pi$ continuum contribution to the inelastic contribution, which supports its overall numerical significance. Independently of the hyperfine constraints, the continuum contributions lowers the unitarity upper bound for $\mathcal{F}(1)$.

The conclusions of the first part focussing on $\mathcal{F}(1)$ are summarized in Sect. 8, with the numeric values given in Eqs. (131), (132) and (133).

Section 6 opens the second, more theoretical part, where we scrutinize, in a model-independent way, the higher excited heavy quark states contributing to the inelastic transitions. In the heavy quark limit these belong to the radial or D -wave states. This is the framework which allowed us to relate the mass dependence of the hyperfine splitting to $\mathcal{F}(1)$ in an informative way. Within the same framework we could link the observed enhancement of the nonlocal effects to the significant inclusive yield of higher-excited states beyond D , D^* and their P -wave excitations, thereby substantiating a possible resolution of the so-called ‘ $\frac{1}{2} > \frac{3}{2}$ ’ puzzle. As a byproduct of the model-independent description we analyze the nonfactorizable effects in the higher-dimension expectation values, and we give numeric estimates for some representative combinations. The non-resonant $D^{(*)}\pi$ continuum has been studied in the same heavy-quark limit setting, relying on the soft-pion approximation.

In Section 7 we discuss certain theoretical aspects related to both the present and the lattice analyses of $\mathcal{F}(1)$. We also briefly mention what can be gained applying our approach to the vector $B \rightarrow D$ transitions. The main conclusions are summarized in Sect. 8.

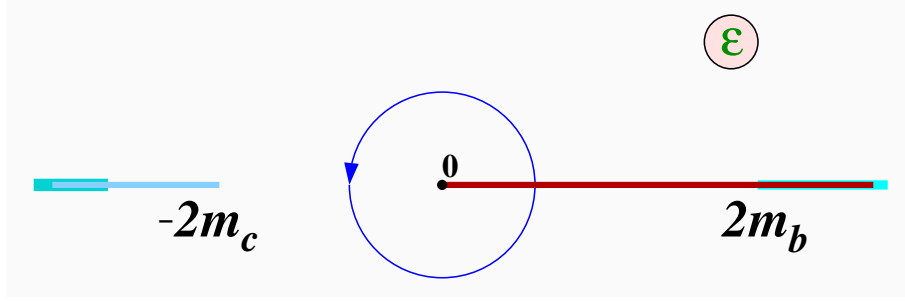


Figure 1: The analytic structure of $T^{\text{zr}}(\varepsilon)$ and the integration contour yielding the sum rule. Distant cuts are shown along with the physical cut. The radius of the circle is ε_M .

The Appendices contain several of the details omitted from the main text. They mostly concern the perturbative calculations; there we discuss some of the conceptual aspects and also give the concrete expressions required in the analysis of $\mathcal{F}(1)$.

2 The framework

We consider the zero-recoil ($\vec{q}=0$) forward scattering amplitude $T^{\text{zr}}(\varepsilon)$ of the flavor-changing axial current $\bar{c}\vec{\gamma}\gamma_5 b$ off a B meson at rest:

$$T^{\text{zr}}(\varepsilon) = \int d^3x \int dx_0 e^{-ix_0(M_B - M_{D^*} - \varepsilon)} \frac{1}{2M_B} \langle B | \frac{1}{3} iT \bar{c}\gamma_k\gamma_5 b(x) \bar{b}\gamma_k\gamma_5 c(0) | B \rangle, \quad (1)$$

where ε is the excitation energy above M_{D^*} in the $B \rightarrow X_c$ transition (the point $\varepsilon = 0$ corresponds to the elastic $B \rightarrow D^*$ transition). The amplitude $T^{\text{zr}}(\varepsilon)$ is an analytic function of ε and has a physical decay cut at $\varepsilon \geq 0$, and other ‘distant’ singularities at $|\varepsilon| \gtrsim 2m_c$. The analytic structure of $T^{\text{zr}}(\varepsilon)$ is illustrated by Fig. 1.

We consider the contour integral

$$I_0(\varepsilon_M) = -\frac{1}{2\pi i} \oint_{|\varepsilon|=\varepsilon_M} T^{\text{zr}}(\varepsilon) d\varepsilon \quad (2)$$

with the contour running counterclockwise from the upper side of the cut, see Fig. 1. Using the analytic properties of $T^{\text{zr}}(\varepsilon)$ the integration contour can be shrunk onto the decay cut; the discontinuity there is related to the weak transition amplitude squared of the axial current into the final charm state with mass $M_X = M_{D^*} + \varepsilon$. If we explicitly single out the elastic transition contribution $B \rightarrow D^*$ at $\varepsilon=0$ then

$$I_0(\varepsilon_M) = \mathcal{F}^2(1) + I_{\text{inel}}(\varepsilon_M), \quad I_{\text{inel}}(\varepsilon_M) \equiv \frac{1}{2\pi i} \int_{\varepsilon>0}^{\varepsilon_M} \text{disc } T^{\text{zr}}(\varepsilon) d\varepsilon \quad (3)$$

holds, where $I_{\text{inel}}(\varepsilon_M)$ is related to the sum of the differential decay probabilities, in the zero recoil kinematics, into the excited states with mass up to $M_{D^*} + \varepsilon_M$.

The OPE allows us to calculate the amplitude in (1) – and hence $I_0(\varepsilon_M)$ – in the short-distance expansion provided $|\varepsilon|$ is sufficiently large compared to the ordinary hadronic mass scale. It should be noted that strong interaction corrections are driven not only by $|\varepsilon|$, but also by the proximity to distant singularities. Therefore, ε_M cannot be taken too large either, and the hierarchy $\varepsilon_M \ll 2m_c$ has to be observed.

The sum rule Eq. (3) can be cast in the form

$$\mathcal{F}(1) = \sqrt{I_0(\varepsilon_M) - I_{\text{inel}}(\varepsilon_M)} \quad (4)$$

which is the master identity for the considerations to follow. Since $I_{\text{inel}}(\varepsilon_M)$ is strictly positive, we get an upper bound on the formfactor

$$\mathcal{F}(1) \leq \sqrt{I_0(\varepsilon_M)} \quad (5)$$

which relies only on the OPE calculation of I_0 . Note that this bound depends on the parameter ε_M , while Eq. (4) is independent of ε_M since the dependence in I_0 and I_{inel} cancel. Furthermore, including an estimate of $I_{\text{inel}}(\varepsilon_M)$ we obtain an evaluation of $\mathcal{F}(1)$.

The correlator in Eq. (1) can be computed using the OPE, resulting in an expansion of $T^{\text{Zr}}(\varepsilon)$ in inverse powers of the masses m_c and m_b . This yields the corresponding expansion of $I_0(\varepsilon_M)$. This OPE takes the following general form:

$$\begin{aligned} I_0(\varepsilon_M) &= \xi_A^{\text{pert}}(\varepsilon_M, \mu) + \sum_k C_k(\varepsilon_M, \mu) \frac{\frac{1}{2M_B} \langle B | O_k | B \rangle_\mu}{m_Q^{d_k-3}} \\ &= \xi_A^{\text{pert}}(\varepsilon_M, \mu) - \Delta_{1/m_Q^2}(\varepsilon_M, \mu) - \Delta_{1/m_Q^3}(\varepsilon_M, \mu) - \Delta_{1/m_Q^4}(\varepsilon_M, \mu) - \dots \\ &\equiv \xi_A^{\text{pert}}(\varepsilon_M, \mu) - \Delta^A(\varepsilon_M, \mu), \end{aligned} \quad (6)$$

where O_k are local b -quark operators $\bar{b} \dots b$ of increasing dimension $d_k \geq 5$, $C_k(\varepsilon_M, \mu)$ are Wilson coefficients for power-suppressed terms, and ξ_A^{pert} is the short-distance renormalization (corresponding to the Wilson coefficient of the unit operator), which is unity at tree level. We have also introduced a Wilsonian cutoff μ used to separate long and short distances. The complete result does not depend on μ since the μ -dependence cancels between the Wilson coefficients and the matrix elements of the operators. At tree level Δ_A does not depend on ε_M . The choice of μ is subject to the same general constraints as that of ε_M , and therefore we will often set $\mu = \varepsilon_M$, in which case we will also use $\xi_A^{\text{pert}}(\mu) \equiv \xi_A^{\text{pert}}(\mu, \mu)$.

3 Perturbative corrections

The leading perturbative renormalization factor $\xi_A^{\text{pert}}(\varepsilon_M, \mu)$ can be expanded in powers of α_s . In the Wilsonian OPE all infrared physics is removed from perturbative corrections; the perturbative series for ξ_A^{pert} is then free from infrared renormalons. The exact form of the perturbative coefficients depends on the concrete definition of the higher-dimension operators used in the OPE; we consistently assume the scheme of Refs. [4, 5] often referred to as “kinetic” (or Small Velocity); see also Ref. [6]. Here we describe a compact method

to calculate ξ_A^{pert} in this scheme; the details as well as the justification of the method can be found in Appendix B.

For the theoretical analysis we need to keep μ and ε_M distinct. Their role is different: ε_M specifies the observable $I_0(\varepsilon_M)$ under study, the energy integral of the spectral density. $I_0(\varepsilon_M)$ depends on ε_M , and the same applies to the Wilson coefficient ξ_A^{pert} for its leading term in the OPE. On the contrary, μ is a technical tool employed in the OPE to separate ‘soft’ and ‘hard’ physics. Since $I_0(\varepsilon_M)$ should not depend on μ , the same applies to the right-hand side of Eq. (6). While ξ_A^{pert} does depend on μ once the perturbative corrections are included, this dependence is canceled by the μ -dependence of the power-suppressed expectation values.

The ε_M -dependence of I_0 is governed by the inelastic spectral density w_{inel} :

$$\frac{dI_0(\varepsilon_M)}{d\varepsilon_M} = \frac{dI_{\text{inel}}(\varepsilon_M)}{d\varepsilon_M} \equiv w_{\text{inel}}(\varepsilon_M). \quad (7)$$

The same holds for the ε_M -dependence of $\xi_A^{\text{pert}}(\varepsilon_M, \mu)$ as long as only the perturbative part of the inelastic spectral density is considered:¹

$$\frac{d\xi_A^{\text{pert}}(\varepsilon_M, \mu)}{d\varepsilon_M} = w^{\text{pert}}(\varepsilon_M), \quad (8)$$

where $w^{\text{pert}}(\varepsilon) \equiv w_{\text{inel}}^{\text{pert}}(\varepsilon)$.

Although both ε_M and μ should be sufficiently large, in a fixed-order perturbative expression one can formally set them equal to zero in $\xi_A^{\text{pert}}(\varepsilon_M, \mu)$. It is evident from the definition of $I_0(\varepsilon_M)$ that this would yield a ‘purely perturbative’ renormalization factor η_A for the zero-recoil axial current to this order, as it is commonly defined in HQET:

$$\xi_A^{\text{pert}}(0, 0) = \eta_A^2. \quad (9)$$

We need, however to keep both mass parameters nonvanishing. Eq. (8) allows one to pass to non-vanishing ε_M . In general, the μ -independence of the overall result is used to fix ξ_A^{pert} at non-vanishing μ .

A relation similar to Eq. (9) holds for a physical choice of the arguments in ξ_A^{pert} if the perturbative calculation of the renormalization factor η_A is performed with an infrared cutoff μ , and provided μ is close to ε_M . There is also a perturbative contribution to I_{inel} , whose soft part is removed by the same cutoff. The precise relation is not trivial, however, even at one loop. An extensive discussion is given in Appendix B.

A direct calculation of the Wilson coefficients implies an infrared cutoff on the internal gluon momentum in the Feynman diagrams. The contribution of soft gluons is subtracted from η_A by a term $\delta\eta_A^{\text{soft}}$. In one-loop diagrams, see Fig. 2, the kinetic scheme cuts off the Feynman integral at $|k| < \mu$ yet the integration over k_0 is always performed from $-\infty$ to ∞ . While the integral is dominated by small $k_0 \lesssim |\vec{k}|$, a power-suppressed contribution comes

¹This is true in general for $\varepsilon_M \gg \mu$, or if we neglect $O(\alpha_s)$ contributions to the Wilson coefficients of the power suppressed operators.

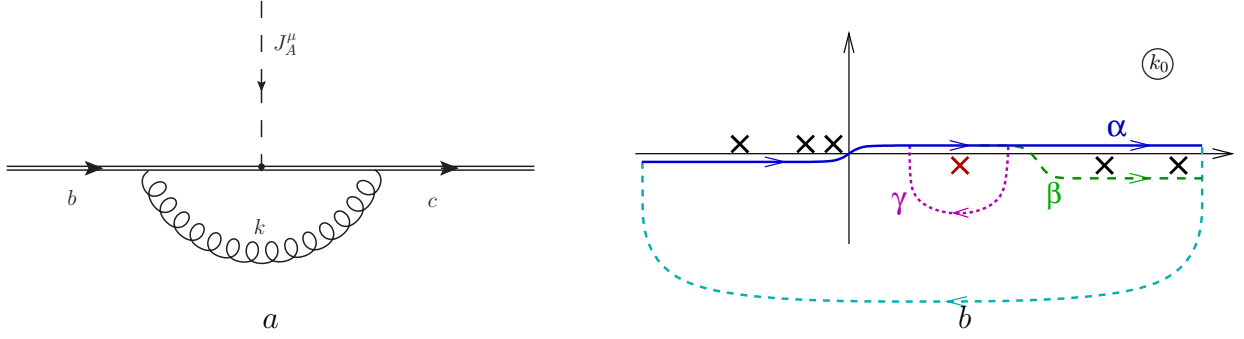


Figure 2: a) Vertex diagram contributing to η_A . b) poles in the complex k_0 -plane encountered in the one-loop diagrams. The standard Feynman propagators lead to contour α (blue); upon closing it into the lower half-plane the integral equals the sum of the three residues. The calculation of $\delta\eta_A^{\text{soft}}(\mu)$ requires to pick up only the ‘near’ gluon pole (red), and is obtained by integration over contour β (the bypass in green).

also from large $k_0 \sim m_Q$. This piece is not soft and would not be properly accounted for if attributed to the matrix elements in the OPE.

This brings us to an important point: the subtraction of the full $|\vec{k}| < \mu$ one-loop contribution to η_A would not yield the correct Wilson coefficient, leading to spurious terms, formally of order $\mathcal{O}(\mu^3/m_Q^3)$. The correct subtraction includes only the residue of the ‘near’ gluon pole at $k_0 = |\vec{k}| - i0$ in the calculation of the integral over k_0 . The other two residues encountered in the conventional Feynman diagram calculation upon closing the k_0 contour into the lower half-plane, see Fig. 2b, correspond in fact to hard physics with gluon virtuality $\sim 2m_Q$ and must be left to the hard Wilson coefficients.

The different physics associated with the ‘distant’ poles in the diagram located near $k_0 = 2m_Q + \vec{k}^2/2m_Q$ can be intuitively understood: picking up the corresponding residue would leave the gluon propagator hard, $k^2 \approx 4m_Q^2$ for small \vec{k} . These poles are actually related to the divergence of the power expansion in \vec{k}/m_Q when the soft scale μ is increased towards m_Q . They contribute terms $\sim d^3\vec{k}/m_Q^3 \propto \mu^3/m_Q^3$ and are seen starting at order $1/m_Q^3$ in the OPE. A detailed discussion of this technical point is given in Appendix B. The validity of this prescription in the kinetic scheme is explicitly checked by the μ -independence of the OPE relations beyond order $1/m_Q^2$. The matching of the μ -dependence of ξ_A to that of the OPE expectation values is demonstrated in Appendix C. We have also verified this for the $1/m_Q$ expansion of the heavy hadron mass.

As a result, the Feynman integration must be modified to exclude the residues of the distant poles in the k_0 plane from the calculation of $\delta\eta_A^{\text{soft}}$. The complete one-loop expression for $\xi_A^{\text{pert}}(\varepsilon_M, \mu)$ accounting for the ε_M -dependence, Eq. (8), takes the following form:

$$\xi_A^{\text{pert}}(\varepsilon_M, \mu) = \eta_A^2 - 2\delta\eta_A^{\text{soft}}(\mu) - \int_{\varepsilon_M}^{\mu'} d\varepsilon w^{\text{pert}}(\varepsilon), \quad (10)$$

where μ' corresponds to the excitation energy of the inelastic transition with emission of a

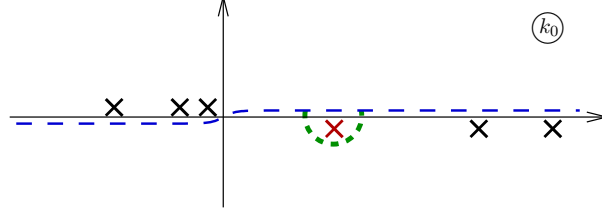


Figure 3: The poles in the integrand and the integration contour in the complex k_0 plane for calculating the Wilson coefficient. At $\vec{k}^2 + \lambda^2 > \mu^2$ the integration is performed in the standard way, dashed line. At $\vec{k}^2 + \lambda^2 < \mu^2$ the ‘near’ gluon pole (red) is moved above the real axis, and the integration contour changes to pass below it, along the green short-dashed path. λ stands for the gluon mass.

gluon with energy $\omega = |\vec{k}| = \mu$,

$$\mu' = \mu + \sqrt{m_c^2 + \mu^2} - m_c. \quad (11)$$

The last term in Eq. (10) describes, at $\mu = \varepsilon_M$, the recoil correction in the relation between the normalization point and the upper limit of energy integration in I_0 . Let us note that the recipe for calculating the combined contribution of the first two terms in Eq. (10) can also be formulated as changing, for $|\vec{k}| < \mu$, the bypass prescription for the gluon pole at $k_0 = |\vec{k}|$ from $k_0 + i0$ to $k_0 - i0$, see Fig. 3. In other words, the proper Wilsonian prescription consists in discarding the gluon pole contribution for gluons softer than the cutoff.

The one-loop renormalization factor η_A without a cutoff is well known:

$$\eta_A = 1 + \frac{3}{4} C_F \frac{\alpha_s}{\pi} \left(\frac{m_b + m_c}{m_b - m_c} \ln \frac{m_b}{m_c} - \frac{8}{3} \right) + \mathcal{O}(\alpha_s^2); \quad (12)$$

the explicit calculations yield for $\delta\eta_A^{\text{soft}}(\mu)$

$$\delta\eta_A^{\text{soft}}(\mu) = -\frac{C_F g_s^2}{4} \int_{|\vec{k}| < \mu} \frac{d^3 \vec{k}}{(2\pi)^3 |\vec{k}|} \left(\frac{1}{m_c^2} + \frac{2}{3m_c m_b} + \frac{1}{m_b^2} \right) = -\frac{C_F \alpha_s}{\pi} \frac{\mu^2}{4} \left(\frac{1}{m_c^2} + \frac{2}{3m_c m_b} + \frac{1}{m_b^2} \right) \quad (13)$$

and the $O(\alpha_s)$ inelastic spectral density is

$$w^{\text{pert}}(\varepsilon) = C_F \frac{\alpha_s}{\pi} \frac{M^2 - m_c^2}{12 M^3 m_b^2} (2M^2 + 3m_b^2 + 2m_b m_c + m_c^2), \quad M = m_c + \varepsilon; \quad (14)$$

M is the invariant hadronic mass in the final state. The integral of the one-loop spectral function that appears in (10) is

$$\begin{aligned} \int_{\mu'}^{\varepsilon_M} d\varepsilon w^{\text{pert}}(\varepsilon) &= C_F \frac{\alpha_s}{\pi} \left\{ \frac{(\varepsilon_M - \mu')(\varepsilon_M + 2m_c + \mu')}{24 m_b^2 (\varepsilon_M + m_c)^2} \left[2\varepsilon_M (\varepsilon_M + 2m_c) \right. \right. \\ &\quad \left. \left. + \frac{m_c^2 (m_c^2 - 3m_b^2 - 2m_b m_c + 4m_c \mu' + 2\mu'^2)}{(m_c + \mu')^2} \right] - \frac{(3m_b - m_c)(m_b + m_c)}{12 m_b^2} \ln \frac{m_c + \mu'}{m_c + \varepsilon_M} \right\}. \end{aligned} \quad (15)$$

Combining these in Eq. (10) we obtain the one-loop $\xi_A^{\text{pert}}(\varepsilon_M, \mu)$ as an explicit function of μ/m_Q . The numeric dependence on μ can be seen in the first-order plot in Fig. 4.

Our analysis of the one-loop corrections can be readily extended to include higher-order BLM corrections which describe the effect of the running of α_s in one-loop diagrams; a complete BLM-summation is also possible. A detailed discussion of the technique, in the context of the Wilsonian OPE, can be found in the Appendix of Ref. [7].² We have recapitulated the salient points in Appendix A. In practice, a fictitious gluon mass λ is introduced in the one-loop diagrams, and eventually a weighted integral over λ^2 is taken. Consequently, the above discussion concerning the Wilsonian cutoff and the OPE applies also to the BLM corrections of any order.

The case of a massive gluon requires the following kinematic modifications. Since the gluon energy is now

$$\omega = \sqrt{\vec{k}^2 + \lambda^2},$$

the range of soft gluon momenta \vec{k} shrinks, $|\vec{k}| < \sqrt{\mu^2 - \lambda^2}$ and the cutoff in the diagrams is now triggered by

$$\theta(\mu^2 - \lambda^2 - \vec{k}^2). \quad (16)$$

Notably, no subtraction is necessary at $\lambda > \mu$. The recoil energy is also modified and μ' in Eqs. (11) is given by

$$\mu' = \sqrt{m_c^2 + \mu^2 - \lambda^2} - m_c + \mu; \quad (17)$$

the perturbative inelastic spectral density is given in Appendix C, Eq. (A.13).

In the Feynman diagrams the relevant gluon pole is now located at $k_0 = \sqrt{\vec{k}^2 + \lambda^2}$ rather than at $k_0 = |\vec{k}|$; this makes the explicit expression for $\delta\eta_A^{\text{soft}}$ more cumbersome:

$$\begin{aligned} \delta\eta_A^{\text{soft}}(\mu) = C_F g_s^2 \int_{k_0 < \mu} \frac{d^3\vec{k}}{(2\pi)^3 2k_0} & \left(\frac{2m_b^2 - 2m_b k_0 - 2k_0^2 + \lambda^2}{(2m_b k_0 - \lambda^2)^2} \right. \\ & \left. + \frac{2m_c^2 - 2m_c k_0 - 2k_0^2 + \lambda^2}{(2m_c k_0 - \lambda^2)^2} - 2 \frac{2m_b m_c - (m_b + m_c)k_0 + \frac{2}{3}\vec{k}^2 + \lambda^2}{(2m_b k_0 - \lambda^2)(2m_c k_0 - \lambda^2)} \right); \quad (18) \end{aligned}$$

the integral can be solved analytically, resulting in a lengthy expression. The expression for η_A at nonvanishing gluon mass is given in Eq. (A.14) of Appendix C.

Combining these elements in Eq. (10) we obtain the one-loop correction to ξ_A^{pert} at arbitrary gluon mass λ , $\xi_A^{\text{pert}}(\varepsilon_M, \mu; \lambda^2)$. Assuming $\mu = \varepsilon_M$, for $\lambda^2 > \mu^2$ the last two terms in Eq. (10) are absent at $\lambda^2 > \mu^2$ and one simply has $\xi_A^{\text{pert}}(\mu; \lambda^2) = \eta_A^2(\lambda^2)$. Using the formulas of Appendix A one readily obtains the BLM corrections of arbitrary order or the resummed result. We performed the final integration over the gluon mass numerically.

The explicit expression for $\eta_A(\lambda^2)$ at small λ^2 shows non-analytic terms in λ^2 , starting with $\frac{\lambda^2}{m_Q^2} \ln \lambda^2$. They signal the infrared sensitivity of η_A and the emergence of infrared

²There was a typo in Eq. (A.6) of paper [8] for the BLM-resummed expression which unfortunately propagated into the later paper [7], Eq. (A.20); in that equation Λ_V^2 must be replaced by Λ_{QCD}^2 (the conventional $\overline{\text{MS}}$ one) in the denominator of the power term. The correct expression is given here in Appendix A, Eq. (A.2).

renormalons, which in turn makes it impossible to assign a definite value to the purely perturbative η_A , and leads to a significant numerical instability from the higher-order corrections. Non-analytic terms are also present in $\delta\eta_A^{\text{soft}}$, and they precisely offset those in $\eta_A(\lambda^2)$: the combined $\xi_A^{\text{pert}}(\varepsilon_M, \mu)$ in Eq. (10) is an analytic function of λ^2 in the vicinity of zero at any positive μ . The radius of convergence of the Taylor series in λ^2 is precisely μ^2 . The cancellation of all the non-analytic pieces is most simply seen directly in the integral representation for $\eta_A - \delta\eta_A^{\text{soft}}(\mu)$, upon closing the contour over the residues at positive k_0 . The recoil integral describes the effect of shifting the normalization point and is purely short-distance. Indeed, the one-loop spectral density $w^{\text{pert}}(\varepsilon; \lambda^2)$ is explicitly analytic at small λ^2 for $\varepsilon > \mu$ where $|\vec{k}|$ is of order μ . Consequently, there are no formal obstacles in deriving either any higher-order BLM coefficient or the fully resummed BLM value for the Wilson coefficient $\xi_A^{\text{pert}}(\varepsilon_M, \mu)$; apart from the ultraviolet domain, its perturbative series has a finite radius of convergence, at least in the BLM approximation.

The advantage of the method described in this section is that it allows to calculate the full μ -dependence of the Wilson coefficient. It does not apply to non-BLM corrections, starting with $\mathcal{O}(\alpha_s^2)$. In that case, the μ -dependence of ξ_A^{pert} has to be determined, order by order in $1/m_Q$, applying the normalization point independence of the OPE relations, and using the initial condition Eq. (9). This was done for the non-BLM $\mathcal{O}(\alpha_s^2)$ corrections in Ref. [9], through $\mathcal{O}(1/m_Q^2)$; in particular, the two-loop spectral density $w^{\text{pert}}(\varepsilon)$ was calculated there to this accuracy. The corresponding non-BLM coefficient was found to be small numerically, which suggests that omitted terms $\mathcal{O}(\alpha_s^2 \mu^3/m_Q^3)$ and higher should not have a noticeable impact.

3.1 Numerical analysis

The perturbative corrections $\xi_A^{\text{pert}}(\varepsilon_M)$ appear to be small for values of ε_M between 0.6 GeV and 1 GeV. Taking, for instance, $\varepsilon_M = \mu = 0.75$ GeV, $m_c = 1.2$ GeV, $m_b = 4.6$ GeV and assuming $\alpha_s(m_b) = 0.22$ we get

$$\sqrt{\xi_A^{\text{pert}}} = 1 - 0.022 + (0.005 - 0.004) + 0.002 - 0.0015 + \dots \quad (19)$$

Here the first term is the tree-level value, the second is the $\mathcal{O}(\alpha_s)$ term evaluated with $\alpha_s = 0.3$, which corresponds to the strong coupling evaluated at an intermediate scale between m_c and m_b . The two values in brackets show the shift, relative the one-loop evaluation with $\alpha_s = 0.3$, due to $\mathcal{O}(\alpha_s^2)$ corrections (positive for the BLM part and negative from the non-BLM contribution); the last two terms are the $\mathcal{O}(\beta_0^2 \alpha_s^3)$ and $\mathcal{O}(\beta_0^3 \alpha_s^4)$, which may serve as an estimate of even higher-order perturbative corrections.

Fig. 4 shows the dependence of $\sqrt{\xi_A^{\text{pert}}(\mu)}$ on μ at different orders in α_s assuming $\alpha_s^{\overline{\text{MS}}}(m_b) = 0.22$. For μ between 0.7 and 0.8 GeV the value of $\sqrt{\xi_A^{\text{pert}}(\mu)}$ is close to 0.98, and we associate to it a rather conservative 1% uncertainty:

$$\sqrt{\xi_A^{\text{pert}}(0.75 \text{ GeV})} = 0.98 \pm 0.01.$$

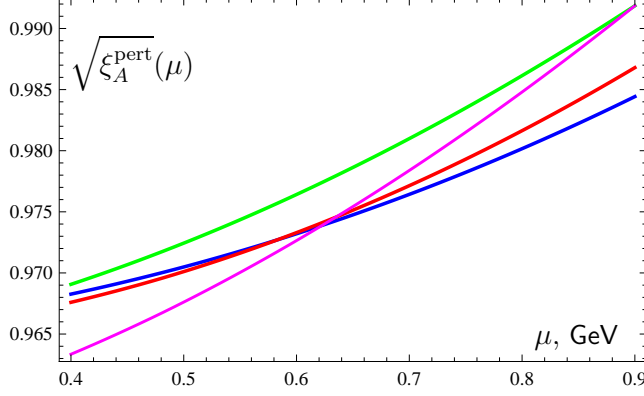


Figure 4: $\sqrt{\xi_A^{\text{pert}}(\mu)}$ as a function of μ for $m_b = 4.6 \text{ GeV}$, $m_c = 1.2 \text{ GeV}$, $\alpha_s(m_b) = 0.22$. The curves represent the one-loop result evaluated with $\alpha_s = 0.3$ (blue), one-loop plus first order BLM (green), complete $\mathcal{O}(\alpha_s^2)$ (red), two-loop plus third-order BLM (maroon).

We emphasize that the observed stability of the perturbative expansion applies only to the perturbative renormalization factor in the Wilsonian OPE, and that the quoted value refers to the specific renormalization scheme which is used in the present analysis.

Let us note here an observation that is relevant when the terms $\mathcal{O}(1/m_Q^3)$ and higher are accounted for. As mentioned in the previous subsection, the calculation of the perturbative factor $\xi_A^{\text{pert}}(\mu)$ which neglects the subtleties related to the ‘distant’ poles yields the correct result through order μ^2/m_Q^2 , and one needs an improved method only to account for the terms μ^3/m_Q^3 and higher. Numerically the two methods yield very close results to order α_s and $\beta_0\alpha_s^2$, but the difference starts to accumulate systematically from order $\beta_0^2\alpha_s^3$ on, even though parametrically the difference between the two methods is still only of order $1/m_Q^3$. For instance, the fully resummed results for the two prescriptions to calculate $\xi_A^{\text{pert}}(\mu)$ differ by about 2%. This is in contrast with the case of the total $b \rightarrow c \ell \nu$ width, where there is no visible difference between the result truncated at order α_s^2 and the fully resummed one. The reason is that the current renormalization at zero recoil has an intrinsically lower scale driven by the charm mass, in contrast to m_b for $\Gamma_{\text{sl}}(B)$.

4 Power corrections to I_0

In this section we investigate the power corrections in the right-hand (OPE) side of the sum rule Eq. (6). The leading power corrections to I_0 were calculated in Refs. [10, 2] to order $1/m_Q^2$ and in Ref. [11] to order $1/m_Q^3$ and read

$$\Delta_{1/m^2} = \frac{\mu_G^2}{3m_c^2} + \frac{\mu_\pi^2 - \mu_G^2}{4} \left(\frac{1}{m_c^2} + \frac{2}{3m_cm_b} + \frac{1}{m_b^2} \right), \quad (20)$$

$$\Delta_{1/m^3} = \frac{\rho_D^3 - \frac{1}{3}\rho_{LS}^3}{4m_c^3} + \frac{1}{12m_b} \left(\frac{1}{m_c^2} + \frac{1}{m_cm_b} + \frac{3}{m_b^2} \right) (\rho_D^3 + \rho_{LS}^3). \quad (21)$$

The nonperturbative parameters μ_π^2 , μ_G^2 , ρ_D^3 and ρ_{LS}^3 all depend on the hard Wilsonian cutoff. In the renormalization scheme we have adopted the inequalities $\mu_\pi^2(\mu) \geq \mu_G^2(\mu)$, $\rho_D^3(\mu) \geq -\rho_{LS}^3(\mu)$ hold at arbitrary normalization point μ . The nonperturbative contributions in Eqs. (20), (21) are therefore positive.

To remain on the conservative side for numeric estimates we can adopt the low values $\mu_\pi^2(0.75 \text{ GeV}) = 0.4 \text{ GeV}^2$, $\rho_D^3(0.75 \text{ GeV}) = 0.15 \text{ GeV}^3$, and the quark masses $m_c = 1.2 \text{ GeV}$ and $m_b = 4.6 \text{ GeV}$ (the scale dependence of the latter plays a role here only at the level formally beyond the accuracy of the calculation). The dependence on μ_G^2 and on ρ_{LS}^3 is minimal and their precise values do not matter; we use for them 0.3 GeV^2 and -0.12 GeV^3 , respectively. We then get

$$\Delta_{1/m^2} = 0.091, \quad \Delta_{1/m^3} = 0.028. \quad (22)$$

It is interesting to compare these estimates with those derived from the constraints on the expectation values of dimension 5 and 6 operators from the semileptonic B -decay moments. If we employ the values of the OPE parameters extracted from the latest official HFAG fit to inclusive semileptonic and radiative decay distributions [12, 13], for $\mu = 0.75 \text{ GeV}$ we find

$$\Delta_{1/m^2} + \Delta_{1/m^3} = 0.102 \pm 0.017,$$

which is consistent with (22). As discussed in [13], this HFAG fit to semileptonic moments depends on several assumptions and does not yet incorporate certain higher-order effects that may be important, including the complete α_s^2 -corrections [14]. In particular, more realistic ansätze for the theoretical correlations have been considered in [15], leading to larger values of the Δ^A , with bigger errors. Typically, one then has

$$\Delta_{1/m^2} + \Delta_{1/m^3} = 0.11 \pm 0.03. \quad (23)$$

On the other hand, combining the semileptonic moments alone with a high precision determination of the charm mass [16] yields [15]

$$\Delta_{1/m^2} = 0.090 \pm 0.013, \quad \Delta_{1/m^3} = 0.029 \pm 0.008, \quad (24)$$

in remarkable agreement with Eq. (22).

The important question is how well the power expansion for the sum rule converges. Recently, the OPE for the semileptonic B -meson structure functions has been extended to order $1/m_Q^4$ and $1/m_Q^5$ [17, 3]. Applying the analysis to the structure functions mediated

by the axial and by the vector currents separately, we find³

$$\begin{aligned}
16m_c^4 \Delta_{1/m^4} &= -(3 + \frac{4}{3}y + y^4)m_1 + (\frac{2}{3}y - \frac{2}{3}y^2 - \frac{2}{3}y^3 - 2y^4)(m_2 + m_5) - (1 + \frac{4}{9}y + \frac{1}{3}y^4)m_4 \\
&\quad + (1 + \frac{4}{3}y - y^4)m_6 - \frac{4}{3}ym_7 + (\frac{1}{4} + \frac{1}{3}y - \frac{1}{4}y^4)m_8, \\
16m_c^5 \Delta_{1/m^5} &= -(2 + \frac{4}{3}y - \frac{2}{3}y^2)r_1 + (6 + 4y + \frac{1}{2}y^2 + \frac{2}{3}y^3 + \frac{4}{3}y^4 + 2y^5)(r_2 - r_3) \\
&\quad + (6 + 4y - \frac{16}{3}y^2 + \frac{2}{3}y^3 + 2y^5)r_4 - (2 + 4y + \frac{1}{3}y^3 + \frac{1}{3}y^4 + y^5)r_5 \\
&\quad - (2 + \frac{4}{3}y + \frac{23}{6}y^2 + \frac{1}{3}y^3 + y^4 + y^5)r_6 + (2 + \frac{4}{3}y + \frac{7}{6}y^2 + \frac{1}{3}y^3 + y^4 + y^5)r_7 \\
&\quad + (\frac{2}{3} - \frac{4}{3}y + \frac{2}{3}y^2)r_8 - (2 + y + \frac{14}{3}y^2 - \frac{2}{3}y^3 - \frac{2}{3}y^4 - 3y^5)(r_9 - r_{12}) \\
&\quad - (2 + y + \frac{7}{2}y^2 - \frac{2}{3}y^3 - \frac{4}{3}y^4 - 3y^5)(r_{10} - r_{11}) - (2 + 6y + \frac{26}{3}y^2 - \frac{2}{3}y^3 - \frac{2}{3}y^4 - 4y^5)r_{13} \\
&\quad - (2 - 4y + \frac{16}{3}y^2 - \frac{2}{3}y^3 - 2y^5)r_{14} + (\frac{4}{3} - \frac{1}{3}y + 4y^2 - \frac{2}{3}y^3 - \frac{2}{3}y^4 - 3y^5)r_{15} \\
&\quad + (\frac{2}{3} + \frac{11}{3}y + 4y^2 - \frac{1}{3}y^3 - \frac{1}{3}y^4 - 2y^5)r_{16} + (\frac{2}{3} - \frac{4}{3}y - \frac{23}{6}y^2 - \frac{1}{3}y^3 - y^4 - y^5)r_{17} \\
&\quad - (\frac{4}{3} + \frac{7}{3}y + \frac{17}{6}y^2 - \frac{2}{3}y^3 - \frac{4}{3}y^4 - 3y^5)r_{18}, \tag{25}
\end{aligned}$$

where $y = m_c/m_b$ and the $D=7$ and $D=8$ expectation values m_{1-9} and r_{1-18} are defined in Ref. [3]. These can be evaluated in the ground-state factorization approximation. Using the expressions given in Ref. [3] we obtain the estimates

$$\Delta_{1/m^4} \simeq -0.023, \quad \Delta_{1/m^5} \simeq -0.013. \tag{26}$$

It is worth noting that retaining only the terms suppressed by the powers of $1/m_c$ (i.e., evaluating the higher-order corrections in the limit $m_b \rightarrow \infty$) yields a perfect numeric approximation to the full expression. In the ground state saturation approximation the dominant contributions to Δ_{1/m^4} and Δ_{1/m^5} are those of $m_{4,8}$ and $r_{2,10}$, respectively, without significant cancellations. We then observe that the power series for I_0 appears well-behaved at the required level of precision.

For what concerns the loop corrections to Δ^A , the α_s -correction to the Wilson coefficient for the kinetic operator in Eq. (20) was calculated in Ref. [9] and turned out numerically insignificant. Generally larger α_s -corrections are expected in the chromomagnetic and Darwin coefficient functions. However, the dependence on μ_G^2 in Eq. (20) turns out negligible; therefore perturbative corrections are not expected to introduce significant numerical changes in the estimate of Δ_{1/m^2} . At order $1/m_Q^3$, even if radiative corrections change the coefficient for the Darwin term by 30% the effect on the sum rule would still be small.

Taking into account all the available information, our estimate for the total power correction at $\varepsilon_M = 0.75$ GeV is

$$\Delta^A = 0.105 \tag{27}$$

with a 0.015 uncertainty due to higher orders. On the theoretical grounds, larger values of μ_π^2 and/or ρ_D^3 are actually favored; they tend to increase Δ^A . Combining the above with the perturbative corrections we arrive at an estimate for I_0 and, according to Eq. (5), at a bound on the form factor, which in terms of the central values at $\varepsilon_M = 0.75$ GeV is

$$\mathcal{F}(1) < 0.925. \tag{28}$$

³We thank S. Turczyk for providing us with the input needed for this calculation.

As stated above, the upper bound in Eq. (5) depends on ε_M , becoming stronger for smaller ε_M . It is advantageous to choose the minimal value of ε_M for which the OPE-based short-distance expansion of the integral (2) for $I_0(\varepsilon_M)$ sets in. This directly depends on how low one can push the renormalization scale μ while still observing the expectation values actual μ -dependence in the kinetic scheme approximated by the perturbative one. Since in this scheme $\mu_\pi^2(\mu) \geq \mu_G^2(\mu)$ holds for arbitrary μ , in essence this boils down to the question at which scale μ_{\min} the spin sum rule and the one for μ_G^2 get approximately saturated, e.g. $\mu_G^2(\mu_{\min}) \simeq 0.3 \text{ GeV}^2$. The only vital assumption in the analysis is that the onset of the short-distance regime is not unexpectedly delayed in actual QCD and hence does not require $\varepsilon_M > 1 \text{ GeV}$. This principal question can and should be verified on the lattice. This will complement already available evidence from preliminary lattice data [18] as well as from the successful experimental confirmation [19] in nonleptonic B decays of the predicted $\frac{3}{2}^-$ -dominance.

5 Estimates of I_{inel}

We now turn to the actual estimate for the inelastic contribution. On general grounds [10] I_{inel} is expected to be comparable to the power correction Δ^A considered above; therefore the inelastic contributions should be important numerically.

Our starting point is the first moment of the scattering amplitude spectral density given by the contour integral

$$I_1(\mu) = -\frac{1}{2\pi i} \oint_{|\varepsilon|=\varepsilon_M} T^{\text{zr}}(\varepsilon) \varepsilon \, d\varepsilon; \quad (29)$$

we can write

$$I_{\text{inel}}(\varepsilon_M) = \frac{I_1(\varepsilon_M)}{\tilde{\varepsilon}}, \quad (30)$$

where $\tilde{\varepsilon}$ is an average excitation energy which depends on ε_M . For moderate ε_M the integral is expected to be dominated by the lowest ‘radial’ excitations⁴ of the ground state, with $\tilde{\varepsilon} \approx \varepsilon_{\text{rad}} \approx 700 \text{ MeV}$. The first moment $I_1(\varepsilon_M)$ can also be calculated in the OPE [2]; the result reads

$$I_1 = \frac{-(\rho_{\pi G}^3 + \rho_A^3)}{3m_c^2} + \frac{-2\rho_{\pi\pi}^3 - \rho_{\pi G}^3}{3m_c m_b} + \frac{\rho_{\pi\pi}^3 + \rho_{\pi G}^3 + \rho_S^3 + \rho_A^3}{4} \left(\frac{1}{m_c^2} + \frac{2}{3m_c m_b} + \frac{1}{m_b^2} \right) + \mathcal{O}\left(\frac{1}{m_Q^3}\right). \quad (31)$$

The nonlocal zero momentum transfer correlators $\rho_{\pi\pi}^3$, $\rho_{\pi G}^3$, ρ_S^3 and ρ_A^3 have been introduced in [2] and are given by

$$\rho_{\pi\pi}^3 = \int d^4x \frac{1}{4M_B} \langle B | iT \{ \bar{b} \vec{\pi}^2 b(x), \bar{b} \vec{\pi}^2 b(0) \} | B \rangle',$$

⁴These excited states play an important role in the analysis of power corrections in the HQE, and we clarify our terminology. In the heavy quark limit these are either the true radial excitations of the ground state, or the counterparts of the D -waves. The former have spin-parity of the light cloud $\frac{1}{2}^+$ while for the latter it is $\frac{3}{2}^+$. At finite quark masses by ‘‘radial excitation’’ we refer to the descendants of any hyperfine multiplet member of these heavy-quark states. More details are addressed in Sect. 6.

$$\rho_{\pi G}^3 = \int d^4x \frac{1}{2M_B} \langle B | iT \{ \bar{b} \vec{\pi}^2 b(x), \bar{b} \vec{\sigma} \vec{B} b(0) \} | B \rangle',$$

$$\frac{1}{3} \rho_S^3 \delta_{ij} \delta_{kl} + \frac{1}{6} \rho_A^3 (\delta_{ik} \delta_{jl} - \delta_{il} \delta_{jk}) = \int d^4x \frac{1}{4M_B} \langle B | iT \{ \bar{b} \sigma_i B_k b(x), \bar{b} \sigma_j B_l b(0) \} | B \rangle', \quad (32)$$

where \vec{B} denotes the chromomagnetic field strength operator. The prime indicates that the ground-state contribution is subtracted – otherwise the integral diverges at large x_0 where the correlators approach a constant determined by the ground-state factorization contribution.

At higher orders in $1/m_Q$ the expansion (31) will include, along with the local expectation values of higher dimensional operators, more intricate nonlocal T -products. The latter are poorly known. Moreover, the quantum-mechanical interpretation of these relations tells us that there will be significant cancellations among different terms in higher orders; say, the factorizable terms must drop out.

Since our goal is only to obtain a reasonable estimate, we discard higher-order corrections and keep only the leading $\mathcal{O}(1/m_Q^2)$ terms. This implies that the expectation values can be considered in the static theory. The nonlocal correlators appear in I_1 because the energy variable ε is defined with respect to the physical threshold $q_0 = M_B - M_{D^*}$ rather than relative to the parton-level threshold at $q_0 = m_b - m_c$ native to the OPE. The terms given by the local operators cancel out in I_1 to the leading order, as becomes transparent in the quantum-mechanical interpretation of Ref. [2], Sect. 6. The latter also explains the explicit field-theoretic expression for $w_{\text{inel}}(\varepsilon)$, which is given in Sec. 6.1. It is important to stress that the third term in (31) is positive since the combination $\rho_{\pi\pi}^3 + \rho_{\pi G}^3 + \rho_S^3 + \rho_A^3$ is actually equivalent to the correlator of two identical operators $\bar{b}(\vec{\sigma}\vec{\pi})^2 b$.

An important piece of information is provided by the heavy quark mass dependence of the hyperfine splitting ΔM^2 , which allows us to estimate the overall magnitude of the non-local correlators in Eqs. (31). The $1/m_Q$ scaling of the vector-pseudoscalar mass splitting is nonperturbatively affected by the values of two $D=3$ spin-triplet parameters, ρ_{LS}^3 and $\rho_{\pi G}^3 + \rho_A^3$:

$$M_{B^*} - M_B = \frac{2}{3} \frac{\mu_G^2}{m_b} + \frac{\rho_{\pi G}^3 + \rho_A^3 - \rho_{LS}^3}{3 m_b^2} + \mathcal{O}\left(\frac{1}{m_b^3}\right), \quad (33)$$

and likewise for charm. Since the spin-orbit expectation value is reasonably constrained by the heavy quark sum rules, (33) yields information on the combination

$$-(\rho_{\pi G}^3 + \rho_A^3).$$

A preliminary analysis was outlined in Ref. [6] and indicated a large value exceeding the naive expectations. We reconsider it carefully in Sect. 6 and confirm the observation. This combination enters directly the expression (31) for I_{inel} and is particularly important, as will become clear in the following subsection, where we combine the theoretical expressions for I_{inel} with the numerical analysis of the hyperfine splitting to arrive at our estimate for I_{inel} . Additional technical details are given in Sect. 6.3.

5.1 Numerical estimate of I_{inel}

It turns out advantageous to analyze I_{inel} from the perspective of the BPS approximation for B mesons [20]. In the BPS limit $\mu_\pi^2 = \mu_G^2$ and, since $\mu_\pi^2 - \mu_G^2 = \langle (\vec{\sigma}\vec{\pi})^2 \rangle$ in the B meson, one concludes that $\bar{b}(\vec{\sigma}\vec{\pi})b|B\rangle = 0$. This would also imply $-\rho_{LS}^3 = \rho_D^3$. The deviation from the BPS limit is quantified by the smallness of the difference $\mu_\pi^2 - \mu_G^2$ compared to μ_π^2 itself [20]. Many remarkable relations hold in the BPS limit; for instance, among the spectral densities of the correlators of $\bar{b}\vec{\pi}^2 b$ and $\bar{b}\vec{\sigma}\vec{B}b$ that we will introduce in Sec. 6,

$$\rho_p^{(\frac{1}{2}^+)}(\omega) = \rho_{pg}^{(\frac{1}{2}^+)}(\omega) = \rho_g^{(\frac{1}{2}^+)}(\omega), \quad \rho_f^{(\frac{3}{2}^+)}(\omega) = \rho_{fg}^{(\frac{3}{2}^+)}(\omega) = \rho_g^{(\frac{3}{2}^+)}(\omega), \quad (34)$$

and among their integrals determining the ρ^3 correlators:

$$\rho_{\pi G}^3 = -2\rho_{\pi\pi}^3, \quad \rho_{\pi G}^3 + \rho_A^3 = -(\rho_{\pi\pi}^3 + \rho_S^3). \quad (35)$$

In the BPS limit I_1 in Eq. (31) is then given by the same combination of the nonlocal correlators that drives, besides ρ_{LS}^3 , the hyperfine splitting to order $1/m_Q^2$, cf. Eq. (33):

$$I_1 \stackrel{\text{BPS}}{=} \frac{-(\rho_{\pi G}^3 + \rho_A^3)}{3m_c^2} + \mathcal{O}\left(\frac{1}{m_c^3}\right). \quad (36)$$

The second term in Eq. (31) for I_1 is of the first order in the deviation from BPS; as such it is not sign-definite. However, it is suppressed by the b -quark mass. The third term is of the second order in the BPS violation and is positive; it comes with a large coefficient. Therefore, the full expression develops only a shallow minimum where the whole sum differs from the BPS value by a factor of no less than 0.93, see Section 6.3.1. In fact, I_1 may exceed the BPS value by a larger amount, although our analysis favors a negative sign for the second term. This typically results, at small deviations, in an overall slight decrease.

A simple minimal – and most physical – ansatz for the spectral densities determining the correlators elucidates the role of the constraints the correlators obey to. It assumes that they are saturated by a single multiplet of excited states, for each angular momentum of light degrees of freedom. Apart from the excitation mass gap the relevant contributions are then determined by three residues; they are introduced in Sect. 6.1 and are denoted by P , G (for the radially excited $\frac{1}{2}^+$) and by g (for the $\frac{3}{2}^+$ state). In the BPS limit $P=G$.

At a fixed hyperfine constraint on $-(\rho_{\pi G}^3 + \rho_A^3)$ the full expression for I_1 in Eq. (31) depends on two dimensionless ratios, P/G and on the relative contribution of the $\frac{3}{2}^+$ state proportional to g^2 . The minimum value for I_1 occurs where the latter vanishes, $g=0$; whenever $\frac{3}{2}^+$ dominates, I_1 uniformly approaches its BPS value. The value of P/G for which there is a minimum depends only on the ratio of the quark masses, see Eq. (85). Fig. 5 shows the variation of I_1/I_1^{BPS} with P/G for a few values of the relative contribution ν of the $\frac{3}{2}^+$ state into the combination determining the hyperfine splitting. More details of the analysis are given in Sect. 6.3.1.

Neglecting a possible few percent relative decrease in I_1 we should, therefore, adopt the BPS relation Eq. (36) as a reasonably accurate lower bound estimate; this leads to the

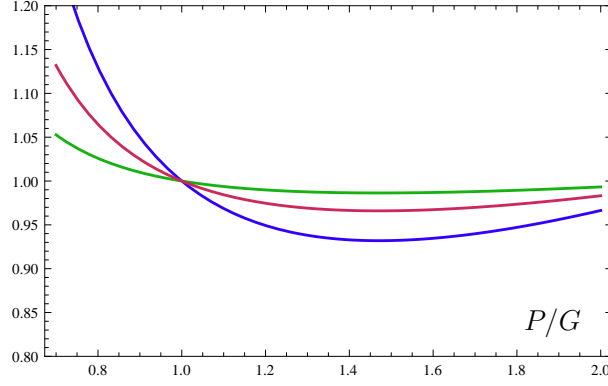


Figure 5: Variation of I_1/I_1^{BPS} with P/G for different relative contribution ν of $\frac{3}{2}^+$ to $\frac{1}{2}^+$ states to the hyperfine splitting, $\nu = 0$ (blue), 0.5 (red), 0.8 (green).

estimate

$$I_{\text{inel}}(\varepsilon_M \approx 0.75 \text{ GeV}) \gtrsim \frac{0.45 \text{ GeV}^3 + (\kappa + 0.2) \cdot 0.35 \text{ GeV}^3}{3m_c^2 \tilde{\varepsilon}}, \quad (37)$$

where the dimensionless κ , introduced in Eq. (73), parameterizes the exact value of the correlator $-(\rho_{\pi G}^2 + \rho_A^3)$. κ is uncertain due to unknown higher power corrections and due to the limited accuracy of the perturbative renormalization. Here ε_M is assumed to be around 0.75 GeV to include the families of the lowest ‘radial’ excitations. Our analysis in Sect. 6.2 suggests that κ is relatively small, between -0.4 and 0 .

Equating $\tilde{\varepsilon}$ in Eq. (37) with $\epsilon_{\text{rad}} \simeq 700 \text{ MeV}$ we estimate

$$I_{\text{inel}} \gtrsim 0.14. \quad (38)$$

We recall that, in contrast to the OPE for $I_0(\mu)$, this estimate assumes only the leading μ_{hadr}/m_Q pieces in the transition amplitudes. The subleading $1/m_c$ corrections can be numerically significant – this is illustrated, for instance, by Eq. (22) – and can potentially modify the actual I_{inel} by as much as 30% of the estimate, even though the inclusive sums like I_{inel} are usually affected less than the individual transitions.

The precise value of μ_π^2 is not yet well known; it mainly affects the degree of proximity of actual B mesons to the BPS regime. The BPS expansion would become more qualitative than quantitative if μ_π^2 eventually exceeds 0.45 GeV^2 by a significant amount. At the same time, as illustrated in this section, this would not affect significantly our estimates. Moreover, larger μ_π^2 lowers the model-independent upper bound which only assumes positivity of the inelastic contribution. Complementarily, from the full set of the heavy quark sum rules we should expect larger transition amplitudes to the excited states at larger μ_π^2 . This conforms the physical intuition which suggests $\sqrt{\mu_\pi^2}$ to quantify the mass scale μ_{hadr} governing the strength of the suppressed transition amplitudes $\propto \mu_{\text{hadr}}/m_Q$. There is no a priori reason to have small power corrections in $\mathcal{F}(1)$ at large μ_π^2 .

5.2 Continuum $D^{(*)}\pi$ contribution

The resonant states are expected to dominate the inelastic transitions at low excitation energy. Continuum effects are formally $1/N_c$ suppressed and are usually numerically small, unless the chiral singularity for the soft pion is strong enough; in the case of I_{inel} it is only logarithmic. Here we give the continuum states $D^{(*)}\pi$ a dedicated consideration since they populate the lowest energy domain and are characterized by an average excitation gap that can be noticeably lower than ε_{rad} . Moreover, these states contribute to the deviation from the BPS regime, possibly dominating the deviation in the low-energy regime. In this subsection we compute their contribution to the zero recoil sum rule with the soft pion technique (see [21] for a review). Complementary theoretical considerations can be found in Sect. 6.4. Here we follow and extend the analysis of Ref. [10].

Both $D\pi$ and $D^*\pi$ channels contribute to I_{inel} . The $D\pi$ amplitude is given by the sum of the two pole graphs in Fig. 6. The pion vertex is parameterized by the effective Lagrangian

$$\mathcal{L}_\chi = 2 g_{D^*D\pi} (M_D D_\mu^* D \partial^\mu \pi + r M_B B_\mu^* B \partial^\mu \pi). \quad (39)$$

where $r = g_{B^*B\pi}/g_{D^*D\pi}$; heavy quark symmetry implies $r=1$. In the heavy quark limit the two diagrams in Fig. 6 cancel each other; all inelastic transitions vanish due to heavy quark symmetry. A nonvanishing result emerges once the mass shifts in the virtual propagators of heavy mesons are accounted for, or due to $r \neq 1$. The amplitude, for a charged pion, then becomes

$$\frac{1}{2\sqrt{M_B M_D}} \langle D^- \pi^+ | \vec{A} | B^+ \rangle = -g_{D^*D\pi} \vec{p}_\pi \left(\frac{1}{\varepsilon} - \frac{r}{\varepsilon + \Delta} \right), \quad (40)$$

where (E_π, \vec{p}_π) is the pion four-momentum and we have neglected subleading terms. We have set the weak vertex to unity, which is legitimate to the first order in the deviations of $\mathcal{F}(1)$ from unity. In terms of the D meson energy, E_D , the excitation energy is $\varepsilon = E_D + E_\pi - M_{D^*} \simeq E_\pi + M_D - M_{D^*} + \vec{p}_\pi^2/2M_D$. Δ represents a power correction: $\Delta \simeq 2/3 \mu_G^2 (1/m_c + 1/m_b) + \mathcal{O}(\vec{p}_\pi^2/m_Q)$. Expanding the amplitude in powers of $1/m_Q$ we would get, for $r=1$,

$$\frac{1}{2\sqrt{M_B M_D}} \langle D^- \pi^+ | \vec{A} | B^+ \rangle = -g_{D^*D\pi} \vec{p}_\pi \frac{\Delta}{\varepsilon^2},$$

which has the correct scaling $\propto 1/m_Q$ for non-diagonal transitions that violate the heavy quark symmetry. However, the hadronic mass scale in the denominator of the amplitude is peculiar: it is the pion energy E_π , which for a light pion can be significantly lower than the typical QCD mass gap ε_{rad} .

The amplitude of Eq. (40) at $r=1$ gives rise to the spectral density

$$w_{\text{inel}}^{D\pi} = \frac{g_{D^*D\pi}^2}{12\pi^2} |\vec{p}_\pi|^3 \frac{\Delta^2}{\varepsilon^2(\varepsilon + \Delta)^2}; \quad (41)$$

the logarithmic chiral singularity that emerges upon integration in the heavy quark limit is regulated by the spin symmetry breaking term $2/3 \mu_G^2 (1/m_c + 1/m_b)$ in Δ , even for a

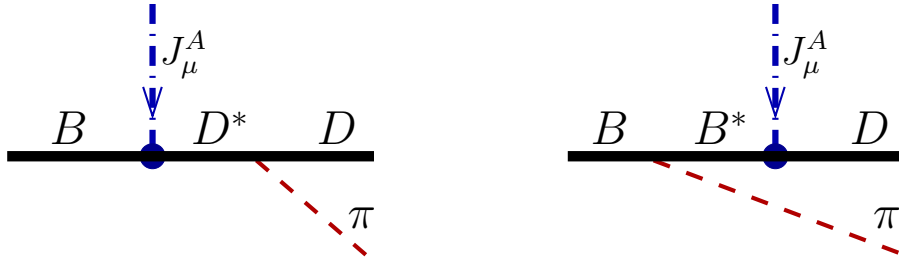


Figure 6: Pole diagrams for the $B \rightarrow D + \pi$ amplitude.

massless pion. As noted in [10], however, the constant term is numerically larger than the chiral logarithm, $\ln \Delta$. The contribution due to neutral pions is half of the one related to charged pions.

The $B \rightarrow D\pi$ amplitude in Eq. (40) in fact receives additional relativistic corrections; it is unique because of the soft pion enhancement we have discussed. Since this enhancement is mild in the integrated probability, the regular contribution to the amplitude should be included. In the actual calculations we use the complete relativistic propagators for B^* and D^* and invariant vertices, and do not rely on an expansion in $1/m_Q$. In other words, we only use the soft-pion Lagrangian to model the pion emission amplitude, assuming that the couplings do not vary significantly with energy. In effect, this implies a certain form for the contact terms which appear in the chiral Lagrangian at the subleading $1/m_Q$ order.

In the calculation of the integrated inelastic probability, there is a subtlety that requires some care and was discussed already in [10]. Since $M_{D^*} > M_D + m_\pi$, the point $\varepsilon = 0$ corresponds to $|\vec{p}_\pi| \simeq 39 \text{ MeV}$ and the integration extends to small negative ε . At $\varepsilon = 0$ the integral has a singularity related to the $D\pi$ decay of the unstable D^* , which should be distinguished from the actual continuum contribution, and has to be removed. In practice, the physical regularization is to introduce the Breit-Wigner factor, replacing $1/\varepsilon^2$ in Eq. (41) by $1/(\varepsilon^2 + \Gamma^2/4)$, where Γ is the decay width of D^* . In actuality Γ is small compared even to the energy release in $D^* \rightarrow D\pi$. Therefore including the width serves only to regularize the integral. Adopting it, integration around $\varepsilon = 0$ yields unity, the probability of $B \rightarrow D^*$ we start with, where D^* is represented by the $D\pi$ -resonance. The integration over ε is then carried out with $|\varepsilon| > \varepsilon_{\min} \gg \Gamma$. The resulting inelastic integral does not depend on the choice of ε_{\min} as long as $\Gamma \ll \varepsilon_{\min} \ll M_{D^*} - M_D - m_\pi$ holds. An accurate analysis shows that for all practical purposes the integral can simply be evaluated by setting $m_\pi = M_{D^*} - M_D$.

It turns out that numerically the most important effect comes from the difference in the pion-meson couplings in the charm and beauty sectors, $r \neq 1$. Various studies suggest $r \lesssim 1$ [22]. Fig. 7 shows the integrated $w_{\text{inel}}^{D\pi}$ as a function of the upper cutoff on the pion momentum, p_π^{\max} , for a few values of r . Formally, p_π^{\max} is related to the maximum excitation energy ε_M :

$$\varepsilon_M = \sqrt{(p_\pi^{\max})^2 + m_\pi^2} + \sqrt{(p_\pi^{\max})^2 + M_D^2} - M_{D^*};$$

however, a lower cutoff may effectively be set by the domain of applicability of the soft-

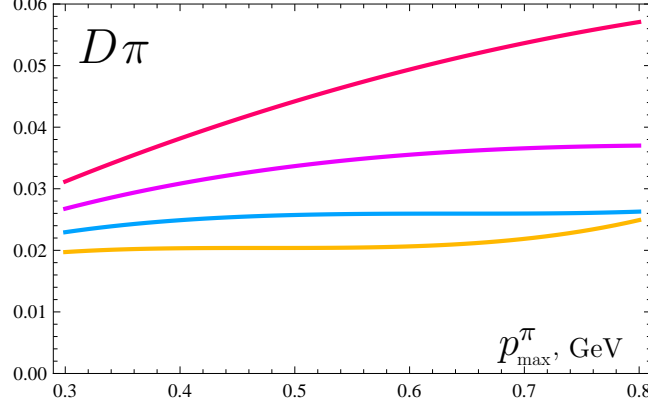


Figure 7: Nonresonant $D\pi$ contribution including both charged and neutral pion depending on the maximal pion momentum, at $g_{D^*\pi} = 4.9 \text{ GeV}^{-1}$ which corresponds to $\Gamma_{D^*} = 96 \text{ keV}$. The plots show, from bottom to top, $r=1, 0.8, 0.6$ and 0.4 .

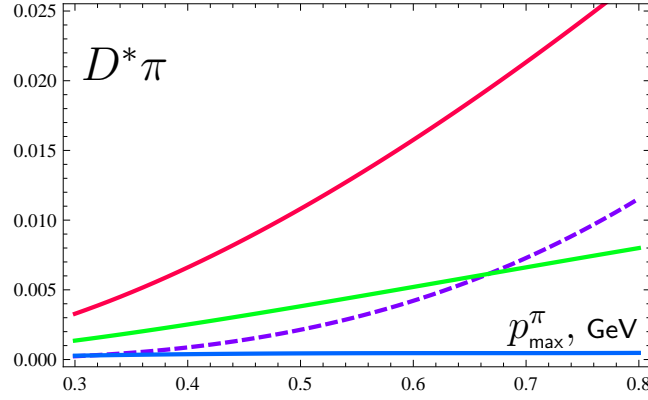


Figure 8: Nonresonant $D^*\pi$ contribution depending on the maximal pion momentum, at $g_{D^*\pi} = 4.9 \text{ GeV}^{-1}$. The solid lines correspond, from bottom to top, to $\tilde{r}=1, 0.8$ and 0.6 , while the dashed line refers to $\tilde{r}=1.3$.

pion approximation. It is reasonable to stop at least somewhat below the expected ‘radial’ resonance domain, around $p_\pi^{\text{max}} \approx 0.6 \text{ GeV}$: even if the amplitude grows with \vec{p}_π , at some point this contribution starts to belong to the resonant radial excitations and should be excluded to avoid double counting.

The $D^*\pi$ channel has been considered only in Ref. [1], even though it is required for consistency with the spin-symmetry structure of the corrections already at $1/m_Q^2$. The pattern of the $1/m_Q$ mass corrections in the intermediate poles is now reversed, and the contribution at low pion momentum is suppressed. Altogether it turns out very small unless the difference between $B^*B\pi$ and $D^*D\pi$ vertices is appreciable. The numerical results are shown in Fig. 8.⁵

The calculation for $D^*\pi$ proceeds in a way similar to the $D\pi$ case. The ‘bare’ weak

⁵Due to a typo in the plotting notebook the plot in Ref. [1] showed values larger by a factor of π .

vertices for the mesons are now

$$\begin{aligned}\langle D^*(\varepsilon)|\bar{c}\gamma_\mu\gamma_5 b|B\rangle &= 2\sqrt{M_B M_{D^*}} \varepsilon_\mu^*, \\ \langle D^*(\varepsilon)|\bar{c}\gamma_\mu\gamma_5 b|B^*(\varepsilon')\rangle &= i\sqrt{M_{B^*} M_{D^*}} \epsilon_{\mu\nu\rho\lambda} \varepsilon_\nu^* \varepsilon'_\rho \left(\frac{P_\lambda}{M_{D^*}} + \frac{P'_\lambda}{M_{B^*}} \right),\end{aligned}\quad (42)$$

where P and P' are the four-momenta of D^* and B^* mesons, respectively. The pion Lagrangian paralleling Eq. (39) is

$$\mathcal{L}_{D^*D^*\pi} = 2g_{D^*D^*\pi} \epsilon_{\mu\nu\rho\lambda} D_\mu^* \partial_\nu D_\rho^* \partial_\lambda \pi, \quad g_{D^*D^*\pi} = \tilde{r} g_{D^*D\pi}, \quad (43)$$

from which the $D^* \rightarrow D^*\pi$ vertex is derived. The required diagrams mirror Figs. (6), with D replaced by D^* . The point $\varepsilon = 0$ is now below the threshold and no subtleties in the integration occurs. Again, the neutral pion contribution to w_{inel} is half of that for the charged pion.

The pion couplings $g_{B^*B\pi}$ and $g_{D^*D^*\pi}$ have not been measured experimentally. There is theoretical evidence that $1/m_c$ corrections in the coupling should indeed be significant [22]; similar conclusions have been reported from the lattice studies [23]. The spin symmetry violating difference between $g_{D^*D^*\pi}$ and $g_{D^*D\pi}$ has not been addressed yet. On general grounds it may likewise be thought to be significant; we expect to have its estimate from the QCD sum rules.

We finally arrive at a few percent continuum contribution to I_{inel} :

$$I_{\text{inel}}^{D^{(*)}\pi} \approx 3 \text{ to } 5\%.$$

This is about a fourth of the resonance estimate Eq. (38) and therefore conforms to the general expectation. A clarifying comment is in order in this respect.

The above estimate of the $D^{(*)}\pi$ effects should not be added to the principal numeric estimate of Eq. (38). The corresponding hadronic states contribute to the nonlocal correlators along with the resonant states and therefore have been accounted for in the observed meson masses used there as inputs. We will come back to this subject in Section 6.3. The $D^{(*)}\pi$ states effectively lower the average excitation energy $\tilde{\varepsilon}$ compared to ε_{rad} ; however, the continuum contribution is relatively suppressed and this is not a prominent effect. On the other hand, should one discard the estimate of the inelastic contribution of Eq. (38), it is reasonable to include at least $I_{\text{inel}}^{D^{(*)}\pi}$ in the unitarity upper bound for $\mathcal{F}(1)$; this lowers it by about 2% down to approximately $\mathcal{F}(1) < 0.90$.

To conclude the first part of the paper, we refer the reader to Sect. 8, where our numeric conclusions for $\mathcal{F}(1)$ can be found, see Eqs. (131), (132) and (133).

6 A closer look at the heavy quark excited states

The zero-recoil transition amplitudes between the B meson and the excited charm states appeared in Sec. 5, where they gave the part of the power-suppressed correction to $\mathcal{F}(1)$ associated with the overlap of nonrelativistic wavefunctions. They are encountered in various

applications of the heavy quark expansion, together with the spectrum of the corresponding states, and deserve a dedicated analysis.

So far mostly the P -wave excitations of the ground-state mesons have been considered in the literature. They play a primary role in the small velocity regime and enter the sum rules which strongly constrain possible values of the main nonperturbative heavy quark parameters [11, 24]. Here we extend the analysis to higher states, in particular to those which are commonly referred to as radial or D -wave excitations, assuming the heavy quark (static) limit. In the actual heavy mesons we may have additional excited states associated with the interacting spin and gauge field degrees of freedom.

In our analysis we will use heavy quarks deprived of their spin [11, 24]; this is physically motivated since in the static limit heavy quark spin degrees of freedom decouple, and this greatly simplifies all the expressions, as long as no velocity change is considered. This formalism leads in a simple and transparent manner to the trace formalism of the rest frame; a discussion of the connection to the conventional formalism can be found in Re. [3]. We remind that with spinless heavy quarks the ground-state heavy mesons are spin- $\frac{1}{2}$ particles; the corresponding states are denoted by $|\Omega_0\rangle$ and their two-component spinor wavefunctions, when needed explicitly, are denoted by Ψ_0 . The Pauli matrices $\vec{\sigma}$ act on the spinor indices of the heavy hadron wavefunctions. To specify our convention we set the parity of Ω_0 positive.

Translating the relations in this formalism to the case of expectation values in actual B mesons is straightforward. The spin-singlet quantities are in a one-to-one correspondence. For the spin-triplet ones the fact that $\vec{\sigma}_Q = -\vec{\sigma}$ for the spinless state like B meson ($\vec{\sigma}_Q$ is the spin matrix acting on the heavy quark indices) immediately gives the required translation.

6.1 Model-independent spectral representation

Heavy quark theory requires the tower of heavy quark transition matrix elements with zero spatial momentum transfer, ordered according to the number of covariant derivatives (heavy quark momentum). They enter both the expansion in velocity and the non-relativistic $1/m_Q$ expansion. In practice we are interested in the matrix elements of the ground state.

The unit operator $\bar{Q}Q$ has trivial matrix elements at vanishing velocity change. The operator $\bar{Q}\pi_k Q$ with a single derivative describes the dipole transitions which connect Ω_0 to the $\frac{1}{2}$ and $\frac{3}{2}$ P -wave states with negative parity. At the lowest order in the expansion we need the general inclusive two-point correlator with two derivatives, or its absorptive part:

$$\begin{aligned} \frac{1}{\pi} \text{Im } P_{jk}(\omega) &= \frac{1}{2\pi} \int d^3x \int dx_0 e^{-i\omega x_0} \frac{1}{2M_Q} \langle \Omega_0 | Q^\dagger \pi_j Q(x) Q^\dagger \pi_k Q(0) | \Omega_0 \rangle \\ &= \mathcal{T}^{(\frac{1}{2}-)}(\omega) \Psi_0^\dagger (\delta_{jk} + \sigma_{jk}) \Psi_0 + \mathcal{T}^{(\frac{3}{2}-)}(\omega) \Psi_0^\dagger (2\delta_{jk} - \sigma_{jk}) \Psi_0; \quad (44) \end{aligned}$$

here and in what follows we use the notation

$$\sigma_i \sigma_j = \delta_{ij} + \sigma_{ij}, \quad \sigma_{ij} = i\epsilon_{ijk} \sigma_k.$$

The two spectral densities generalize the conventional $\frac{1}{2}$ and $\frac{3}{2}$ SV amplitudes to continuum states:

$$\mathcal{T}^{(\frac{1}{2}-)}(\omega) = \omega^2 \frac{d|\tau_{1/2}(\omega)|^2}{d\omega}, \quad \mathcal{T}^{(\frac{3}{2}-)}(\omega) = \omega^2 \frac{d|\tau_{3/2}(\omega)|^2}{d\omega}; \quad (45)$$

their relation to the inelastic part of the SV structure functions $W_{\pm}(\omega)$ introduced in Ref. [25] is

$$W_+(\omega) = \frac{2\mathcal{T}^{(\frac{3}{2}-)}(\omega) + \mathcal{T}^{(\frac{1}{2}-)}(\omega)}{\omega^2}, \quad W_-(\omega) = \frac{2\mathcal{T}^{(\frac{3}{2}-)}(\omega) - \mathcal{T}^{(\frac{1}{2}-)}(\omega)}{\omega^2}, \quad \omega > 0. \quad (46)$$

To extend the analysis to the relevant radially excited states we consider the spectral density of the general two-point correlation function of the products of two spatial covariant derivatives acting on the heavy quark:

$$R_{ijkl}(\omega) = \frac{1}{2\pi} \int d^3x \int dx_0 e^{-i\omega x_0} \frac{1}{2M_Q} \langle \Omega_0 | Q^\dagger \pi_i \pi_j Q(x) Q^\dagger \pi_k \pi_l Q(0) | \Omega_0 \rangle. \quad (47)$$

It can be decomposed into the invariant structures corresponding to three possible classes of the intermediate heavy quark states with $j = \frac{1}{2}$, $j = \frac{3}{2}$ and $j = \frac{5}{2}$, respectively:

$$\begin{aligned} R_{ijkl}(\omega) = & \Psi_0^\dagger \left[\frac{1}{9} \rho_p^{(\frac{1}{2}+)}(\omega) \delta_{ij} \delta_{kl} - \frac{1}{18} \rho_{pg}^{(\frac{1}{2}+)}(\omega) (\delta_{ij} \sigma_{kl} + \sigma_{ij} \delta_{kl}) + \frac{1}{36} \rho_g^{(\frac{1}{2}+)}(\omega) \sigma_{ij} \sigma_{kl} \right] \Psi_0 \\ & + \Psi_0^\dagger \left[\frac{1}{200} \rho_f^{(\frac{3}{2}+)}(\omega) \left(\delta_{ik} \delta_{jl} + \delta_{il} \delta_{jk} - \frac{2}{3} \delta_{ij} \delta_{kl} + \frac{1}{2} (\sigma_{ik} \delta_{jl} + \sigma_{il} \delta_{jk} + \sigma_{jk} \delta_{il} + \sigma_{jl} \delta_{ik}) \right) \right. \\ & + \frac{1}{80} \rho_{fg}^{(\frac{3}{2}+)}(\omega) \left(i\epsilon_{ijk} \sigma_l + i\epsilon_{ijl} \sigma_k + i\epsilon_{jkl} \sigma_i + i\epsilon_{ikl} \sigma_j - \frac{2}{3} (\delta_{ij} \sigma_{kl} + \delta_{kl} \sigma_{ij}) \right) \\ & \left. - \frac{1}{16} \rho_g^{(\frac{3}{2}+)}(\omega) \left(\frac{2}{3} (\delta_{ik} \delta_{jl} - \delta_{il} \delta_{jk}) + \frac{1}{3} (i\epsilon_{ijk} \sigma_l - i\epsilon_{ijl} \sigma_k) \right) \right] \Psi_0 \\ & + \frac{1}{10} \rho^{(\frac{5}{2}+)}(\omega) \Psi_0^\dagger \left[3(\delta_{ik} \delta_{jl} + \delta_{il} \delta_{jk} - \frac{2}{3} \delta_{ij} \delta_{kl}) - (\sigma_{ik} \delta_{jl} + \sigma_{il} \delta_{jk} + \sigma_{jk} \delta_{il} + \sigma_{jl} \delta_{ik}) \right] \Psi_0. \end{aligned} \quad (48)$$

The meaning of the three invariant functions for $j = \frac{1}{2}$ and $j = \frac{3}{2}$ will become clear shortly.

The nonlocal correlators which are relevant to our analysis of I_{inel} have been introduced in Eqs. (32). In addition, it is also useful to introduce

$$\begin{aligned} \tilde{\rho}_{\pi\pi} &= \int d^4x i|x_0| \frac{1}{4M_B} \langle B | iT \{ \bar{b} \vec{\pi}^2 b(x), \bar{b} \vec{\pi}^2 b(0) \} | B \rangle', \\ \tilde{\rho}_{\pi G} &= \int d^4x i|x_0| \frac{1}{2M_B} \langle B | iT \{ \bar{b} \vec{\pi}^2 b(x), \bar{b} \vec{\sigma} \vec{B} b(0) \} | B \rangle', \\ \frac{1}{3} \tilde{\rho}_S \delta_{ij} \delta_{kl} + \frac{1}{6} \tilde{\rho}_A (\delta_{ik} \delta_{jl} - \delta_{il} \delta_{jk}) &= \int d^4x i|x_0| \frac{1}{4M_B} \langle B | iT \{ \bar{b} \sigma_i B_k b(x), \bar{b} \sigma_j B_l b(0) \} | B \rangle'. \end{aligned} \quad (49)$$

The extra factor $i|x_0|$ compared to Eqs. (32) is simply an extra power of excitation energy ε in the denominator in the spectral representation, see Eqs. (51) below. Using the $\tilde{\rho}$ correlators one can directly write the inelastic contribution to the sum rule (3), cf. Eq. (31):

$$I_{\text{inel}} = \frac{-(\tilde{\rho}_{\pi G} + \tilde{\rho}_A)}{3m_c^2} - \frac{2\tilde{\rho}_{\pi\pi} + \tilde{\rho}_{\pi G}}{3m_c m_b} + \frac{\tilde{\rho}_{\pi\pi} + \tilde{\rho}_{\pi G} + \tilde{\rho}_S + \tilde{\rho}_A}{4} \left(\frac{1}{m_c^2} + \frac{2}{3m_c m_b} + \frac{1}{m_b^2} \right) + \mathcal{O}\left(\frac{1}{m_Q^3}\right). \quad (50)$$

All these nonlocal correlators are readily expressed in terms of the above spectral densities:

$$\begin{aligned} \rho_{\pi\pi}^3 &= \int d\omega \frac{\rho_p^{(\frac{1}{2}^+)}(\omega)}{\omega} & \tilde{\rho}_{\pi\pi} &= \int d\omega \frac{\rho_p^{(\frac{1}{2}^+)}(\omega)}{\omega^2} \\ -\rho_{\pi G}^3 &= \int d\omega \frac{2\rho_{pg}^{(\frac{1}{2}^+)}(\omega)}{\omega} & -\tilde{\rho}_{\pi G} &= \int d\omega \frac{2\rho_{pg}^{(\frac{1}{2}^+)}(\omega)}{\omega^2} \\ \rho_S^3 &= \int d\omega \left(\frac{\rho_g^{(\frac{1}{2}^+)}(\omega)}{3\omega} + \frac{\rho_g^{(\frac{3}{2}^+)}(\omega)}{2\omega} \right) & \tilde{\rho}_S &= \int d\omega \left(\frac{\rho_g^{(\frac{1}{2}^+)}(\omega)}{3\omega^2} + \frac{\rho_g^{(\frac{3}{2}^+)}(\omega)}{2\omega^2} \right) \\ \rho_A^3 &= \int d\omega \left(\frac{2\rho_g^{(\frac{1}{2}^+)}(\omega)}{3\omega} - \frac{\rho_g^{(\frac{3}{2}^+)}(\omega)}{2\omega} \right), & \tilde{\rho}_A &= \int d\omega \left(\frac{2\rho_g^{(\frac{1}{2}^+)}(\omega)}{3\omega^2} - \frac{\rho_g^{(\frac{3}{2}^+)}(\omega)}{2\omega^2} \right). \end{aligned} \quad (51)$$

The integration runs over positive ω ; the point $\omega=0$ is excluded. The integration is also cut at large ω for $\omega > \mu$ according to the normalization prescription in the kinetic scheme.

Note that neither $\rho_{f,fg}^{(\frac{3}{2}^+)}$ nor $\rho^{(\frac{5}{2}^+)}$ can contribute above. Using these relations one can express the $1/m_Q^2$ inelastic transition probabilities for actual B mesons. The following form appears particularly convenient for the analysis:

$$\begin{aligned} w_{\text{inel}}(\omega) &= \left(\frac{1}{2m_c} - \frac{1}{2m_b} \right)^2 \frac{\rho_p^{(\frac{1}{2}^+)}(\omega)}{\omega^2} + \left(\frac{1}{2m_c} - \frac{1}{2m_b} \right) \left(\frac{1}{3m_c} + \frac{1}{m_b} \right) \frac{\rho_{pg}^{(\frac{1}{2}^+)}(\omega)}{\omega^2} \\ &\quad + \frac{1}{4} \left(\frac{1}{3m_c} + \frac{1}{m_b} \right)^2 \frac{\rho_g^{(\frac{1}{2}^+)}(\omega)}{\omega^2} + \frac{1}{6m_c^2} \frac{\rho_g^{(\frac{3}{2}^+)}(\omega)}{\omega^2}. \end{aligned} \quad (52)$$

The analogous representation for the vector current-induced transitions is given in Eq. (A.28).

6.1.1 Intermediate state contributions

Here we consider the contribution of an individual positive-parity state to the above correlators. Again, we first briefly remind what happens for the P -wave states.

Following Ref. [11] we denote the $\frac{1}{2}$ and $\frac{3}{2}$ P -wave states by ϕ and χ and describe them with the two-dimensional spinor ϕ and the non-relativistic Rarita-Schwinger spinors χ_j , respectively. There are successive families of these states which differ by their excitation

energy $\epsilon_n = M_n - M_0$; we typically omit the index marking the excitation number. The $\frac{3}{2}$ -spinors χ_j satisfy $\sigma_j \chi_j = 0$ and the normalization fixes the sum over their polarizations:

$$\sum_{\lambda} \chi_i(\lambda) \chi_j^{\dagger}(\lambda) = \delta_{ij} - \frac{1}{3} \sigma_i \sigma_j. \quad (53)$$

The dipole amplitudes are related to the conventional small-velocity amplitudes τ by

$$\langle \phi^{(n)} | \pi_j | \Omega_0 \rangle = \epsilon_n \tau_{1/2}^{(n)} \phi^{(n)\dagger} \sigma_j \Psi_0, \quad \langle \chi^{(m)} | \pi_j | \Omega_0 \rangle = \sqrt{3} \epsilon_m \tau_{3/2}^{(m)} \chi_j^{(m)\dagger} \Psi_0. \quad (54)$$

The two-derivative heavy quark operators at vanishing total spatial momentum acting on Ω_0 may create $\frac{1}{2}^+$, $\frac{3}{2}^+$ or $\frac{5}{2}^+$ states. The ground state itself has $j^P = \frac{1}{2}^+$; we will always assume however that $\frac{1}{2}^+$ refers to an excited multiplet. We describe the $\frac{1}{2}^+$, $\frac{3}{2}^+$ and $\frac{5}{2}^+$ states by a conventional spinor χ and by the Rarita-Schwinger spinors χ_j and χ_{jl} , respectively, with the following constraints:⁶

$$\sigma_j \chi_j = 0; \quad \chi_{jk} = \chi_{kj}, \quad \chi_{jj} = 0, \quad \sigma_j \chi_{jk} = 0. \quad (55)$$

The sum over polarizations λ giving the spin part of the propagator equals to

$$\begin{aligned} \sum_{\lambda=1}^2 \chi(\lambda) \chi^{\dagger}(\lambda) &= 1 \\ \sum_{\lambda=1}^4 \chi_i(\lambda) \chi_j^{\dagger}(\lambda) &= \delta_{ij} - \frac{1}{3} \sigma_i \sigma_j \\ \sum_{\lambda=1}^6 \chi_{ij}(\lambda) \chi_{kl}^{\dagger}(\lambda) &= \frac{3}{10} (\delta_{ik} \delta_{jl} + \delta_{il} \delta_{jk} - \frac{2}{3} \delta_{ij} \delta_{kl}) - \frac{1}{10} (\sigma_{ik} \delta_{jl} + \sigma_{il} \delta_{jk} + \sigma_{jk} \delta_{il} + \sigma_{jl} \delta_{ik}). \end{aligned} \quad (56)$$

Following the standard notation for the diagonal matrix element of the ground state,

$$\langle \Omega_0 | \pi_k \pi_l | \Omega_0 \rangle = \frac{\mu_{\pi}^2}{3} \delta_{kl} \Psi_0^{\dagger} \Psi_0 - \frac{\mu_G^2}{6} \Psi_0^{\dagger} \sigma_{kl} \Psi_0, \quad (57)$$

we parameterize

$$\langle \frac{1}{2}^+ | \pi_k \pi_l | \Omega_0 \rangle = \frac{P}{3} \delta_{kl} \chi^{\dagger} \Psi_0 - \frac{G}{6} \chi^{\dagger} \sigma_{kl} \Psi_0. \quad (58)$$

The transitions amplitude into $\frac{3}{2}^+$ -states have a symmetric and an antisymmetric structure parameterized by constants f and g :

$$\langle \frac{3}{2}^+ | \pi_k \pi_l | \Omega_0 \rangle = \frac{f}{20} (\chi_k^{\dagger} \sigma_l + \chi_l^{\dagger} \sigma_k) \Psi_0 + \frac{g}{4} i \epsilon_{klm} \chi_m^{\dagger} \Psi_0, \quad (59)$$

⁶The P -wave wave-functions will no longer appear in what follows and we use the same notation for the $\frac{3}{2}$ -hadrons of opposite parity.

while the $\frac{5}{2}^+$ amplitude depends on a single parameter h :

$$\langle \frac{5}{2}^+ | \pi_k \pi_l | \Omega_0 \rangle = h \chi_{kl}^\dagger \Psi_0. \quad (60)$$

The residues P, G, f, g and h are different for each multiplet of the excited heavy state.

A particular hadronic state with excitation energy ϵ_n is associated with the following factorized contributions to the invariant spectral densities $\rho_{p,pg,g}^{(\frac{1}{2}^+)}(\omega)$, $\rho_{f,fg,g}^{(\frac{3}{2}^+)}(\omega)$ and $\rho^{(\frac{5}{2}^+)}(\omega)$ in Eq. (48):

$$\begin{aligned} \delta\rho_p^{(\frac{1}{2}^+)}(\omega) &= P^2 \delta(\omega - \epsilon_n), & \delta\rho_g^{(\frac{1}{2}^+)}(\omega) &= G^2 \delta(\omega - \epsilon_n), & \delta\rho_{pg}^{(\frac{1}{2}^+)}(\omega) &= PG \delta(\omega - \epsilon_n) \\ \delta\rho_f^{(\frac{3}{2}^+)}(\omega) &= f^2 \delta(\omega - \epsilon_n), & \delta\rho_g^{(\frac{3}{2}^+)}(\omega) &= g^2 \delta(\omega - \epsilon_n), & \delta\rho_{fg}^{(\frac{3}{2}^+)}(\omega) &= fg \delta(\omega - \epsilon_n) \\ \delta\rho^{(\frac{5}{2}^+)}(\omega) &= h^2 \delta(\omega - \epsilon_n). \end{aligned} \quad (61)$$

The ground-state contribution to R_{ijkl} is located at $\omega=0$ and is excluded from the nonlocal correlators ρ^3 and $\tilde{\rho}$ of Eqs. (51); it is obtained by taking $P_{(0)} = \mu_\pi^2$ and $G_{(0)} = \mu_G^2$ with $\epsilon_0=0$.

The spin- $\frac{5}{2}$ contribution $\delta\rho^{(\frac{5}{2}^+)}(\omega)$ is given by the square of a single residue h and is non-negative. The factorization relations lead to the Cauchy inequalities

$$(\rho_{pg}^{(\frac{1}{2}^+)})^2 \leq \rho_p^{(\frac{1}{2}^+)} \rho_g^{(\frac{1}{2}^+)}, \quad (\rho_{fg}^{(\frac{3}{2}^+)})^2 \leq \rho_f^{(\frac{3}{2}^+)} \rho_g^{(\frac{3}{2}^+)} \quad (62)$$

which turn into equalities for a particular single state contribution. Furthermore, one has the general inequalities

$$2|\rho_{pg}^{(\frac{1}{2}^+)}(\omega)| \leq \rho_p^{(\frac{1}{2}^+)} + \rho_g^{(\frac{1}{2}^+)}, \quad 2|\rho_{fg}^{(\frac{3}{2}^+)}(\omega)| \leq \rho_f^{(\frac{3}{2}^+)} + \rho_g^{(\frac{3}{2}^+)}, \quad (63)$$

the first of which will soon be useful.

For completeness we mention the constraints imposed by the BPS limit for the ground state, which assumes $\vec{\pi}\vec{\sigma}|\Omega_0\rangle=0$. Similar to the ground-state expectation values, for transitions into $\frac{1}{2}^+$ states the BPS condition implies $P=G$; however the relations for the excited states are accurate only to first order in the deviation from the BPS limit. No constraint emerges on h , while for the transitions into $\frac{3}{2}^+$ states BPS implies $f=g$:

$$\langle \frac{3}{2}^+ | \pi_k \vec{\pi} \vec{\sigma} | \Omega_0 \rangle = (\frac{1}{4}f - \frac{1}{4}g) \chi_k^\dagger \Psi_0. \quad (64)$$

For the invariant structures in the spectral density $R_{ijkl}(\omega)$ in Eq. (48) the BPS condition leads to the relations

$$\rho_p^{(\frac{1}{2}^+)}(\omega) = \rho_{pg}^{(\frac{1}{2}^+)}(\omega) = \rho_g^{(\frac{1}{2}^+)}(\omega), \quad \rho_f^{(\frac{3}{2}^+)}(\omega) = \rho_{fg}^{(\frac{3}{2}^+)}(\omega) = \rho_g^{(\frac{3}{2}^+)}(\omega). \quad (65)$$

Let us note that when the spin- $\frac{1}{2}$ degrees of freedom associated with light antiquark in the meson decouple, as in the case of purely perturbative calculations, the correlator

decomposition can be based on the angular momentum only, $L=0, 1, 2$, of the intermediate states composed of the QCD degrees of freedom still interacting with heavy quark:

$$R_{ijkl}^{\text{Fact}}(\omega) = \left[\frac{\rho_0(\omega)}{9} \delta_{ij} \delta_{kl} + \frac{\rho_1(\omega)}{16} (\delta_{il} \delta_{jk} - \delta_{ik} \delta_{jl}) + \frac{\rho_2(\omega)}{10} (\delta_{ik} \delta_{jl} + \delta_{il} \delta_{jk} - \frac{2}{3} \delta_{ij} \delta_{kl}) \right] \Psi_0^\dagger \Psi_0, \quad (66)$$

with a trivial spinor structure. This would mean

$$\begin{aligned} \rho_p^{(\frac{1}{2}^+)}(\omega) &= \rho_0(\omega), & \rho_g^{(\frac{1}{2}^+)}(\omega) &= \frac{3}{4} \rho_1(\omega), & \rho_g^{(\frac{3}{2}^+)}(\omega) &= \rho_1(\omega), \\ \rho_f^{(\frac{3}{2}^+)}(\omega) &= 8\rho_2(\omega), & \rho^{(\frac{5}{2}^+)}(\omega) &= \frac{1}{5} \rho_2(\omega), & \rho_{pg}^{(\frac{1}{2}^+)}(\omega) &= \rho_{fg}^{(\frac{3}{2}^+)}(\omega) = 0. \end{aligned} \quad (67)$$

We will use these relations when address the perturbative μ -dependence later on.

6.2 Hyperfine splitting and the estimate of the correlators

The analysis of the spin structure and of the factorization properties does not constrain the overall scale of the residues and the significance of the radially excited states, which can however be estimated by considering the heavy quark mass dependence of the hyperfine splitting ΔM^2 . This will allow us to fix the magnitude of the nonlocal correlators in Eqs. (31), (50).

The $B-B^*$ mass splitting basically fixes the value of μ_G^2 . The mass difference between the beauty and charm states mainly reflects $m_b - m_c$. A comparison of $M_{D^*} - M_D$ and $M_{B^*} - M_B$ hyperfine splittings gives information on higher dimensional correlators, and in particular on the values of two $D=3$ spin-triplet parameters, ρ_{LS}^3 and $\rho_{\pi G}^3 + \rho_A^3$:

$$\Delta M_B = M_B^* - M_B = \frac{2}{3} \frac{\mu_G^2}{m_b} + \frac{-\rho_{LS}^3 + \rho_{\pi G}^3 + \rho_A^3}{3 m_b^2} + \mathcal{O}\left(\frac{1}{m_b^3}\right) \quad (68)$$

and likewise for charm. Following Ref. [6], we explore this relation cast in a somewhat different form.

As dictated by the heavy quark expansion, for sufficiently heavy quarks the difference $\Delta M_Q^2 = M_{Q^*}^2 - M_Q^2$ for the vector and the pseudoscalar mesons approaches a constant. Yet it has been noticed long ago that such a relation works well even for light quarks:

$$M_\rho^2 - M_\pi^2 \simeq M_{K^*}^2 - M_K^2 \simeq M_{D^*}^2 - M_D^2 \simeq M_{B^*}^2 - M_B^2. \quad (69)$$

Clearly, the heavy quark expansion cannot explain why such a relation extends down to the light quarks. The approximate equality resembles the universality of the slope for Regge trajectories and may root in the peculiarities of the strong dynamics. Moreover, actual QCD predicts that such a relation must be violated for sufficiently heavy quarks due to the perturbative renormalization of the chromomagnetic operator of the heavy quark which has a nontrivial anomalous dimension. As was also noted long ago, the observed 12% decrease in the mass square difference in the B system compared to D mesons fits reasonably well the naive estimates of this perturbative evolution.

It is therefore tempting to assume the independence of the mass-square splitting as a phenomenological property of *soft* strong dynamics yet to be understood, and to consider its consequences in the context of the heavy quark expansion where we can vary the heavy quark mass. Using the mass formulae we have

$$\Delta M_Q^2 = \Delta M_Q(2M_Q + \Delta M_Q) = \frac{4}{3}c_G(\mu, m_Q)\mu_G^2 + \frac{2}{3}\frac{\rho_{\pi G}^3 + \rho_A^3 - \rho_{LS}^3 + 2\bar{\Lambda}\mu_G^2}{m_Q} + \mathcal{O}\left(\frac{1}{m_Q^2}\right), \quad (70)$$

where c_G is the Wilson coefficient of the chromomagnetic operator in the heavy quark Hamiltonian. If the perturbative m_Q -evolution of c_G accounted completely for the observed difference between ΔM_B^2 and ΔM_D^2 , the m_Q -independence of ΔM_Q^2 to the first nontrivial order in $1/m_Q$ would imply

$$-(-\rho_{LS}^3 + \rho_{\pi G}^3 + \rho_A^3) \simeq 2\bar{\Lambda}\mu_G^2. \quad (71)$$

This relation will guide our analysis below.

Numerically using $\bar{\Lambda} = 600 \text{ MeV}$, $\mu_G^2 = 0.3 \text{ GeV}^2$ and $\rho_{LS}^3 = -0.1 \text{ GeV}^3$ we would get

$$-(\rho_{\pi G}^3 + \rho_A^3) \approx 0.45 \text{ GeV}^3 \quad (72)$$

which indicates that the nonlocal correlators ρ^3 are in general sizable. The negative sign for $\rho_{\pi G}^3 + \rho_A^3$ is expected from BPS arguments [6].

To proceed more quantitatively we introduce a factor κ in Eq. (71), to account for the actual mismatch between the observed mass dependence and the dependence stemming from c_G :

$$-(-\rho_{LS}^3 + \rho_{\pi G}^3 + \rho_A^3) = 2(1 + \kappa)\bar{\Lambda}\mu_G^2. \quad (73)$$

κ does not include higher power corrections, which we address later, and can be defined through

$$\kappa\bar{\Lambda}\mu_G^2 = \lim_{m_Q \rightarrow \infty} m_Q^2 \frac{d}{dm_Q} \left[\frac{3}{4}\Delta M_Q^2 - c_G(m_Q)\mu_G^2 \right], \quad (74)$$

where the logarithmic derivative of $c_G\mu_G^2$ is related to the exact anomalous dimension of the chromomagnetic operator, times ΔM_Q^2 .

In simple words, the soft part of ΔM_Q^2 , identified by subtracting the (Wilsonian) short-distance renormalization factor, approaches a finite limit as $m_Q \rightarrow \infty$. The assumption underlying the approximation of small $|\kappa|$ is that such a soft part is nearly a constant in a wide range of heavy quark masses, as Eq. (69) would naively suggest.

Let us now look at the perturbative renormalization c_G . The one- and two-loop [26] contributions are known. At first glance in the evolution from beauty to charm, namely in the ratio $c_G(m_c)/c_G(m_b)$, the two-loop contribution is quite sizable. However, the bulk of the higher-loop perturbative enhancement comes from growing strong coupling at small momenta of virtual gluons. This large-coupling domain must be removed from the perturbative corrections to avoid double counting. The subtraction piece is power-suppressed yet important for charm, especially in the effect of running of the strong coupling.

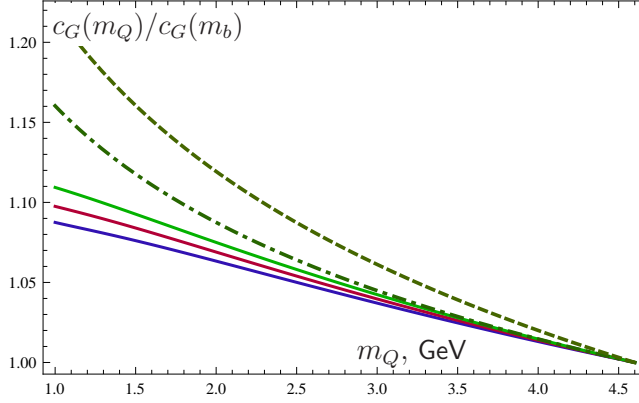


Figure 9: The effect of removing the infrared piece belonging to the nonperturbative expectation values, from the one-loop perturbative evolution from beauty to charm $c_G(m_Q)/c_G(m_b)$, as a function of m_Q . The solid curves correspond to $\mu = 0.8$ GeV (blue), 0.7 GeV (red) and 0.6 GeV (green), respectively; the dashed curve shows the naive perturbative result with no cutoff, all at $\alpha_s = 0.3$. For comparison the dashed-dotted line shows the no-cutoff result at $\alpha_s = 0.22$.

The numeric aspects are illustrated in Fig. 9 in the case of one-loop corrections, using $\alpha_s = 0.3$. The cutoff effects are more important than higher-loop corrections. The two-loop calculation of Ref. [26], which strongly enhanced the first-order renormalization, should not be used in the present context [6]. To get an accurate estimate in the following we will employ the one-loop calculation of $c_G(m_c)/c_G(m_b)$ with Wilsonian cutoff evaluated at $\alpha_s = 0.3$.

A precise determination of κ is not easy since only two data points exist on the ΔM^2 curve in the heavy quark regime. Moreover, the perturbative treatment of charm may have insufficient precision and higher power corrections for $D^{(*)}$ may be significant. The situation is illustrated in Fig. 10, where only the change in the perturbative coefficient c_G is considered. In other words, the continuous lines show the quantity $(M_{B^*}^2 - M_B^2) \frac{c_G(m_Q)}{c_G(m_b)}$, without power corrections associated with using the meson masses.⁷ Clearly, this approximation is valid for sufficiently large masses.

Let us now discuss the implications for the nonlocal correlators that follow from Fig. 10. The *solid* curves correspond to $\kappa = 0$, and do not include any power correction. For $\kappa \neq 0$ a power correction appears according to Eqs. (70) on top of the perturbative renormalization. Therefore, if the actual ΔM^2 below beauty goes lower than the perturbatively continued dependence, κ is positive; conversely, a negative κ corresponds to the case where the actual ΔM^2 increases steeper than the one computed perturbatively from the beauty point. We also note that what matters here is actually the relative position of the curves in the vicinity of the beauty point, or, more generally the difference in the slope of the two curves at any

⁷The physical masses depend on the pseudoscalar meson mass M_P , viz. M_B, M_D, \dots whereas the perturbative renormalization is expressed through the quark masses. To put them on the same plot and to compare we evaluate the perturbative calculations at $m_Q = M_{P_Q} - \bar{\Lambda}$. The dependence on the precise value of m_Q is minor.

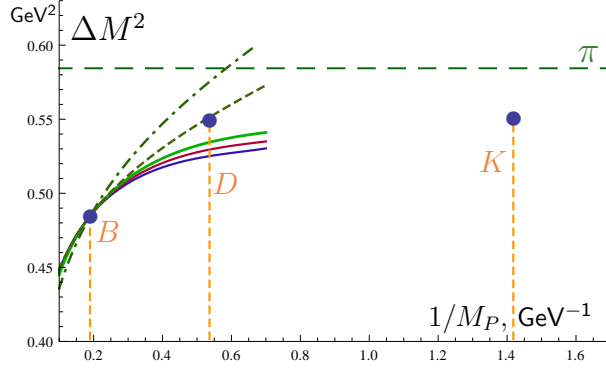


Figure 10: The difference $\Delta M^2 = M_V^2 - M_P^2$ plotted as a function of the inverse meson mass $1/M_P$. The three data points stand for beauty, charm and strangeness, the horizontal line shows the asymptotic value given by the ρ - π splitting. (The K point has been moved leftward.) Solid curves represent the expected perturbative evolution in the case all power corrections are neglected, using the Wilsonian perturbative renormalization factor; they correspond to $\mu = 0.8 \text{ GeV}$, 0.7 GeV , 0.6 GeV , respectively. The dashed curves shows the naive perturbative result without cutoff.

sufficiently large mass where the $1/m_Q^3$ and higher terms in the masses can be neglected.

It looks improbable that the actual ΔM^2 dependence on the inverse meson mass may be significantly steeper around the B meson than the one-loop $\alpha_s = 0.22$ perturbative curve, because that would require an unnatural shape, perhaps with a maximum higher than the charm point. Moreover, in that case sizable power corrections would be necessary to hit the ΔM_D^2 point, and there would be no reason to expect a small value of the nonlocal correlators. Since the ΔM_D^2 point in Fig. 10 is above the Wilsonian perturbative curves, a somewhat steeper dependence on $1/M_P$ is observed. Therefore, κ must be relatively small and negative in the Wilsonian approach.

In order to obtain a numerical prediction for ΔM^2 and refine Eq. (72) we use the expansion for ΔM , Eq. (68), and rewrite it, neglecting, as usual, the perturbative corrections to power corrections, as

$$\Delta M(m_Q) = \frac{m_b c_G(m_Q; \mu)}{m_Q c_G(m_b; \mu)} \frac{1 - \frac{\delta}{m_Q}}{1 - \frac{\delta}{m_b}} \Delta M(m_b) \left[1 + \mathcal{O}\left(\frac{1}{m_Q^2}\right) \right], \quad (75)$$

with the shortcut

$$\delta = \frac{-(\rho_{\pi G}^3 + \rho_A^3 - \rho_{LS}^3)}{2\mu_G^2}, \quad \text{or} \quad 1 + \kappa = \frac{\delta}{\Lambda}.$$

Higher order power terms modify the m_Q -dependence of ΔM^2 . Therefore, in order to obtain definite numerical values for the nonlocal correlators from ΔM^2 in beauty and charm we need to make assumptions on the higher-order terms $\mathcal{O}(1/m_Q^2)$ in Eq. (75). The simplest option is to discard $1/m_Q^2$ and higher terms in the mass difference. An alternative

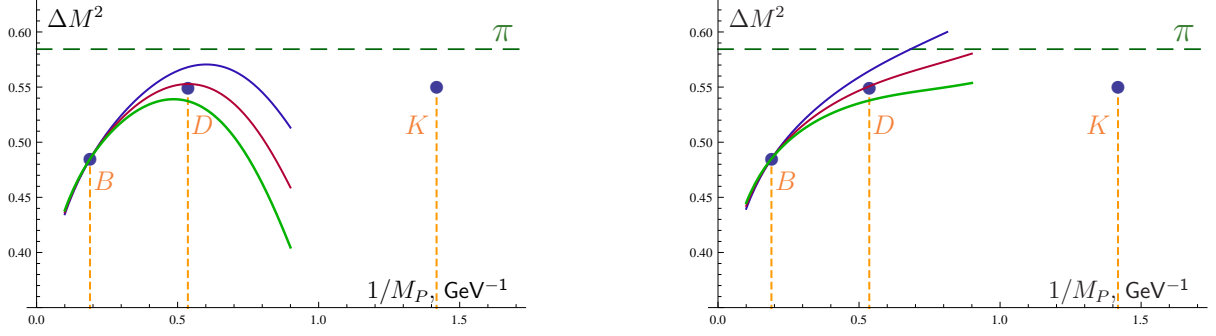


Figure 11: ΔM^2 for different heavy quark masses computed under different assumptions for higher-order power terms: no higher power term (left) and the ansatz in Eq. (76) (right). The two families of curves assume different values for $1+\kappa$ from top to bottom: 0.5, 0.55, 0.6 (left) and 0.7, 0.8, 0.9 (right), respectively. $\bar{\Lambda}=0.65$ GeV, $\mu=0.8$ GeV and $\alpha_s=0.3$.

way is to write the power correction factor as

$$\Delta M(m_Q) = \frac{2}{3} c_G(m_Q) \frac{\mu_G^2}{m_Q} \cdot \frac{1}{1 + \frac{\delta}{m_Q}} \quad (76)$$

as an ansatz for higher-order terms; it expresses them in terms of μ_G^2 and of the powers of δ . The two forms have identical μ_{had}^3/m_Q^2 corrections but differ at higher orders. The latter ansatz has the advantage of yielding a reasonable finite value even at small m_Q .

To depict results graphically as a function of M_P , for the pseudoscalar mass $M_P(m_Q)$ we use its conventional heavy quark expansion well described by just $m_Q + \bar{\Lambda}$ due to the proximity to the BPS regime (for even lighter quark, to continue the plots below charm we use an ad-hoc extrapolation giving a reasonable behavior at small m_Q).

Fig. 11 shows the expected ΔM^2 for three values of κ under the two assumptions about higher-order terms. The difference illustrates the sensitivity to the unknown power corrections in the meson masses. It is modest around the B mass scale, yet becomes significant for charm. We have also tried alternative ansätze for power corrections and found that κ always varies between -0.5 and 0 . The extrapolation of the curves below charm seems to suggest a preference for the smaller $|\kappa|$, as in the right of Figs. 11. Moreover, higher order perturbative effects are qualitatively expected to increase $1+\kappa$. We will therefore use $\kappa = -0.2 \pm 0.2$, arriving at

$$2(1+\kappa)\bar{\Lambda}\mu_G^2 \approx 2(0.8 \pm 0.2)0.65 \cdot 0.35 \text{ GeV}^3 \simeq (0.35 \pm 0.1) \text{ GeV}^3. \quad (77)$$

Combining this estimate with the expected value $\rho_{LS}^3 \approx -0.1 \text{ GeV}^3$ we end up with

$$-(\rho_{\pi G}^3 + \rho_A^3) \approx 0.45 \text{ GeV}^3, \quad (78)$$

as in the original estimate, Eq. (72). One of the reasons is that a larger value for $\bar{\Lambda}$ must be used in the Wilsonian approach, which offsets a negative κ .

The main assumption employed in the above estimate is the possibility to quantitatively use the mass expansion for charm particles, assuming a reasonable magnitude of the higher-order power corrections in a physical scheme. This assumption could be avoided in the case an additional input from lattice calculations were available, with the squared mass splitting reliably computed at one or more intermediate points for quarks heavier than charm. The short-distance expansion there is in a better shape, perturbative corrections under better control, and higher-order power corrections are less important. This would allow to use the differential version of the constraint on the hyperfine splitting in the large- m_Q limit, namely Eq.(74), fixing directly the slope. Even if a first-principle direct measurement of ΔM^2 with sufficient precision turns out difficult for large mass, any intermediate point – and even a point somewhat below charm – would constrain the shape of the curve thereby narrowing down the interval of possible values for the derivative.

Eq. (78) is a strong constraint, especially useful in the analysis of the inelastic contribution to $\mathcal{F}(1)$. This will be discussed in the next subsection. Here we only note that a determination of $-(\rho_{\pi G}^3 + \rho_A^3)$ gives a model-independent constraint on the spectral densities $\rho_g^{(\frac{1}{2}^+)}$, $\rho_{pg}^{(\frac{1}{2}^+)}$ and $\rho_g^{(\frac{3}{2}^+)}$, which are informative due to the factorization property and to the relation to the spectrum of physical states. Since the value in Eq. (78) is quite large, $\rho_{pg}^{(\frac{1}{2}^+)}(\omega)$ together with $-\rho_{\pi G}^3$ is most probably positive, unless the correlators are strongly dominated by the $\frac{3}{2}^+$ states. The predictive power sharpens significantly if additional dynamic information is used, for instance the proximity to the BPS limit or the saturation by a limited number of the heavy quark multiplets.

We conclude this section noting that another interesting constraint on the nonlocal correlators can be obtained from the difference of the spin-averaged B and D meson masses, namely from

$$m_b - m_c = \overline{M}_B - \overline{M}_D + \frac{\mu_\pi^2}{2} \left(\frac{1}{m_c} - \frac{1}{m_b} \right) + \frac{\rho_D^3 - \bar{\rho}^3}{4} \left(\frac{1}{m_c^2} - \frac{1}{m_b^2} \right) + \mathcal{O}\left(\frac{1}{m_Q^3}\right), \quad (79)$$

where $\bar{\rho}^3 = \rho_{\pi\pi}^3 + \rho_S^3$. The use of this relation to determine $\bar{\rho}^3$ requires a good control of the heavy quark mass difference and a precise knowledge of μ_π^2 and ρ_D^3 , which can in principle be provided by the global fits to semileptonic moments. We have considered the fits employed in Sec. 4; they typically give $\bar{\rho}^3 = (0.33 \pm 0.17) \text{ GeV}^3$. Notice that the semileptonic fits determine μ_π^2 in the actual B meson, while its static approximation appears in Eq. (79). As the difference is BPS and $1/m_b$ suppressed, it is certainly smaller than the fit uncertainty on μ_π^2 , and we have neglected it. The value of $\bar{\rho}^3$ can be linked to $(\rho_{\pi G}^3 + \rho_A^3)$ since the sum $\rho_{\pi\pi}^3 + \rho_S^3 + \rho_{\pi G}^3 + \rho_A^3$ is positive definite, vanishes in the BPS limit, and receives only second order corrections to the limit. Therefore, $-(\rho_{\pi G}^3 + \rho_A^3) \lesssim (0.33 \pm 0.17) \text{ GeV}^3$, which is compatible with our primary estimate, Eq. (78).

6.3 The hyperfine constraint and the excited states

The hyperfine splitting constraint Eq. (78) fixes the overall scale of the correlators which are the focus of our study:

$$\int \frac{d\omega}{\omega} \left(\frac{\rho_g^{(\frac{3}{2}^+)}(\omega)}{2} + 2\rho_{pg}^{(\frac{1}{2}^+)}(\omega) - \frac{2\rho_g^{(\frac{1}{2}^+)}(\omega)}{3} \right) \simeq 0.45 \text{ GeV}^3 + (\kappa+0.2) \cdot 0.36 \text{ GeV}^3. \quad (80)$$

The normalization point enters here as the upper cutoff in the integral over ω ; we assume it is around 0.8 GeV. At first glance we have a single relation among four spectral functions; nevertheless this relation turns out to be very useful thanks to the positivity and factorization properties discussed in Sec. 6.1.1.

The principal observation is that according to the estimate Eq. (78) the nonlocal correlators are numerically large. The particular combination constrained significantly exceeds the estimated size of the expectation values of local heavy quark operators of $D=6$, most notably ρ_D^3 which by itself is large. Alternatively, the value in Eq. (78) can be compared to $\bar{\Lambda}^3$: it exceeds it, even though $\bar{\Lambda}$ is already numerically large. Likewise, the square of the kinetic expectation value $(\mu_\pi^2)^2$ can be used to gauge the scale of hadronic parameters of mass dimension 3 if it is divided by a typical energy of the radial excitations, yielding again a value close to 0.35 GeV³.

For more quantitative statements it is advantageous to separate the resonant and the soft continuum contributions to the spectral densities: the inclusion of the continuum makes the effective value of ω identified with ε_{rad} more uncertain numerically. The separation can be done since the $\Omega_0+\pi$ states are readily analyzed in the soft-pion technique; for instance, Sect. 5.2 estimated the continuum part of I_{inel} at actual values of m_c and m_b . This analysis is performed in Sect. 6.4 and suggests that a relatively small fraction should be subtracted from the value in Eq. (80) if we want to keep only the resonant contribution.

Once only the resonant contribution are retained, a meaningful approximation well illustrating the physics of the constraints is a model where a single multiplet in each channel involved is considered. This model has a very few parameters essentially reduced to the residues P , G and g (f and h do not enter), and all the constraints can be easily analyzed.

To gauge the size of the related hadronic parameters we take the sum of the two spin-singlet nonlocal correlators $\rho_{\pi\pi}^3$ and ρ_S^3 as a measure of their overall significance; each of these correlators is positive. On the other hand, we have a relation

$$\rho_{\pi\pi}^3 + \rho_S^3 = -(\rho_{\pi G}^3 + \rho_A^3) + \int \frac{d\omega}{\omega} \left[\rho_p^{\frac{1}{2}^+} - 2\rho_{pg}^{\frac{1}{2}^+} + \rho_g^{\frac{1}{2}^+} \right]. \quad (81)$$

The last bracket on the right is positive; it can be represented as a correlator of a certain operator. This shows that the l.h.s. of (81) always exceeds the combination $-\rho_{\pi G}^3 - \rho_A^3$ fixed by the ‘hyperfine’ constraint; the minimum is attained at the BPS point where the two combinations coincide. The inequality actually holds at arbitrary spectral parameter ω ; it is the numeric hyperfine constraint that applies only upon integration over the energy.

Eq. (81) shows that the $1/m_Q^2$ spin-averaged meson mass shift must always be larger than $3/4$ times the $1/m_Q^2$ correction to the hyperfine splitting. This is not difficult to trace directly:

$$\frac{3\delta M_B^* + \delta M_B}{4} = \frac{3}{4}(\delta M_B^* - \delta M_B) + \delta M_B; \quad (82)$$

$\delta_{1/m_Q^2} M_B$ receives a positive contribution $(\rho_D^3 + \rho_{LS}^3)/4m_b^2$ from the local piece and a negative contribution from the T -product of two $(\sigma\pi)^2$. Both vanish at the BPS point.

The last positive term in Eq. (81) is of the second order in the deviation from BPS, therefore it may be a good approximation to neglect it in numerical estimates unless the BPS is strongly violated in the actual B mesons. For what follows we do not need this additional assumption, the positivity is sufficient.

Now we can see that the sum of the two correlators $\rho_{\pi\pi}^3$ and ρ_S^3 is also quite large numerically; this implies large $1/m_Q$ corrections to the meson states, in particular averaged over the spin multiplet. However, experiment tells us that the heavy quark symmetry works reasonably well even in charm. This means the correlators driving power corrections should not be excessively large. In order to have both $\rho_{\pi\pi}^3$ and ρ_S^3 as small as possible, besides the BPS condition, we can assume that $\rho_{\pi\pi}^3$ and ρ_S^3 are equal, in which case $\rho_g^{\frac{1}{2}+} = \frac{3}{4}\rho_g^{\frac{3}{2}+}$ must hold upon corresponding integration over energy.

On the other hand, since the r.h.s. of Eq. (80) is large, it is reasonable to expect that $\rho_{pg}^{(\frac{1}{2}+)}$ is positive, and that $\rho_p^{(\frac{1}{2}+)}$ is not much smaller than $\rho_g^{(\frac{1}{2}+)}$. In this case the left-hand side is a sum of two positive contributions from $\frac{1}{2}^+$ and $\frac{3}{2}^+$ channels.

It makes sense to parameterize the relative contribution of the $\frac{1}{2}^+$ and $\frac{3}{2}^+$ states, introducing a parameter ν :

$$\int \frac{d\omega}{\omega} \frac{\rho_g^{(\frac{3}{2}+)}(\omega)}{2} \equiv \nu \int \frac{d\omega}{\omega} \left(\frac{\rho_g^{(\frac{3}{2}+)}(\omega)}{2} + 2\rho_{pg}^{(\frac{1}{2}+)}(\omega) - \frac{2\rho_g^{(\frac{1}{2}+)}(\omega)}{3} \right), \quad \nu > 0. \quad (83)$$

The large numeric value of the the r.h.s. of Eq. (80) points at ν between 0 and 1 as the most natural solution; ν exceeding unity is highly improbable.

6.3.1 Estimate of I_1

The spectral representation together with the hyperfine constraint allows one to analyze the possible values of I_{inel} . Ignoring a possible spread in the values of average excitation energy we equate I_{inel} with $I_1/\varepsilon_{\text{rad}}$ or, equivalently, express the $\tilde{\rho}$ correlators in Eq. (51) through the conventional ρ^3 . The evaluation of I_{inel} then depends directly on the size of the corresponding nonlocal correlators. For instance, the last positive term in Eq. (31) is immediately recognized as the square bracket in Eq. (81); it is given solely by the BPS-violating transitions into the $\frac{1}{2}^+$ multiplet.

All the terms in I_1 but the leading BPS piece fixed by the hyperfine constraint are independent of the $\frac{3}{2}^+$ contributions, and the l.h.s. of Eq. (80) gets a positive piece from

them. Therefore the minimum of I_1 is attained at vanishing $\rho_g^{(\frac{3}{2}^+)}$ which also corresponds to $\rho_A^3 = 2\rho_S^3$.

We now refer to Eq. (52) for the structure of I_{inel} and express it in terms of the transition amplitudes P, G, g . At fixed G and g , I_{inel} is a quadratic trinomial in the ratio P/G , with the positive leading power coefficient proportional to $(1/m_c - 1/m_b)^2$. We recall that in the BPS limit $P/G = 1$. The hyperfine splitting implies an additional constraint on P, G, g , which can be taken into account. The result is that

$$\frac{3m_c^2 I_1}{-(\rho_{\pi G}^3 + \rho_A^3)} \geq 1 - (1 - \nu) \frac{m_c^2}{m_b^2} \simeq 1 - 0.07(1 - \nu), \quad (84)$$

and I_1 has a minimum at a value of $P/G > 1$, whose exact position depends only on the heavy quark mass ratio but not on g . The minimum is attained, with the inequality saturated, at

$$\frac{P}{G} = \frac{1}{3} + \frac{2}{3} \frac{m_b + m_c}{m_b - m_c} \simeq 1.47, \quad (85)$$

where the numeric values correspond to $m_c/m_b = 1.2/4.6$. This result was referred to in Sect. 5.1. For $\nu = 0$ it implies $G \approx 0.37 \text{ GeV}^2$.

The minimum, however, is rather shallow, see Fig. 5, because the coefficient of the term quadratic in P/G is large while the linear term is small. While I_1 may, in principle, significantly exceed its BPS value I_1^{BPS} , Eq. (36), for strong BPS violation if P/G is negative, at more natural positive P/G (a regime where both $\rho_{\pi\pi}^3$ and ρ_s^3 are not too large) the value of I_1/I_1^{BPS} is typically slightly smaller than unity, as illustrated in Fig. 5.

6.3.2 The inclusive $\frac{1}{2}^+$ and $\frac{3}{2}^+$ yield

The hyperfine constraint implies relatively large values of the transition matrix elements to $\frac{1}{2}^+$ and/or $\frac{3}{2}^+$ states and an enhancement of the overall yield of the corresponding excited charm states in the semileptonic decays of actual B mesons. This is quantified by the estimate of I_{inel} constituting, roughly speaking, 15% of the D^* probability, in the zero-recoil kinematics. This comparison does not include the phase-space suppression of excited states resonances which becomes significant when one integrates over all available phase space. Other kinematic effects may work in the opposite direction, however, and a more substantiated estimate is desirable.

Our preceding analysis constrains directly the $1/m_Q$ squared transition amplitudes into the corresponding hadronic states at zero velocity transfer. At first glance, this seems too crude an estimate at non-zero recoil, where contributions not suppressed by $1/m_Q$ appear. However, since we consider states with the quantum numbers of radials or of D -waves, the leading-order amplitude is proportional to the second power of the velocity of the charmed meson — roughly speaking, it is generated by replacing the momentum operators π_k with $m_Q v_k$. Since for excited mesons v_k is always relatively small, the zero-recoil amplitude receives only a minor correction when integrated over the whole phase space. Therefore, we can retain only the $1/m_Q$ part of the transition amplitude. For comparison, the leading heavy-quark transition amplitude into the P -waves provides only a suppressed correction

to the $1/m_Q$ term [27], even though the leading amplitude in that case is of the first order in the velocity, and the P -wave states are lighter.

We will therefore relate the transition probabilities into radially excited states directly to the zero-recoil observables we have studied in the previous sections. The total yield is also fed by vector-current transitions, even though we do not expect them to provide a large contribution, as their amplitudes vanish in the BPS limit. These transitions can be considered in the same way as the axial timelike component, see Appendix D.

The total yields are roughly proportional to $(M_B - M)^5 \equiv \Delta^5$ where M is the mass of the corresponding charm multiplet. Numerically we equate Δ with $M_B - M_D - \epsilon_{\text{rad}}$, leading to $\Delta \simeq 2.6$ GeV. However, for $\Delta/M_B \gtrsim 0.5$ relativistic effects modify significantly the nonrelativistic Δ^5 dependence. A more accurate approach is the following (see Appendix D for details). Instead of considering the transition amplitudes between the B meson and all the excited mesons belonging to a multiplet, we evaluate the decay rate of the Ω_0 spin- $\frac{1}{2}$ heavy state into the corresponding excited half-integer spin multiplets. The weak current coupling of these fictitious hadrons is then fixed by the corresponding transition probabilities near zero recoil.

In practice, we parameterize the transition amplitudes to $\frac{1}{2}^+$ and $\frac{3}{2}^+$ states, for axial and vector currents, and compute the decay rate integrating over all the available phase space. The overall normalization of the amplitudes is fixed at zero recoil by the corresponding nonlocal correlator. Let us illustrate this in the case of the transitions into $\frac{1}{2}^+$ states.

The most general vector or axial vertices in terms of full Lorentz spinor wavefunctions have the form

$$\begin{aligned} J_\mu^A &= g_A \bar{\chi} \gamma_\mu \gamma_5 \Psi_0 + b_A \bar{\chi} i \sigma_{\mu\nu} \frac{q_\nu}{M_B} \gamma_5 \Psi_0 + c_A \frac{q_\mu}{M_B} \bar{\chi} i \gamma_5 \Psi_0, \\ J_\mu^V &= g_V \bar{\chi} \gamma_\mu \Psi_0 + b_V \bar{\chi} \sigma_{\mu\nu} \frac{q_\nu}{M_B} \Psi_0 + c_V \frac{q_\mu}{M_B} \bar{\chi} \Psi_0. \end{aligned} \quad (86)$$

At zero recoil the effect of b_A reduces to a change in g_A of $(M_B - M)/M_B b_A$, while the term proportional to c_A vanishes. However, for generic recoil these are all independent structures. Similar considerations apply to the vector current. We neglect the additional contributions at non-zero recoil and effectively set the formfactors $b_{A,V}$, $c_{A,V}$ to zero. Likewise we neglect the velocity-dependence of the formfactors. The corresponding decay rates are then given by

$$\Gamma_{V,A}^{(\frac{1}{2})} = |g_{V,A}|^2 \frac{G_F^2 |V_{cb}|^2 M_B^5}{192\pi^3} z_{A,V}(r), \quad (87)$$

where

$$\begin{aligned} z_{A,V}(r) &= \frac{z_0(r) \pm \tilde{z}_0(r)}{2}, & z_0(r) &= 1 - 8r + 8r^3 - r^4 - 12r^2 \ln r, \\ r &= \frac{M^2}{M_B^2}, & \tilde{z}_0(r) &= 2\sqrt{r} [1 + 9r - 9r^2 - r^3 + 6r(1+r) \ln r], \end{aligned} \quad (88)$$

are the weighted phase space factors for the axial and vector transitions, respectively; $z_0(r)$ is the standard kinematic factor for $V - A$ decays.

The value of $|g_A|^2$ is directly given by the $\frac{1}{2}^+$ contribution in $w_{\text{inel}}(\omega)$ in Eq. (52) for one multiplet, and the transition amplitudes G and P are constrained by our analysis of the hyperfine splitting. $|g_V|^2$ follows from the analogous relation for vector-induced probabilities, Eq. (A.28). The vector-induced probability is significantly suppressed compared to the axial one.

As already mentioned, we neglect additional recoil corrections. A justification for this is the ‘extended’ SV regime relevant in the context of a large-5 expansion [4] where the enhanced corrections reside in the lepton phase space. The deviations from the small-recoil kinematics in the amplitude are not enhanced, but rather suppressed by the large power of energy release decreasing the average recoil.

The case of the decays into the $\frac{3}{2}^+$ is treated similarly — the details are given in Appendix D. We describe these states by complete relativistic Rarita-Schwinger wavefunctions at arbitrary velocity, and calculate the corresponding contribution to the (unpolarized) structure functions of Ω_0 . Their integration yields the total decay rate, and we fix the normalization of the formfactors at zero recoil.

In this way the decay rates are calculate separately for the $\frac{1}{2}^+$ and $\frac{3}{2}^+$ states and separately for the axial and the vector transitions. Numerically we get for the combined yield

$$\frac{\Gamma_{\text{rad}}}{\Gamma_{\text{sl}}} \approx 0.07, \quad (89)$$

with the axial part strongly dominating (we have included perturbative corrections in the denominator). While the relative weight of $\frac{1}{2}^+$ and $\frac{3}{2}^+$ states varies depending on their couplings, their sum is approximately fixed by the hyperfine condition (80).

In our approach the total decay rate is computed in the heavy quark limit. We included the $1/m_Q$ symmetry-breaking terms which mediate the transitions in question, and exploited the fact that the total decay rate does not depend on the exact mixing of the final heavy-quark eigenstates in the actual QCD hadrons.

To apply the estimates to the yield of actual individual charmed mesons in QCD one would need to properly construct the corresponding states in terms of $\frac{1}{2}^+$ and $\frac{3}{2}^+$ states. While straightforward in practice, this may yield unreliable predictions in practice since the heavy quark symmetry is probably quite strongly violated for the excited charm states. We expect much more robust predictions for the total yield summing up all the associated channels. Such inclusive probabilities are insensitive to the details of the strong Hamiltonian in the final states, are not affected by possible degeneracies and altogether enjoy smaller preasymptotic corrections. Therefore, we view Eq. (89) as a good starting estimate of the overall yield of the descendants of the ‘radial’ states. It refines the earlier estimate given in Ref. [1], and probably represents a natural lower limit. A compatible number has recently been suggested in Ref. [28].

It is worth noting that the semileptonic phase space factor strongly suppresses the yield of the states with higher mass; in particular, for a wide resonance with mass $M = \bar{M} + \delta m$ one has

$$(M_B - M)^5 = (\Delta - \delta m)^5 \approx \Delta^5 \left(1 - \frac{\delta m}{600 \text{ MeV}} + \dots \right) \quad (90)$$

This shows that for broad resonances the phase space factor averaged over the whole decay kinematics significantly distorts the Breit-Wigner shape and shifts the apparent peak towards lower mass. The factor in Eq. (90) applied to a wide resonance may easily mimic a typical non-resonant continuum yield with a threshold suppression.

The above estimate suggests that the total yield of the discussed ‘radial’ excitations with mass below $M_D + 1 \text{ GeV}$ is expected to be, in terms of Γ_{sl} , at the 7% level. This is close to what is observed in experiment, yet traditionally is attributed to the ‘wide’ $\frac{1}{2}$ P -wave states. The conventional allocation creates a problem: theory predicts that the $\frac{3}{2}$ -states must strongly dominate among the P -waves; they have been measured at the right rate of about 10% of Γ_{sl} , see *e.g.* [29] for a discussion. We are therefore led to argue that the decays into the $\frac{1}{2}^-$ states are indeed suppressed, while the bulk of the experimentally observed “wide” structure is actually the result of the significant fraction of the ‘radial’ states.

6.3.3 The radial and D -wave excited states

The phenomenological analysis earlier in this section suggests, as the most natural solution that both the $\frac{1}{2}^+$ true radial excitations and the $\frac{3}{2}^+$ D -wave states contribute significantly the spectral functions involved and are produced at appreciable rate in the semileptonic B decays. At present we do not have accurate enough data to state which of the two channels dominate; we have only observed that the solutions where one of them, say, the D -wave, is small is disfavored.

In fact, the identification of the two families of states with the S - or D -waves is not strict in the actual mesons in QCD even in the limit of a large mass m_Q . For instance, the $\frac{3}{2}^+$ states can instead be a result of excitation of gauge degrees of freedom. Whether this is so or not is an open question, and the fact that we expect a numerically large transition matrix element of the chromomagnetic field,

$$\langle \frac{3}{2}^+ | \bar{Q} B_k Q | \Omega_0 \rangle_{\vec{q}=0} = \frac{g}{4} \chi_k^\dagger \Psi_0, \quad (91)$$

is not directly related to it. It appears that so far the radial states attracted more attention in the literature, while the D -waves were marginally considered [30]. At the same time we expect the dominant mechanism for the production of the corresponding charmed states to be the $1/m_c$ -component of the amplitude, and it is qualitatively similar for both of them. Their masses are also expected to be in the same range about 700 MeV above the ground state.

A challenging question is how one can disentangle these states in experiment. In the simplest constituent quark model one expects the hyperfine splitting inside the D -wave multiplet to be particularly suppressed. However, it is not evident to which extent this would be the property of the actual QCD states. Moreover, the hyperfine splitting may well happen to be suppressed within the radially excited multiplet as well.

Some differences are expected in the decay pattern. (We reason in terms of the asymptotic states deprived of the heavy quark spin; the translation into the actual mesons is

standard.) The radially excited states can decay into the ground state Ω_0 and a single pion in the P -wave, or into Ω_0 plus two pions in S -wave. We expect the dominant channel to be the latter where two pions have a σ -meson enhancement; that is, they must predominantly be in the isospin-singlet S -wave state.

This particular two-pion channel is not allowed for the $\frac{3}{2}^+$ state which should then decay mostly into Ω_0 and a pion. A weaker two-pion channel cannot show the resonance enhancement associated with σ -meson. We naturally expect the $\frac{3}{2}^+$ states to have a smaller width. It is possible that the excited mesons recently reported by BaBar [31] with mass around 2.75 GeV are related to these states. The states with the lower mass around 2.6 GeV may be the radial states.

Another decay chain where the first decay proceeds into a single pion in the S -wave and a P -wave charm state, either $\frac{1}{2}^-$ or $\frac{3}{2}^-$, can be competitive and may provide an additional handle through the identification of the P -wave state via its subsequent decay. These questions deserve further consideration. Since the two multiplets are expected to have close masses, the actual excited vector D^* states may show significant mixture, which has to be considered.

6.4 Nonresonant $D^{(*)}\pi$ in the spectral representation

The special role of the nonresonant $D^{(*)}\pi$ states manifested itself already in the analysis of $\mathcal{F}(1)$. In the heavy quark limit we consider their counterpart, the non-resonant states $\Omega_0 + \pi$ (kaon or η may also be included). They are of special interest for a relatively soft pion where its energy is essentially below the resonance excitation gap. This gap depends on the orbital momentum of the pion: for the P -wave states it is about 400 MeV. Our focus is on the radial (or D -wave) excitations where it is about 700 MeV.

The traditional classification over spin-parity of the light degrees of freedom is equally applicable to multi-particle states, including the $\Omega_0\pi$ continuum. They can be classified in a way similar to the ground-state excitations, the analogies of P -waves etc., and only have to be additionally labeled by the continuum excitation energy. In the static limit the latter is equal to the pion energy. The quantum numbers of $\Omega_0\pi$ are not fixed a priori: a continuum state is generally a mixture with different quantum numbers depending on the production amplitude. For instance, this would apply to the relative weight of the $\frac{3}{2}^-$ and $\frac{1}{2}^-$ states in P -wave.

The advantage of the expansion we employ is that only the heavy quark states with vanishing total spatial momentum are involved, and they are considered in the static limit. This fixes the structure of the transition amplitudes appearing to a particular order in the $1/m_Q$ expansion; the relative weight of different spin-orbit multiplets is then determined as well. In this section we obtain the decomposition into $\frac{1}{2}$, $\frac{3}{2}$ etc. states for $\Omega_0\pi$ and calculate the corresponding spectral densities as a function of the pion energy. They then determine the contributions to $|\tau_{1/2}|^2$, $|\tau_{3/2}|^2$, $\rho_{\pi\pi}^3$ etc. For instance, we will see that the pion loop has a $\tau_{1/2} = \tau_{3/2}$ property [32]. The associated continuum states do not contribute to μ_G^2 or ρ_{LS}^3 , yet they change the IW slope or $\bar{\Lambda}$ in a predictable way, and mediate a positive contribution to $\mu_\pi^2 - \mu_G^2$.

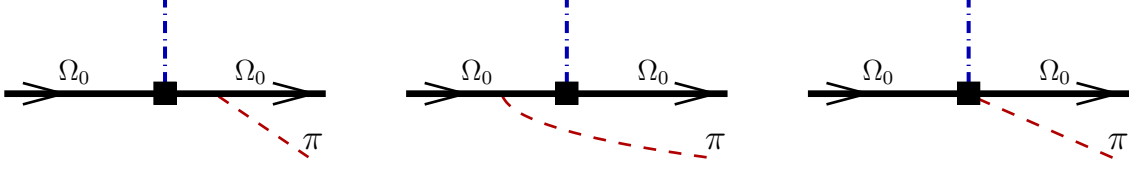


Figure 12: The pion emission diagrams in the static limit. The solid blocks denote the $\bar{Q}iD_jQ$ or $\bar{Q}iD_jiD_lQ$ operators with $\vec{q}=0$. Pion carries spatial momentum \vec{k} ; incoming Ω_0 have vanishing spatial momentum and outgoing $-\vec{k}$.

The $\Omega_0\pi$ states at rest are uniquely characterized by the energy and by the pion orbital momentum L . Indeed, the total angular momentum j consists of $\frac{1}{2}$ of Ω_0 and of L of pion: $L = j \pm \frac{1}{2}$. Its parity relative to parity of Ω_0 is $(-1)^{L+1}$. Therefore, the combination of j and parity unambiguously specifies L . For instance, $L=0$ are $\frac{1}{2}^-$ P -wave states, $L=1$ give $\frac{1}{2}^+$ and $\frac{3}{2}^+$ ‘radial’ excitations and the $\frac{3}{2}^-$ P -wave states require $L=2$.

The combination of the ‘ P -waves’ appearing to the leading order in either $1/m_Q$ or in velocity is mediated explicitly by the operator $\bar{Q}i\vec{D}Q$; the relative mixture is determined by a concrete form of the amplitude which involves the spin of Ω_0 . The most straightforward approach is to consider the $\Omega_0\pi$ contribution to the zero-recoil correlation function of operators $\bar{Q}iD_jQ$ and $\bar{Q}iD_kQ$, as we did in Sect. 6.1, Eq. (44).

The effective low-energy Lagrangian of the $\pi\Omega_0\Omega_0$ -interaction corresponding to Eqs. (39) and (43) in relativistic notations is

$$\mathcal{L}_{\text{chi}} = -g_{B^*B\pi}\bar{\Omega}_0\gamma_\mu\gamma_5\Omega_0\partial^\mu\pi = -2g_{B^*B\pi}M_\Omega\bar{\Omega}_0i\gamma_5\Omega_0\pi \quad (92)$$

(total derivatives are omitted). The diagrams to be calculated are shown in Fig. 12 where the heavy hadron lines now all refer to Ω_0 and the solid vertex stands for the operator $\bar{Q}iD_jQ$. The vertex is simple:

$$\frac{1}{2M_{\Omega_0}}\langle\Omega_0(p_2)|\bar{Q}(i\overleftarrow{D}_j \pm i\overrightarrow{D}_j)Q|\Omega_0(p_1)\rangle = (p_2 \pm p_1)_j\Psi_0^\dagger\Psi_0, \quad (93)$$

where we have generally distinguished the left and right derivatives for the case of different momenta of Ω_0 . Since in our case the spatial momentum flowing into the vertex vanishes, this specification is superfluous.

The diagram **a)** vanishes, while **b)** yields an amplitude with a simple spin structure:

$$\frac{1}{2M_{\Omega_0}}\langle\Omega_0\pi|\bar{Q}iD_jQ|\Omega_0(0)\rangle = -g_{B^*B\pi}\frac{k_j}{\omega}\Psi_0^\dagger i\vec{\sigma}\vec{k}\Psi_0, \quad (94)$$

where \vec{k} is the pion momentum. The resulting correlator $P_{jk}(\omega)$ obtained by squaring the amplitude and summing over polarizations of intermediate Ω_0 has only a part symmetric in j, k :

$$\frac{1}{\pi}\text{Im} P_{jk}(\omega) = \frac{g_{B^*B\pi}^2}{12\pi^2}\frac{|\vec{k}|^5}{\omega^2}\delta_{jk}\Psi_0^\dagger\Psi_0. \quad (95)$$

From this we read off

$$\mathcal{T}^{(\frac{1}{2}^-)}(\omega) = \mathcal{T}^{(\frac{3}{2}^-)}(\omega) = \frac{g_{B^*B\pi}^2}{36\pi^2} \theta(\omega - m_\pi) (\omega^2 - m_\pi^2)^{3/2} \left(1 - \frac{m_\pi^2}{\omega^2}\right), \quad (96)$$

where the overall factor refers to a single charged pion loop contribution. The neutral pion additionally contributes a half of that. Relations (45) give the values of the corresponding $|\tau_{1/2}|$ and $|\tau_{3/2}|$, which are equal.

It is worth noting that the equality $\tau_{1/2} = \tau_{3/2}$ is not an automatic property of quantum numbers in the $D\pi$ system. It rather follows from the form of the soft-pion amplitude for heavy mesons. For instance, a structure $\bar{\Psi}_0 \sigma_j \Psi_0$ would have produced only $\frac{1}{2}^-$ but not $\frac{3}{2}^-$. The relation generally changes already due to the final state interaction (FSI) in the $\Omega_0\pi$ system, although the latter is suppressed by extra powers of pion momentum. Before the three-pion threshold the amplitude is completely characterized by the pion- Ω_0 scattering phases which are different in the $\frac{1}{2}^-$ and $\frac{3}{2}^-$ states, $\delta_{1/2}(\omega)$ and $\delta_{3/2}(\omega)$:

$$\frac{1}{2M_{\Omega_0}} \langle (\Omega_0\pi)_j | A | \Omega_0(0) \rangle \propto |A| e^{i\delta_j(\omega)} \quad (97)$$

for arbitrary operator A . These phases, strictly speaking, should be included into $\tau_{1/2}(\omega)$ and $\tau_{3/2}(\omega)$. The FSI phases also depend on the isospin state, $I = \frac{1}{2}$ or $I = \frac{3}{2}$, but we now abstract from the light flavor symmetries.

The scattering phases emerge via iterations of the Ω_0 -pion interaction along with renormalization of the coupling constant, and they must vanish in the limit of small pion four-momentum due to the pseudoscalar nature of the interaction. This fixes the physical value of the coupling as its value renormalized at the threshold. We identify this coupling with the one in the ‘bare’ chiral Lagrangian Eq. (92). Although the higher-order terms in pion momentum, including both scattering phases, can formally be obtained in perturbation theory in $g_{B^*B\pi}$ from the Yukawa-type Lagrangian in Eq. (92), this would make no sense for a number of evident physical reasons. What is relevant here is that even a naive perturbative expansion yields different scattering phases $\delta_{1/2}(\omega)$ and $\delta_{3/2}(\omega)$.

The net effect of FSI is to introduce an effective phase $e^{i\delta_j(\omega)}$ in τ_j and to replace the threshold $g_{B^*B\pi}$ in Eq. (96) by an energy-dependent coupling. In principle, the phases together with the couplings are constrained by analyticity of the amplitude and its unitarity property which are restrictive before the higher thresholds open. However, these may not fix the amplitude completely since the resulting relations are not local in energy and depend on the multiparticle domain. Likewise, the solution generically admits resonances in a particular channel whose number, position in energy and residues may vary.

We shall neglect all such effects in what follows, assuming that the bulk of them is included in the resonance contributions, and subtracting the latter largely results in an effective cutoff of the soft-pion amplitudes at a certain scale near or below the lowest resonance. In particular, we attribute the difference between the $\frac{1}{2}^-$ and $\frac{3}{2}^-$ channels to the resonant states.

Next on our list is $L=1$ producing the true $\frac{1}{2}^+$ radial and $\frac{3}{2}^+$ states; in our treatment they will again appear along with the $\frac{5}{2}^+$ ‘D-wave’ states. For the heavy quark expansion

we need to calculate the matrix elements for the operator with two derivatives,

$$\frac{1}{2M_{\Omega_0}} \langle \Omega_0 \pi | \bar{Q} i D_j i D_l Q | \Omega_0(0) \rangle, \quad (98)$$

contracted with δ_{jl} , ϵ_{mjl} and $(\delta_{mj}\delta_{nl} + \delta_{ml}\delta_{nj} - \frac{2}{3}\delta_{mn}\delta_{jl})$ to yield the spin-0, spin-1 and spin-2 operators, respectively.

To evaluate the pole diagrams for them we need the couplings analogous to Eq. (93), at zero momentum transfer. These expectation values, however, are required over the heavy hadron moving with a small momentum of order $\omega \sim \mu_{\text{hadr.}}$. They are related by Lorentz invariance to the generic rest frame matrix elements with up to two spatial derivatives. Namely, the matrix elements of a product of any number of full covariant derivatives $m_Q v_\mu + \pi_\mu$ form a Lorentz tensor of the corresponding rank, and its value in an arbitrary frame is obtained, regardless of m_Q , from the rest frame components by the corresponding Lorentz transformation. In the case at hand we get

$$\begin{aligned} \frac{1}{2M_{\Omega_0}} \langle \Omega_0(\vec{p}) | \bar{Q} \vec{\pi}^2 Q | \Omega_0(\vec{p}) \rangle &= (\vec{p}^2 + \mu_\pi^2) \Psi_0^\dagger \Psi_0, \\ \frac{1}{2M_{\Omega_0}} \langle \Omega_0(\vec{p}) | \bar{Q} (\pi_j \pi_l - \pi_l \pi_j) Q | \Omega_0(\vec{p}) \rangle &= -\frac{\mu_G^2}{3} \Psi_0^\dagger \sigma_{jl} \Psi_0, \\ \frac{1}{2M_{\Omega_0}} (\delta_{mj}\delta_{nl} + \delta_{ml}\delta_{nj} - \frac{2}{3}\delta_{mn}\delta_{jl}) \langle \Omega_0(\vec{p}) | \bar{Q} \pi_j \pi_l Q | \Omega_0(\vec{p}) \rangle &= (2p_m p_n - \frac{2}{3}\delta_{mn} \vec{p}^2) \Psi_0^\dagger \Psi_0. \end{aligned} \quad (99)$$

Additional p -independent terms are absent since no spin-2 or higher current can be constructed with a spin- $\frac{1}{2}$ particle at rest. Similar relations hold for any higher order product as well; basically, the result for a non-zero momentum is obtained by incrementing each $\vec{\pi}$ by \vec{p} :

$$\langle \Omega_0(\vec{p}) | \bar{Q} \pi_{j_1} \dots \pi_{j_k} Q | \Omega_0(\vec{p}) \rangle = \langle \Omega_0(\vec{p}=0) | \bar{Q} (\pi_{j_1} + p_{j_1}) \dots (\pi_{j_k} + p_{j_k}) Q | \Omega_0(\vec{p}=0) \rangle. \quad (100)$$

Otherwise the calculation of the transition amplitude proceeds exactly like for P -waves and yields

$$\frac{1}{2M_{\Omega_0}} \langle \Omega_0 \pi | \bar{Q} \pi_j \pi_l Q | \Omega_0(0) \rangle = g_{B^* B \pi} \frac{1}{\omega} \Psi_0^\dagger i \left(\frac{\mu_G^2}{3} (k_j \sigma_l - k_l \sigma_j) + (\vec{\sigma} \vec{k}) k_j k_l \right) \Psi_0. \quad (101)$$

The amplitude above calculated for spin-0 and spin-1 operators has a nontrivial ‘diagonal’ Ω_0 matrix element at rest, with the diagram **a)** not vanishing. The ‘diagonal’ piece of the matrix elements in Eqs. (99) (in this case it is the value at $\vec{p}=0$) is independent of the momentum. The propagators in diagrams **a)** and **b)** have opposite sign; this contribution then enters universally as a commutator with the pion interaction Hamiltonian, in accord with stationary perturbation theory:

$$A_{mn} = \frac{[\delta \mathcal{H}, \mathcal{H}]_{mn}}{(E_m - E_n)^2}. \quad (102)$$

For instance, the kinetic expectation value μ_π^2 always drops out, but a contribution remains proportional to the chromomagnetic interaction μ_G^2 which does not commute with the spin-dependent pion vertex. This yields the most IR-singular contribution for a soft pion due to the double pole in Eq. (102).

Strictly speaking, the pole diagrams with virtual Ω_0 – they have a pole at $\omega=0$ (\vec{k} is assumed to be fixed, and the overall \vec{k} from the pion interaction is factored out) – does not describe the pion emission amplitude completely. It contains a piece finite at $\omega=0$ coming from the contact interactions, see Fig. 12c. These contact vertices assume some values in QCD; we only know they are proportional to \vec{k} since the heavy quark operators we consider are chirally sterile so that their (light flavor) axial charge vanishes:

$$\lim_{k_\mu \rightarrow 0} \langle \Omega_0 \pi^a(k) | \bar{Q} i D_j i D_l Q | \Omega_0 \rangle = -\frac{1}{F_\pi} \int d^3x \langle \Omega_0 \pi^a | [\bar{Q} i D_j i D_l Q(0), J_0^{5(a)}(0, \vec{x})] | \Omega_0 \rangle = 0. \quad (103)$$

Otherwise they are arbitrary, and we can only parameterize them by four constants of dimension mass:

$$\begin{aligned} \frac{1}{g_{B^*B\pi}} \langle \Omega_0 \pi | \bar{Q} i D_j i D_l Q | \Omega_0 \rangle = & \alpha \Psi_0^\dagger (k_j \sigma_l - k_l \sigma_j) \Psi_0 + \beta i \epsilon_{jlm} k_m \Psi_0^\dagger \Psi_0 + \gamma \delta_{jl} \Psi_0^\dagger i \vec{\sigma} \vec{k} \Psi_0 + \\ & \tau i \Psi_0^\dagger (\sigma_j k_l + \sigma_l k_j - \frac{2}{3} \delta_{jl} \vec{\sigma} \vec{k}) \Psi_0, \end{aligned} \quad (104)$$

plus higher terms in k . Such terms are induced, in particular, by intermediate excited heavy quark meson resonance states propagating in diagrams Fig. 12, a), b), with their relative size depending on spin. Unequal meson-to-pion couplings in Sect. 5.2 correspond to particular values of the constants α to γ ; based on the QCD sum rule analysis Ref. [22] they appear large. While these terms are parametrically smaller than the pole amplitudes for small pion momenta, in general they contribute, especially the quantities regular in the chiral limit.

There are also terms next order in p_π/μ_{hadr} . They would have the same scaling as the last term in Eq. (101). Nevertheless, we shall neglect them in what follows when address the pion loop effects proper: we relegate the corresponding contributions to the effects of resonances. This parallels the pole-dominance assumption employed in the calculation of the $D^{(*)}\pi$ amplitudes in Sect. 5.2, however the Z -diagrams included in the relativistic propagators of intermediate B^* and D^* mesons also induce such terms. If an argument can be put forward that one should retain only the D^* or B^* in the normal diagrams, there is no physical reason to exclude the higher states in the Z -diagrams: they all have the same large virtuality. Therefore, it may be natural to assume that in aggregate the Z -induced contact terms are suppressed or vanish in the nonrelativistic expansion.

The result for the pion loop in $R(\omega)$ takes the following form:

$$\begin{aligned} R_{ijkl}^\pi(\omega) = & \frac{g_{B^*B\pi}^2}{12\pi^2} \theta(\omega - m_\pi) \frac{|\vec{k}|^3}{\omega^2} \Psi_0^\dagger \left[\frac{(\mu_G^2)^2}{9} (2\delta_{ik}\delta_{jl} - 2\delta_{il}\delta_{jk} + \delta_{ik}\sigma_{jl} + \delta_{jl}\sigma_{ik} - \delta_{il}\sigma_{jk} - \delta_{jk}\sigma_{il}) \right. \\ & \left. + \frac{\mu_G^2}{3} \frac{2\vec{k}^2}{5} (\delta_{ik}\sigma_{jl} - \delta_{kl}\sigma_{ij} + \delta_{ij}\sigma_{kl} - \delta_{jl}\sigma_{ik}) + \frac{\vec{k}^4}{5} (\delta_{ij}\delta_{kl} + \delta_{ik}\delta_{jl} + \delta_{il}\delta_{jk}) \right] \Psi_0. \end{aligned} \quad (105)$$

This can be decomposed into the invariant structures; introducing the common factor

$$W \equiv \frac{g_{B^*B\pi}^2}{12\pi^2} \theta(\omega - m_\pi)$$

we get

$$\begin{aligned} \rho_p^{(\frac{1}{2}^+)}(\omega) &= W \frac{3|\vec{k}|^7}{\omega^2}, & \rho_{pg}^{(\frac{1}{2}^+)}(\omega) &= -W \frac{4\mu_G^2|\vec{k}|^5}{\omega^2}, & \rho_g^{(\frac{1}{2}^+)}(\omega) &= W \frac{16(\mu_G^2)^2|\vec{k}|^3}{3\omega^2}, \\ \rho_f^{(\frac{3}{2}^+)}(\omega) &= W \frac{16|\vec{k}|^7}{\omega^2}, & \rho_{fg}^{(\frac{3}{2}^+)}(\omega) &= W \frac{8\mu_G^2|\vec{k}|^5}{3\omega^2}, & \rho_g^{(\frac{3}{2}^+)}(\omega) &= W \frac{16(\mu_G^2)^2|\vec{k}|^3}{9\omega^2}, \\ \rho^{(\frac{5}{2}^+)}(\omega) &= W \frac{2|\vec{k}|^7}{5\omega^2}. \end{aligned} \quad (106)$$

The factorization properties stated in Sect. 6.1.1 are manifest here.

For practical applications it is important to include in the amplitude the next-to-leading ‘contact’ terms described by α, β and γ in Eq. (104); they can actually be derived in a model-independent way and do not depend on the form of the resonance ansatz. Calculating the full $R_{ijkl}^\pi(\omega)$ with them is straightforward, but we postpone it to future work.

The above calculation of the pion loop can be readily generalized to higher-dimensional heavy quark momentum operators, including the case of different number of derivatives in the two vertices. The expressions are particularly simple where no timelike momentum or antisymmetric spatial indices are involved; then the corresponding vertices simply amount to products of pion momentum and the resulting integrals can be simply calculated.

We now return to our practical need. We are concerned with only the zero-momentum correlators of the $1/m_Q$ -terms in the heavy quark Lagrangian, and we use the above derived spectral densities to estimate

$$\delta\rho_{\pi\pi}^3 \approx 0.02 \text{ GeV}^3, \quad \delta\rho_{\pi G}^3 \approx 0.065 \text{ GeV}^3, \quad \delta\rho_S^3 = \delta\rho_A^3 \approx 0.03 \text{ GeV}^3, \quad (107)$$

and

$$\delta\tilde{\rho}_{\pi\pi}^3 \approx 0.03 \text{ GeV}^2, \quad \delta\tilde{\rho}_{\pi G}^3 \approx 0.1 \text{ GeV}^2, \quad \delta\tilde{\rho}_S^3 = \delta\tilde{\rho}_A^3 \approx 0.07 \text{ GeV}^2, \quad (108)$$

where we have assumed the upper cutoff at $\omega = 700 \text{ MeV}$ and have adopted $g_{B^*B\pi} = 4 \text{ GeV}^{-1}$. The loops with charged and neutral pions are included, but not the kaon and η contributions. Of special interest is the ‘hyperfine’ combination of Eq. (78) for which we get

$$\delta(-\rho_{\pi G}^3 - \rho_A^3) \approx -0.09 \text{ GeV}^3; \quad (109)$$

as expected, the pion contribution is suppressed, but it is negative and, taken at face value, would strengthen the lower bound on the resonant contributions. This is due to the positive sign of $\delta\rho_{\pi G}^3$, opposite to the BPS regime.

With the same choice for $g_{B^*B\pi}$ we would have

$$\begin{aligned} \delta\varrho^2 &\approx 0.015 \left(\frac{\omega_{\max}}{0.5 \text{ GeV}} \right)^2, & \delta\bar{\Lambda} &\approx \left(\frac{\omega_{\max}}{0.5 \text{ GeV}} \right)^3 10 \text{ MeV}, \\ \delta\mu_\pi^2 &\approx \left(\frac{\omega_{\max}}{0.5 \text{ GeV}} \right)^4 0.006 \text{ GeV}^2, & \delta\rho_D^3 &\approx \left(\frac{\omega_{\max}}{0.5 \text{ GeV}} \right)^5 0.0025 \text{ GeV}^3 \end{aligned} \quad (110)$$

where we have anticipated a lower effective cutoff in the P -wave channel (the spin-triplet counterparts are not affected). We see that generally the pion loop contributes only a small fraction of the nonlocal correlators and a tiny amount of the local expectation values. A possible exception are quantities vanishing in the BPS limit where the pion loop may constitute a significant part of the deviation.

The first calculation [33] of the chiral correction to the formfactor to order $1/m_Q^2$ accounted for the terms proportional to $(\mu_G^2)^2$ from the HQS-breaking masses in the meson propagators and picked up only the $\tilde{\rho}_S^3$ and $\tilde{\rho}_A^3$ pieces in Eq. (108), yet leaves out $\tilde{\rho}_{\pi\pi}^3$ and $\tilde{\rho}_{\pi G}^3$. We see, however that the latter contribution has the same size even though it is not singular in the chiral limit.

One can combine the above description of the nonresonant $D^{(*)}\pi$ states with the method of Sect. 6.3.2 for the inclusive yield, to get an estimate of the total continuum contribution to the inclusive yield. To that end one only needs to integrate the expressions in Eq. (106) over the mass of the $\Omega_0\pi$ state; due to the strong phase-space suppression the integral is effectively cut off at relatively soft pions. In this way we arrive at the yield in the ball park of 1% of Γ_{sl} . This, however, refers to only the specified j^P of the $D^{(*)}\pi$ states. The P -wave continuum is an independent channel.

6.5 Nonfactorizable contributions to higher-dimensional local expectation values

The size of the expectation values of local heavy quark operators of $D = 7$ and $D = 8$ is important to estimate the impact of higher-order power corrections both in beauty and charm, to assess the accuracy of the OPE predictions and to study the convergence of the OPE series. The relevant operators here are those which emerge in the calculation of power corrections at tree level; they are sometimes called ‘color-through’ operators. Ref. [3] illustrated their effect in inclusive B decays for the semileptonic $b \rightarrow c$ transitions and for $B \rightarrow X_s + \gamma$ used in measuring $|V_{cb}|$. They have also appeared in Sect. 4 in our analysis of $B \rightarrow D^* \ell \nu$ at zero recoil.

In order to estimate the significance of the expectation values a ground-state factorization method has been devised in Ref. [3] which contains a derivation of the formalism and the explicit expressions for the factorization contributions to all nine dimension-7, m_{1-9} , and eighteen dimension-8, r_{1-18} , B -meson expectation values. Using the intermediate state saturation representation of Ref. [3] together with the relations elaborated in the previous sections we can now supplement the ground-state factorization values with the contributions from the excited states: the analysis of hyperfine splitting allows to quantify their effect. This enables us to assess the accuracy of the factorization ansatz, the potential scale of the corrections to factorization and, ultimately, may elucidate the pattern of the higher-order effects in a more quantitative manner.

Once again we start with infinitely heavy spinless quarks. The intermediate state representation for the operators with four spatial derivatives reads

$$\frac{1}{2M_Q} \langle \Omega_0 | Q^\dagger \pi_i \pi_j \pi_k \pi_l Q(0) | \Omega_0 \rangle = \int d\omega R_{ijkl}(\omega), \quad (111)$$

with $R_{ijkl}(\omega)$ introduced in Eq. (47). The factorization contribution is located at $\omega = 0$; the upper limit of integration over ω is determined by the normalization point assumed for the operator. The non-factorized pieces take a different form for each class of intermediate states.

Contracting indices in $R_{ijkl}(\omega)$ and multiplying the tensor, for the spin-triplet operators, by the spin matrix with an appropriate index, we obtain for the actual B mesons

$$\begin{aligned}
\delta^{\text{nf}} m_1 &= \frac{5}{9} \rho_p^{(\frac{1}{2}^+)} + \frac{1}{30} \rho_f^{(\frac{3}{2}^+)} + 2 \rho^{(\frac{5}{2}^+)} & \delta^{\text{nf}} m_3 &= -\frac{2}{3} \rho_g^{(\frac{1}{2}^+)} - \rho_g^{(\frac{3}{2}^+)} \\
\delta^{\text{nf}} m_4 &= \frac{4}{3} \rho_p^{(\frac{1}{2}^+)} + \rho_g^{(\frac{1}{2}^+)} - \frac{1}{10} \rho_f^{(\frac{3}{2}^+)} + \frac{3}{2} \rho_g^{(\frac{3}{2}^+)} - 6 \rho^{(\frac{5}{2}^+)} \\
\delta^{\text{nf}} m_6 &= \frac{2}{3} \rho_g^{(\frac{1}{2}^+)} - \frac{1}{4} \rho_g^{(\frac{3}{2}^+)} & \delta^{\text{nf}} m_7 &= -\frac{8}{3} \rho_{pg}^{(\frac{1}{2}^+)} - 2 \rho_{fg}^{(\frac{3}{2}^+)} \\
\delta^{\text{nf}} m_8 &= -8 \rho_{pg}^{(\frac{1}{2}^+)} \\
\delta^{\text{nf}} m_9 &= -\frac{10}{3} \rho_{pg}^{(\frac{1}{2}^+)} + \rho_g^{(\frac{1}{2}^+)} - \frac{3}{20} \rho_f^{(\frac{3}{2}^+)} - \rho_{fg}^{(\frac{3}{2}^+)} - \frac{3}{4} \rho_g^{(\frac{3}{2}^+)} + 6 \rho^{(\frac{5}{2}^+)}.
\end{aligned} \tag{112}$$

In the above equations the integration over ω is assumed, it has not been shown explicitly for compactness. We remind that m_2 and m_5 are given by the fourth moment of the standard SV (P -wave) structure functions and have no conventional ground-state factorizable contributions.

For numeric estimates one simply considers the contributions of the individual multiplets of the excited states using their spectral densities in Eq. (61). The contribution of $\frac{1}{2}^+$ is obvious beforehand: it follows the factorizable one, see Ref. [3], and only requires to replace $(\mu_\pi^2)^2$ by P^2 , $(\mu_G^2)^2$ by G^2 and $\mu_\pi^2 \mu_G^2$ by PG . The effect of the higher-spin states has a different structure. Since the basis $\{m_1 - m_9\}$ has been selected arbitrarily, the impact of nonfactorizable contributions should be gauged in specific cases; this is easily done based on Eqs. (112).

To quantify the overall scale of the effect we consider here three representative combinations M_1, M_2, M_3 corresponding to the expectation values $\bar{b} \vec{\pi}^2 \vec{\pi}^2 b$, $\bar{b}(\vec{\sigma} \vec{B})(\vec{\sigma} \vec{B})b$ and $-\bar{b}(\vec{\sigma} \vec{B}) \vec{\pi}^2 b$, respectively:

$$M_1 = m_1 + \frac{1}{2} m_3 + \frac{1}{3} m_4, \quad M_2 = -m_3, \quad M_3 = -\frac{1}{8} m_8, \tag{113}$$

for which we have

$$\begin{aligned}
M_1 &= (\mu_\pi^2)^2 + \int d\omega \rho_p^{(\frac{1}{2}^+)}(\omega) \\
M_2 &= \frac{2}{3} (\mu_G^2)^2 + \int d\omega \left(\frac{2}{3} \rho_g^{(\frac{1}{2}^+)}(\omega) + \rho_g^{(\frac{3}{2}^+)}(\omega) \right) \\
M_3 &= \mu_\pi^2 \mu_g^2 + \int d\omega \rho_{pg}^{(\frac{1}{2}^+)}(\omega).
\end{aligned} \tag{114}$$

Numerically the corrections depend to some extent on the ratio of the $\frac{3}{2}^+$ and $\frac{1}{2}^+$ contributions and on P/G in the latter. Taking, for instance, $\varepsilon_{\text{rad}} \approx 700 \text{ MeV}$, $\int d\omega \rho_g^{(\frac{1}{2}^+)}(\omega) \approx$

$\int d\omega \rho_{pg}^{(\frac{1}{2}^+)}(\omega) \approx \int d\omega \rho_g^{(\frac{3}{2}^+)}(\omega)$ ($P \approx G$, see Sect. 6.3) and using the hyperfine constraint Eq. (80) with $\kappa \approx -0.2$ we obtain

$$\begin{aligned} M_1 &\approx 0.2 \text{ GeV}_{\text{fact}}^4 + 0.17 \text{ GeV}_{\text{n-fact}}^4 \\ M_2 &\approx 0.08 \text{ GeV}_{\text{fact}}^4 + 0.28 \text{ GeV}_{\text{n-fact}}^4 \\ M_3 &\approx 0.15 \text{ GeV}_{\text{fact}}^4 + 0.17 \text{ GeV}_{\text{n-fact}}^4. \end{aligned} \quad (115)$$

A more definite value is obtained for the special combination

$$-\frac{1}{5}m_3 - \frac{6}{5}m_6 - \frac{1}{4}m_8$$

which has the same structure as the hyperfine constraint; here we get

$$-\frac{1}{5}m_3 - \frac{6}{5}m_6 - \frac{1}{4}m_8 \simeq -\frac{2}{3}(\mu_G^2)^2 + 2\mu_\pi^2\mu_G^2 - \varepsilon_{\text{rad}}(\rho_{\pi G}^3 + \rho_A^3) \approx (0.23 + 0.32_{\text{nf}}) \text{ GeV}^4. \quad (116)$$

From this brief comparison we conclude that the factorization ansatz generally provides no more than a reasonable starting approximation for the expectation values not affected by cancellations.

The hyperfine constraint and the approximations we complemented it with have nothing to say about the contribution of spin- $\frac{5}{2}$ states which require a different theoretical input. Positivity and various relations between different nonfactorizable contributions are implicit in Eqs. (112); these constraints should, in principle, be applied only after the contributions from the non-resonant continuum are subtracted.

The $D=8$ operators with five derivatives were found to contribute at a lower level to the inclusive moments in B decays [3]; their precise expectation values are therefore less important in practice. Nevertheless, in this case it would also be useful to have at least a crude estimate of the potential error in the factorization ansatz, to be more confident in the assessment of the impact of $1/m_Q^5$ terms.

The nonfactorizable effects for the $D=8$ operators can be analyzed along the same lines as the $D=7$ operators, identifying iD_0 adjacent to the intermediate state in question with $-\varepsilon$. Most notably, the excited states contribute to a few combinations of r_i which vanish in the ground-state factorization:

$$\begin{aligned} r_5 &= -\omega \rho_p^{(\frac{1}{2}^+)}(\omega) \approx -0.13 \text{ GeV}^5 & r_{15} &= -\omega \frac{1}{2} \rho_{pg}^{(\frac{1}{2}^+)}(\omega) \approx -0.06 \text{ GeV}^5 \\ r_6 - r_1 &= -\omega \left(\frac{1}{3} \rho_p^{(\frac{1}{2}^+)} + \frac{1}{6} \rho_g^{(\frac{1}{2}^+)} + \frac{1}{20} \rho_f^{(\frac{3}{2}^+)} + \frac{1}{4} \rho_g^{(\frac{3}{2}^+)} + 3\rho^{(\frac{5}{2}^+)} \right) \\ r_7 &= -\omega \left(\frac{1}{3} \rho_p^{(\frac{1}{2}^+)} - \frac{1}{6} \rho_g^{(\frac{1}{2}^+)} + \frac{1}{20} \rho_f^{(\frac{3}{2}^+)} - \frac{1}{4} \rho_g^{(\frac{3}{2}^+)} + 3\rho^{(\frac{5}{2}^+)} \right) \\ r_{16} &= -\omega \left(-\frac{2}{3} \rho_{pg}^{(\frac{1}{2}^+)} - \frac{1}{6} \rho_g^{(\frac{1}{2}^+)} - \frac{3}{40} \rho_f^{(\frac{3}{2}^+)} - \frac{1}{2} \rho_{fg}^{(\frac{3}{2}^+)} + \frac{1}{8} \rho_g^{(\frac{3}{2}^+)} + 3\rho^{(\frac{5}{2}^+)} \right) \\ r_{17} - r_8 &= -\omega \left(\frac{2}{3} \rho_{pg}^{(\frac{1}{2}^+)} - \frac{1}{6} \rho_g^{(\frac{1}{2}^+)} - \frac{3}{40} \rho_f^{(\frac{3}{2}^+)} + \frac{1}{2} \rho_{fg}^{(\frac{3}{2}^+)} + \frac{1}{8} \rho_g^{(\frac{3}{2}^+)} + 3\rho^{(\frac{5}{2}^+)} \right) \\ r_{18} &= -\omega \left(\frac{1}{6} \rho_g^{(\frac{1}{2}^+)} - \frac{3}{40} \rho_f^{(\frac{3}{2}^+)} - \frac{1}{8} \rho_g^{(\frac{3}{2}^+)} + 3\rho^{(\frac{5}{2}^+)} \right). \end{aligned} \quad (117)$$

In the above equations the integration over ω is again assumed; the numeric estimates for r_5 and r_{15} are obtained under the same assumptions as Eqs. (115).

The most general analysis of the nonfactorizable corrections for the other operators (except for r_1 and r_8 given by the fifth moment of the generalized SV structure functions) requires considering

$$\tilde{R}_{ijkl}(\omega) = \frac{1}{2\pi} \int d^3x \int dx_0 e^{-i\omega x_0} \frac{1}{2M_Q} \langle \Omega_0 | Q^\dagger \pi_i \pi_j Q(x) Q^\dagger \pi_k \pi_0 \pi_l Q(0) | B \rangle \quad (118)$$

which is an analogue of the tensor spectral density $R_{ijkl}(\omega)$ in Eq. (47). One of the operators now includes an extra time derivative. The corresponding decomposition is lengthier than Eq. (48) since there is no symmetry between pairs of indices. The factorization of Eqs. (61) is modified for the new invariant structures: along with the transition matrix elements in Eqs. (58), (59) and (60) we need to introduce the similar ones $\tilde{P}, \tilde{G}, \tilde{f}, \tilde{g}$ and \tilde{h} for the operators $\bar{Q} \pi_l \pi_0 \pi_l Q$ (it is assumed that π_0 acts on the right which matters for non-diagonal matrix elements). The analogue of Eq. (111) for the operators with five derivatives in terms of $\tilde{R}_{ijkl}(\omega)$ holds and the general relations for the remaining r_i similar to Eqs. (112) or (114) can readily be derived.

The hyperfine splitting constraint cannot, however be directly applied to $\tilde{R}_{ijkl}(\omega)$ and the corresponding tilded residues remain largely unconstrained even in the single excited multiplet approximation. The BPS approximation in this case yields $\tilde{P} = \tilde{G}$ and $\tilde{f} = \tilde{g}$, but it is not too helpful. Therefore we do not quote here the corresponding expressions.

It is nevertheless possible to get a rough estimate by making the assumption that the first P -wave excitation(s) approximately saturate, as an intermediate state, the transition amplitudes into the radial or the D -wave states:

$$\langle \rho | \pi_j \pi_0 \pi_k | \Omega_0 \rangle \approx \langle \rho | \pi_j | P_{\frac{3}{2}}^{(1)} \rangle \langle P_{\frac{3}{2}}^{(1)} | \pi_0 \pi_k | \Omega_0 \rangle + \langle \rho | \pi_j | P_{\frac{1}{2}}^{(1)} \rangle \langle P_{\frac{1}{2}}^{(1)} | \pi_0 \pi_k | \Omega_0 \rangle, \quad (119)$$

where ρ generically refers to the $\frac{1}{2}^+$, $\frac{3}{2}^+$ or $\frac{5}{2}^+$ states under consideration. This can also be regarded as an approximate relation obtained by truncating the complete representation

$$\pi_j | \Omega_0 \rangle = \sum_m \sqrt{3} \epsilon_m \tau_{3/2}^{(m)} | \chi^{(m)} \rangle_j + \sum_n \epsilon_n \tau_{1/2}^{(n)} \sigma_j | \phi^{(k)} \rangle \approx \sqrt{3} \epsilon_{3/2}^{(1)} \tau_{3/2}^{(1)} | \chi^{(1)} \rangle_j + \epsilon_{1/2}^{(1)} \tau_{1/2}^{(1)} \sigma_j | \phi^{(1)} \rangle \quad (120)$$

after the lowest P -wave families. Such an assumption seems to work satisfactorily for the transition between the ground states, yet may be expected to degrade with higher initial and/or final states. Identifying $\epsilon_{1/2}$ and $\epsilon_{3/2}$ with $\tilde{\epsilon}$ this would yield

$$\tilde{P} \approx -\tilde{\epsilon} P, \quad \tilde{G} \approx -\tilde{\epsilon} G, \quad \tilde{f} \approx -\tilde{\epsilon} f, \quad \tilde{g} \approx -\tilde{\epsilon} g, \quad \tilde{h} \approx -\tilde{\epsilon} h \quad (121)$$

for individual residues, and

$$\tilde{\rho}^{(\frac{l}{2}^+)} \approx -\tilde{\epsilon} \rho^{(\frac{l}{2}^+)} \quad (122)$$

for all invariant tensor structures with $l=1$ and $l=3$, and, most generally,

$$\tilde{R}_{ijkl}(\omega) \approx -\tilde{\epsilon} \cdot R_{ijkl}(\omega). \quad (123)$$

Adopting for orientation such an approximation we obtain

$$\begin{aligned}
\delta^{\text{nf}} r_2 &\approx -\tilde{\epsilon} \rho_p^{(\frac{1}{2}^+)} \approx -0.07 \text{ GeV}^5 \\
\delta^{\text{nf}} r_3 &\approx -\tilde{\epsilon} \left(\frac{1}{3} \rho_p^{(\frac{1}{2}^+)} - \frac{1}{6} \rho_g^{(\frac{1}{2}^+)} + \frac{1}{20} \rho_f^{(\frac{3}{2}^+)} - \frac{1}{4} \rho_g^{(\frac{3}{2}^+)} + 3 \rho^{(\frac{5}{2}^+)} \right) \\
\delta^{\text{nf}} r_4 &\approx -\tilde{\epsilon} \left(\frac{1}{3} \rho_p^{(\frac{1}{2}^+)} + \frac{1}{6} \rho_g^{(\frac{1}{2}^+)} + \frac{1}{20} \rho_f^{(\frac{3}{2}^+)} + \frac{1}{4} \rho_g^{(\frac{3}{2}^+)} + 3 \rho^{(\frac{5}{2}^+)} \right) \\
\delta^{\text{nf}} r_9 &\approx \delta^{\text{nf}} r_{10} \approx -\tilde{\epsilon} \rho_{pg}^{(\frac{1}{2}^+)} \approx -0.07 \text{ GeV}^5 \\
\delta^{\text{nf}} r_{11} &\approx \delta^{\text{nf}} r_{12} \approx -\tilde{\epsilon} \left(\frac{1}{6} \rho_g^{(\frac{1}{2}^+)} - \frac{3}{40} \rho_f^{(\frac{3}{2}^+)} - \frac{1}{8} \rho_g^{(\frac{3}{2}^+)} + 3 \rho^{(\frac{5}{2}^+)} \right) \\
\delta^{\text{nf}} r_{13} &\approx -\tilde{\epsilon} \left(-\frac{2}{3} \rho_{pg}^{(\frac{1}{2}^+)} - \frac{1}{6} \rho_g^{(\frac{1}{2}^+)} - \frac{3}{40} \rho_f^{(\frac{3}{2}^+)} - \frac{1}{2} \rho_{fg}^{(\frac{3}{2}^+)} + \frac{1}{8} \rho_g^{(\frac{3}{2}^+)} + 3 \rho^{(\frac{5}{2}^+)} \right) \\
\delta^{\text{nf}} r_{14} &\approx -\tilde{\epsilon} \left(\frac{2}{3} \rho_{pg}^{(\frac{1}{2}^+)} - \frac{1}{6} \rho_g^{(\frac{1}{2}^+)} - \frac{3}{40} \rho_f^{(\frac{3}{2}^+)} + \frac{1}{2} \rho_{fg}^{(\frac{3}{2}^+)} + \frac{1}{8} \rho_g^{(\frac{3}{2}^+)} + 3 \rho^{(\frac{5}{2}^+)} \right) \quad (124)
\end{aligned}$$

where the integration over ω is assumed similar to Eqs. (112). Taking $\tilde{\epsilon} \approx 400 \text{ MeV}$ the numerical estimates for the relevant combinations of the expectation values are then as straightforward as those for the $D = 7$ operators. The nonfactorizable corrections to the typical non-suppressed expectation values are of the order of 50 to 100%.

Bearing in mind the dependence of all the contributions on a few poorly known hadronic parameters we cannot regard the calculation of general nonfactorizable effects accurate. They should be used primarily to assess the potential scale of the corrections to factorization and to clarify the expected sign pattern. The corrections associated with the $\frac{5}{2}^+$ states, for instance in $\langle \vec{\pi}^2 \vec{\pi}^2 \rangle$ or in $\langle \vec{\pi}^2 \pi_0 \vec{\pi}^2 \rangle$ are largely unconstrained since only physics related to the $\frac{1}{2}^+$ and $\frac{3}{2}^+$ have been considered.

The formalism employed in this subsection could be used together with the results of Sec. 6.4 to find the nonfactorizable contributions due to non-resonant states composed of the ground-state multiplet and a pion. However, we expect these contributions to be relatively small, as they come with higher powers of the excitation energy which is lower for the soft pion continuum than for the principal resonances, and therefore we do not consider them here.

6.5.1 Ground-state factorization and N_c

The expectation values like $\langle \bar{Q} \vec{\sigma} \cdot \vec{B} \times \vec{B} Q \rangle$ or $\langle \bar{Q} \vec{\sigma} \cdot \vec{E} \times \vec{E} Q \rangle$ are possible due to the non-Abelian nature of QCD; in the factorization approximation they are proportional to $\frac{2}{3}(\mu_G^2)^2$ or to $-\tilde{\epsilon}^2 \mu_G^2$. Such expectation values must vanish, on the other hand, in the bound states of Abelian theories like QED. In QCD proper one can consider similar time correlators for the usual magnetic and/or electric fields; they would enter, for instance, the electromagnetic corrections. The correlators can be decomposed into the same set of invariant spectral densities with different residues. For such Abelian fields certain expectation values must vanish

reflecting the commutativity of the different components of the Abelian field strength. For instance, this is the case for the counterpart of the ρ_A^3 structure:

$$\int_{\omega>0} d\omega \rho_A^{\text{Abel}} = \int_{\omega>0} d\omega \left(\frac{2}{3} \rho_{g,\text{Abel}}^{(\frac{1}{2}^+)} - \frac{1}{2} \rho_{g,\text{Abel}}^{(\frac{3}{2}^+)} \right) = -\frac{2(\mu_{G,\text{Abel}}^2)^2}{3} \quad (125)$$

must hold for the Abelian analogies of the spectral densities and of the B -meson local expectation values. This may be reminiscent of Eqs. (67), but is more general. Such a sum rule shows that the ground-state saturation itself may not be a universally applicable approximation. Eq. (125) may even be regarded as an indication of the importance of the $\frac{3}{2}^+$ state.

In actual QCD such local antisymmetric products of the gluon field strength do not need to vanish; all the considered correlators and the factorized pieces count as constants in the large- N_c limit. One may think that the ground-state factorization approximation is generally representative at not too small N_c .

6.5.2 Perturbative normalization point dependence

Having at our disposal the perturbative heavy quark spectral functions of Eqs. (A.22) and (A.17) we can easily incorporate the leading powerlike mixing for the operators to order α_s and to any BLM order using the preceding analysis. The corrections to the expectation values are obtained from Eqs. (112), (117), etc.; the B -meson spectral densities themselves are given by Eqs. (67). This gives the one-loop renormalization-scale evolution of the expectation values, except for the scale-dependence of the factorizable contributions themselves, like $(\mu_\pi^2(\mu))^2$, which in practice may be significant.

As a typical example, the one-loop and two-loop BLM piece in the combination M_2 in Eqs. (114) is

$$M_2^{\text{pert}}(\mu) = C_F \frac{\alpha_s(\bar{M})}{\pi} \mu^4 \left[1 + \frac{\beta_0 \alpha_s}{2\pi} \left(\ln \frac{\bar{M}}{2\mu} + \frac{29}{12} \right) \right], \quad (126)$$

with \bar{M} denoting the normalization scale for α_s (in the $\overline{\text{MS}}$ scheme). It is obtained using Eqs. (A.25). The first-order correction to M_1 vanishes and the second-order term is negative (although quite suppressed).⁸ Of course, the perturbative calculation is meaningful only for not too low values of μ . At a numeric value of the strong coupling such estimates can be used to gauge the relative importance of the scale-dependence effects. The one-loop term with fixed $\alpha_s=0.3$ would yield

$$M_2^{\text{pert}}(0.7 \text{ GeV}) \approx 0.03 \text{ GeV}^4,$$

and is relatively small for μ between 0.7 and 1 GeV.

To extend this to the complete set of $D=8$ operators including those in Eqs. (124) an additional class of the spectral functions would be needed where one of the pair products

⁸This shows a typical problem of applying naive non-Abelization to cases where the order- α_s effect is absent; the full $\mathcal{O}(\alpha_s^2)$ contribution to $\rho_{\pi\pi}^2$ is, of course positive, paralleling the similar term in the Abelian theory.

$\pi_k \pi_l$ is replaced by $\pi_k \pi_0 \pi_l$, cf. Eq. (118). The one-loop answer for it is simple, because the transition amplitude for such operators into a state with a single extra gluon amounts to $-\omega$ times the amplitude for the corresponding operator without extra π_0 :

$$\langle Qg|\bar{Q}\pi_k\pi_0\pi_l Q|Q\rangle = -k_0\langle Qg|\bar{Q}\pi_k\pi_l Q|Q\rangle + \mathcal{O}(g_s^3).$$

In other words, $\tilde{\epsilon} = \omega$ in terms of Eqs. (124) to this accuracy. This exactly parallels the result for the P -wave SV operators. In this way both $\mathcal{O}(\alpha_s)$ and the higher BLM corrections to the mixing are readily obtained for the $D=8$ operators alongside the power mixing for $D=7$.

7 Discussion

7.1 On a resummation of the $1/m_c^k$ corrections

The accuracy in the estimate of $\mathcal{F}(1)$ is limited, in particular, by significant higher-order power corrections in $1/m_c$. We mention here a possibility to consider all these potentially dangerous corrections together and, therefore, in a certain sense, to resum them. The price to pay is the appearance of a limited number of new hadronic expectation values.

The idea is to apply the OPE to the reversed zero-recoil transition $D^* \rightarrow B$ instead of $B \rightarrow D^*$. At first glance this amounts only to exchanging c and b in Eq. (1) and taking the expectation values over the vector rather than pseudoscalar state.⁹ However, the axial $\bar{c}b$ current produces not only B out of D^* , but also B^* . Therefore a scattering amplitude of two arbitrary spatial components j, l should instead be considered, and the corresponding indices contracted with the polarizations of D^* ,

$$\tilde{T}^{\text{zr}}(q_0) = \int d^3x \int dx_0 e^{-iq_0 x_0} \frac{1}{2M_{D^*}} \langle D_j^* | \frac{1}{3} iT \bar{c}\gamma_j \gamma_5 b(x) \bar{b}\gamma_k \gamma_5 c(0) | D_k^* \rangle. \quad (127)$$

The analogue of Eq. (6) will still contain terms with powers of $1/m_c$. However, they only come from the nonrelativistic expansion of the full-QCD charm quark operators $\bar{c}O_k c$, starting with the leading $\bar{c}c$. Consequently, the full set of the $1/m_c^k$ corrections originate from the heavy charm expansion of the finite- m_c expectation value over actual D^* states, $\langle D^* | \bar{c}c | D^* \rangle$. The latter is a physical quantity and can in principle be measured on the lattice. Similarly, for a given power l of $1/m_b$ all the terms $1/m_b^l 1/m_c^k$ come from the heavy charm expansion of the finite- m_c expectation value of the corresponding $\bar{c}c$ operator with l derivatives. Likewise, the $1/m_c$ power effects in the inelastic transition amplitudes combine to yield directly the non-diagonal transition probabilities for the finite- m_c charm states. The nontrivial explicit OPE corrections to the corresponding sum rule may only depend on powers of $1/m_b$ since they come from the dynamic expansion of the intermediate-quark propagator. For what concerns the perturbative corrections, they are the same as in the sum rule Eq. (1), modulo the $m_c \leftrightarrow m_b$ replacement.

⁹The fact that D^* is not a stable particle is not an issue since the width of D^* is extremely small. To completely bypass the complication one may simply assume that the pion mass is a few MeV larger than it is in reality; the properly defined $B \rightarrow D^*$ formfactor may not depend on this.

An attractive element of such an approach is that the m_c -dependence of these matrix elements must be regular in the whole m_c range and it should be possible to construct accurate interpolating functions, which would replace a large number of different coefficients appearing in the expansion in $1/m_c$. Theory-wise, the regularity puts constraints on the higher-order behavior of the $1/m_c$ series and suggests that the series is sign-alternating, implying numerical cancellations between successive orders for actual charm mass.

The series in $1/m_b$ is not resummed in this approach. As was discussed in Sect. 4, numerically these corrections can be discarded to a good approximation, and retaining the known leading $1/m_b^2$ terms for them would be sufficient for all practical purposes.

Guided by the quantum-mechanical interpretation of the sum rules it is not difficult to verify that the leading, $1/m_Q^2$ corrections are identical to those in the direct approach, separately for the local OPE piece and for the inelastic contribution. Therefore the actual difference between the expansions would appear when the higher-order power corrections are addressed.

7.2 Vector formfactor in $B \rightarrow D$ transitions

The present study focused on the $B \rightarrow D^*$ decay mediated by the axial current. A similar analysis may be applied to the $B \rightarrow D$ transitions where only the vector current contributes. Two different aspects can be addressed here.

The direct zero-recoil vector-current analogue F_D of \mathcal{F}_{D^*} is related to the matrix element $\langle D | \bar{c} \gamma_0 b | B \rangle$ and does not determine the semileptonic decay rate near zero recoil for massless leptons, unlike $B \rightarrow D^*$. It can be measured in the decay $B \rightarrow D \tau \nu_\tau$ whose amplitude is proportional to m_τ at $\vec{q}=0$, and this may represent an interesting opportunity for a new generation Super-B facility.

The more conventional decays $B \rightarrow D \ell \nu$ with nearly massless leptons are P -wave at small recoil and are more difficult to measure in this corner of the phase space. Of the two general vector formfactors $f_+(q^2)$ and $f_-(q^2)$ the latter does not contribute for massless leptons; the former, on the other hand, depends on both the time and the spatial components of the current (see, e.g. Ref. [20]). The spatial component assumes a change of the heavy meson velocity, is not related to a conserved Noether current in the heavy quark limit, and generally suffers from linear power corrections $\mathcal{O}(1/m_Q)$. This fact fed, for a long time, a theoretical prejudice against the precision evaluation of the corresponding formfactor

$$\mathcal{F}_+ \equiv \frac{2\sqrt{M_B M_D}}{M_B + M_D} f_+((M_B - M_D)^2).$$

It was nevertheless argued later [20], based on the BPS expansion, that in fact the power corrections in \mathcal{F}_+ are smaller, and may even enjoy a better numeric control than in \mathcal{F}_{D^*} :

$$\mathcal{F}_+ = 1.04 \pm 0.01_{\text{pert}} \pm 0.01_{\text{power}}. \quad (128)$$

The analysis developed in the present paper can be applied to both formfactors, F_D and \mathcal{F}_+ . For F_D the required modifications are minimal. The case of \mathcal{F}_+ is somewhat different

both technically and conceptually; in particular, the physical interpretation is different, and there is no simple probabilistic interpretation that would mean positivity already for the $1/m_Q^2$ corrections. The positivity holds for the leading $1/m_Q$ power correction, however it can simply be regarded as known within the required numeric precision.

The analysis of the perturbative corrections follows closely that of Sect. 3 in the case of F_D , with corrections generally smaller. This kind of analysis cannot be directly applied to \mathcal{F}_+ due to subtleties at nonvanishing recoil; the treatment is more complicated here and has to be analyzed ad hoc [20].

For what concerns the power corrections, we do not expect improvements in either cases. The main reason is that the power corrections (in the kinetic scheme we consistently use) are numerically small to start with, since they all vanish in the exact BPS limit. Moreover, to any order in $1/m_Q$ the terms are of the second order in the deviation from the BPS limit [20], an analogue of the Ademollo-Gatto theorem [34] which applies to the BPS expansion for both F_D and \mathcal{F}_+ . As a consequence, any numeric result strongly depends on the degree of proximity of the actual-QCD dynamics in B mesons to the BPS limit, for instance, on the excess of μ_π^2 over μ_G^2 . This appears as a significant cancellation between terms belonging to different spin structures. It is therefore difficult to expect an increase in defendable accuracy in F_D and \mathcal{F}_+ unless the numerical aspects of the BPS breaking are experimentally scrutinized. Once this aspect of the strong dynamics is studied, we would have more theory constraints to improve the accuracy of the nonperturbative predictions, in particular if the BPS regime turns out a good starting approximation.

7.3 Lattice determination of \mathcal{F}_{D^*}

The recent PDG policy has been to rely solely on the lattice evaluation of \mathcal{F}_{D^*} for the exclusive extraction of $|V_{cb}|$ from the $B \rightarrow D^* \ell \nu$ differential rate extrapolated to the no-recoil kinematics. The lattice values for $\mathcal{F}_{D^*}(1)$ have always been on the higher side, well above 0.9 and carried small error bars, in particular since unquenched simulations were first employed [35]:

$$\mathcal{F}_{D^*}(1) = 0.924 \pm 0.012 \pm 0.019. \quad (129)$$

An update of this result was presented by the FNAL-MILC collaboration [36] after our first publication [1]. It has a lower central value,¹⁰

$$\mathcal{F}_{D^*}(1) = 0.902 \pm 0.005 \pm 0.016 \quad (130)$$

and is closer to our number. The other recent lattice result is based on a quenched simulation by the Tor Vergata group [37], $\mathcal{F}_{D^*}(1) = 0.924 \pm 0.008 \pm 0.005$ and has an even smaller nominal error.

Confronting our evaluation of $\mathcal{F}_{D^*}(1)$ with the lattice ones, we should first emphasize that the latter are not direct calculations of this formfactor. The lattice theory with heavy quarks and continuum QCD are two different theories, and there is no limit at $m_Q a \sim 1$ (a

¹⁰The last FNAL paper included the electroweak decay enhancement factor 1.007 into F ; we have removed it in Eq. (130). We thank A. Kronfeld for the communication.

is the lattice spacing) where they would coincide nonperturbatively. Present simulations do not reach values of $m_c a$ below about 0.3-0.4. The fact that the two theories share the same heavy quark symmetry was emphasized as the key point behind the approach pursued by the FNAL group [38]. However, it is the power-suppressed deviations from the symmetry that matter in this case, and in principle they are different.

This becomes transparent if one takes a closer look at the $1/m_Q$ corrections. In QCD, as a consequence of Lorentz symmetry, the mass entering the nonrelativistic kinetic energy $\vec{p}^2/2m_Q$ is the same rest-energy mass m_Q controlling also the power-suppressed terms in the currents (from equations of motion and from the Foldy-Wouthuysen transformation), the role of the correlators of the subleading operators, etc. No symmetry, however, enforces their equality on the lattice, and all these terms are driven by different effective masses.

The FNAL lattice approach appreciates this complication [39]. To handle it the heavy quark sector is modified by adding *ad hoc* power-suppressed terms allowing to change the corresponding effective masses; in turn this changes the power corrections. The outcome for the $1/m_Q^k$ effects in $\mathcal{F}(1)$ is then determined by the *ad hoc* constants which have to be specified through a matching. However, such a matching has only been performed at tree level. Furthermore, the matching was performed only to the leading power effects, corresponding to the $1/m_Q^2$ corrections in $\mathcal{F}(1)$. All $1/m_Q^3$ and higher effects are therefore not under control,¹¹ although it can be argued that these discretization effects are somewhat suppressed for charm, at low a .

In view of these practical limitations the FNAL approach cannot be regarded a first-principle evaluation of the zero-recoil $B \rightarrow D^*$ formfactor in QCD. Some of the related potential biases are included in the error budget detailed in the publications. However, the error assignment may not be realistic. In fact, the recent value in Eq. (130) has a reduced discrepancy with the estimate Eq. (133); a more conservative treatment of the systematic errors would make it compatible with the central value of the present analysis.

We also note that, comparing the earlier and the more recent FNAL lattice simulations, the group did not find a noticeable effect of the light quark unquenching. This differs from the estimated size of the chiral loop contributions discussed in Sect. 5.2 related to the non-resonant states with light dynamic pions, although there may be no formal contradiction.

The above reservations apply to the lattice determination of the vector $B \rightarrow D$ formfactor \mathcal{F}_+ as well. In this case larger corrections to the symmetry limit were found [41]

$$\mathcal{F}_+ = 1.074 \pm 0.018 \pm 0.015$$

compared to the theoretical prediction in Eq. (128). Here, however, the disagreement is less significant than for \mathcal{F}_{D^*} .¹²

¹¹Earlier FNAL evaluations [40] claimed to extract the principal $1/m_Q^3$ terms, however they were determined in an effective theory essentially different from the actual QCD. The later analyses considered only $1/m_Q^2$ corrections.

¹²More recently, the Tor Vergata group reported the value $\mathcal{F}_+ = 1.026 \pm 0.017$, based on quenched simulations [42] and a new preliminary value $\mathcal{F}_+ = 1.058 \pm 0.009_{stat}$ [43] has been presented, where the systematic uncertainty still needs to be evaluated.

8 Conclusions

The present study has been motivated by the need for an updated evaluation of the phenomenologically important $B \rightarrow D^*$ semileptonic transition formfactor near the zero-recoil point, $\mathcal{F}(1)$, that could account for the latest progress in heavy quark theory. The main numeric outcome has been reported in [1] and the details have been given here.

Numerically we conclude that the unitarity upper bound for the formfactor is

$$\mathcal{F}(1) < 0.92 \quad (131)$$

assuming only positivity of the inelastic contributions. Including the soft $D^{(*)}\pi$ continuum the bound becomes

$$\mathcal{F}(1) < 0.90. \quad (132)$$

These numbers refer to values of μ_π^2 close to its lower bound. The bounds on $\mathcal{F}(1)$ become stronger if the actual μ_π^2 value is larger, which is more natural on theory grounds. Our analysis of the inelastic transitions into the low-lying channels incorporating the constraints following from the observed amount of the hyperfine splitting in B and D mesons allows us to go beyond the unitarity upper bound and to obtain an estimate. The actual value for $\mathcal{F}(1)$ comes out about

$$\mathcal{F}(1) \approx 0.86 \quad (133)$$

at low values of μ_π^2 ; it somewhat decreases at larger μ_π^2 and/or ρ_D^3 .

The quoted numbers for the unitarity bounds Eqs. (131), (132) carry a theoretical uncertainty of about 1%. The estimated central value has a larger uncertainty, of around 2%. We quote here the value literally obtained in our estimate (for low μ_π^2 , ρ_D^3); it is not implied that this value peaks the expectation probability.

Thus, $\mathcal{F}(1)$ in excess of 0.9 would be consistent with unitarity and the short-distance expansion of the QCD amplitude only under contrived assumptions. Values larger than 0.92 should be viewed in violation of unitarity assuming that the conventional short-distance expansion in QCD works in the case of the zero-recoil scattering amplitude off heavy quarks.

In earlier analyses of the power corrections to $\mathcal{F}(1)$ the “wavefunction overlap” effect used to be uncertain and, essentially was only parameterized; in the language of the heavy quark sum rules it was

$$I_{\text{inel}} = \chi \cdot \Delta \quad (134)$$

with Δ the power corrections in the sum rule, cf. Eq. (6), setting the scale of the nonperturbative effects in $\mathcal{F}(1)$. It was simply guessed following Refs. [10, 2] that χ is somewhere between 0 and 1 leading to an assumption $\chi = 0.5 \pm 0.5$. On the other hand we have linked I_{inel} to measured hadronic parameters in the heavy mesons and found χ to be large,

$$\chi \approx 1.3 \div 1.7.$$

This is the main factor driving the prediction for $\mathcal{F}(1)$ down compared to earlier estimates, along with a shift due to the higher-order power corrections.

Since our conclusion appears in some conflict with the lattice results for $\mathcal{F}(1)$, one may examine how robust this conclusion is. We found that the phenomenology of the heavy mesons suggests that the inelastic contributions, as well as the $1/m_Q^3$ and higher-order power corrections are numerically significant and that they lower the expected value for $\mathcal{F}(1)$. Our derivations, of course, use the power expansion for charm, and this may be a vulnerable point for a precision prediction.

We emphasize, however, that a scenario with smaller corrections from the nonlocal correlators or high orders would not be consistent. If the neglected higher-order effects in charm are relatively small, our analysis of the hyperfine splitting is reliable. If, on the contrary, the higher-order corrections in charm are too significant to affect the credibility of the analysis, this would imply a higher overall mass scale of nonperturbative QCD in heavy quarks. Then there would be no reason to expect small corrections to $\mathcal{F}(1)$ either.

Our numeric predictions involved a number of theoretical improvements. The first to mention concerned the calculation of the Wilsonian perturbative renormalization factor with a hard cutoff. We derived a general ansatz applicable to the one-loop level as well as to arbitrary BLM order, which yields the perturbative correction in the kinetic scheme with a full dependence on μ/m_Q . It appears to be different from the naive prescription for having a cut on the gluon momentum. For the zero-recoil transitions the difference emerges starting with the terms $\mathcal{O}(1/m_Q^3)$. Numerically it is important whenever the hard scale is determined by the charm mass.

The other direction is the treatment of the inelastic contributions, along with a detailed analysis of the continuum soft-pion states in the context of the heavy quark expansion.

We have presented a novel model-independent analysis of the transitions into the radially excited (or D -wave) states near the rest kinematics. So far the excited states considered were mainly the P -wave states. The important new phenomenological constraint comes from the hyperfine splitting in B and D : qualitatively, the latter tells us that the $D=3$ zero-momentum nonlocal correlators are numerically large in actual QCD, and this enhances the predicted size of the inelastic probabilities (the ‘overlap deficit’ in the formfactor) over the naive expectations. The analysis of the spin-averaged B and D meson mass difference supports the same conclusion, albeit with larger uncertainty. Using the hyperfine splitting, one can then set a lower bound on the inelastic contribution. The bound is very close to the value I_{inel} assumes in the BPS limit where a single combination of the four general correlators determines both I_{inel} and the $1/m_Q$ dependence of the hyperfine splitting.

A related implication of the hyperfine splitting analysis is the enhancement of the transition amplitudes into the excited ‘radial’ charm states which must be dominated by the $1/m_c$ -suppressed terms rather than by the velocity-dependent component. This leads to an increased yield of the wide charm hadronic structures from the decays of the ‘radial’ states, and would eliminate the ‘ $\frac{1}{2} > \frac{3}{2}$ ’ puzzle if the observed wide yields are dominated by them rather than by the $\frac{1}{2}$ P -waves predicted to be suppressed. We emphasize that the D -wave states must be produced along with true radially excited mesons, and may even dominate. Some possibilities to distinguish them in experiment were discussed.

Therefore, we have identified a link among three apparently unrelated physics points: the size of the hyperfine splitting in charm and beauty, the reduction in $\mathcal{F}(1)$ through

the enhanced nonlocal power corrections, and the resolution of the ‘ $\frac{1}{2} > \frac{3}{2}$ ’ puzzle in the semileptonic B decays.

On the theoretical side, yet another implication is manifest: we find significant corrections to the factorization for higher-dimension heavy-quark expectation values. Our model-independent analysis provides the basis for a dedicated account of the nonfactorizable effects from higher orders in $1/m_Q$ [3], in particular for the semileptonic B -decay fits.

With respect to the $D^{(*)}\pi$ states, we have expanded the treatment in a few aspects. Our approach allowed us to account for their effect in the analysis of $\mathcal{F}(1)$ beyond the leading order $1/m_Q^2$, relying instead on the soft-pion approximation. The subleading terms turned out significant. In particular, the heavy quark symmetry-breaking corrections in the heavy meson-to-pion couplings seem to yield the dominant effect.

Theoretically, we have presented a consistent treatment of the $D^{(*)}\pi$ states in the heavy quark approximation within the soft-pion approach. The decomposition of the P -wave into the $\frac{1}{2}$ - and the $\frac{3}{2}$ -components has been addressed before yet remained largely unknown. We briefly recapitulated it in Sect. 6.4 and extended it to radial/ D -wave states, with the decomposition into the corresponding $\frac{1}{2}^+$ -, $\frac{3}{2}^+$ - and $\frac{5}{2}^+$ -channels. This made it explicit that earlier studies of the soft-pion corrections were incomplete: they accounted only for the most singular effect at the softest pion momentum, however not dominant in the typical configuration with $|\vec{k}_\pi| \sim \mu_{\text{had}}$. Typically, the pion loops yield negligible contributions, with the notable exception of the contribution to the axial sum rule for $\mathcal{F}(1)$.

We conclude with the following remark. The pattern of the hyperfine splitting in B and D mesons, in particular its precise mass dependence, is important for a few different phenomena and draws novel qualitative conclusions for our understanding of the heavy meson states. The precision interpretation of the splitting, on the other hand, may potentially be hindered by higher-order effects in charm. A sufficiently accurate measurement at a different heavy quark mass would radically improve the credibility of the hyperfine analysis. We have pointed out that a first principle lattice determination of the hyperfine splitting at better than 5% accuracy, if possible, can provide this information, and have discussed how it can be used for mesons either heavier or lighter than charm.

Acknowledgements

We are grateful to S. Turczyk for computing the higher-order power corrections for the axial-vector decays during work on Ref. [3]. It is our pleasure to thank Ikaros Bigi and Alex Khodjamirian for numerous discussions. The work of P.G. is supported in part by the Italian Ministry of Research (MIUR) under contract 2008H8F9RA_002. The work was supported by the German research foundation DFG under contract MA1187/10-1 and by the German Ministry of Research (BMBF), contracts 05H09PSF; it enjoyed a partial support from the NSF grant PHY-0807959 and from the grant RSGSS 4801.2012.2.

9 Appendices

A BLM corrections and summation

The technique that allows the computation and summation of BLM corrections of order $\beta_0^n \alpha_s^{n+1}$ has been concisely reviewed in Ref. [8]; Ref. [7] focussed upon its application to Wilsonian OPE calculations. To BLM-dress a one-loop result one needs to evaluate the generic one-loop correction A_1

$$\mathcal{A} = 1 + \frac{\alpha_s}{\pi} A_1 + \dots$$

with a fictitious gluon mass λ , $A_1(\lambda^2)$, so that the conventional A_1 is $A_1(0)$. The BLM series in terms of the $\overline{\text{MS}}$ coupling α_s normalized at the arbitrary scale M takes the form

$$A^{\text{BLM}} = 1 + A_1(0) \frac{\alpha_s(M)}{\pi} + \sum_{n=0}^{\infty} \frac{4}{\beta_0} \left(\frac{\beta_0 \alpha_s(M)}{4\pi} \right)^{n+2} \times \\ \sum_{k=0}^{\frac{n}{2}} (-\pi^2)^k C_{n+1}^{2k+1} \cdot \int \frac{d\lambda^2}{\lambda^2} \left[\ln \frac{M^2}{\lambda^2} + \frac{5}{3} \right]^{n-2k} \left(A_1(0) \frac{M^2}{M^2 + e^{-5/3} \lambda^2} - A_1(\lambda^2) \right), \quad (\text{A.1})$$

with C denoting the binomial coefficients. Let us remind that the integral over λ^2 here typically has two (or more) domains. The last term depending on $A_1(\lambda^2)$ is integrated from 0 to the threshold value of the gluon mass if there is a threshold (in particular, it would be set by μ in the Wilsonian calculations), whereas the first term in the same brackets should always be integrated over all values of λ^2 regardless of a cutoff or of kinematic details.

When the infrared part is removed from the one-loop diagram to leave a genuinely short-distance correction, the corresponding $A_1(\lambda^2)$ is a real analytic function in the vicinity of zero. This allows to write an integral representation for the resummed series,

$$A^{\text{BLM}} = 1 + A_1(0) \frac{\alpha_s(M)}{\pi} \\ + \int_{-\infty}^{\infty} dt \frac{\frac{\beta_0}{4} \left(\frac{\alpha_s}{\pi} \right)^2}{\left(1 + \frac{\beta_0 \alpha_s}{4\pi} \left(t - \frac{5}{3} \right) \right)^2 + \left(\frac{\beta_0}{4} \alpha_s \right)^2} \left(A_1(0) \frac{1}{1 + e^{t - \frac{5}{3}}} - A_1(e^t M^2) \right) \\ - \frac{4}{\beta_0} \left[\frac{M^2}{M^2 - \Lambda_{\text{QCD}}^2} A_1(0) - A_1(-\Lambda_V^2) \right], \quad (\text{A.2})$$

without any ambiguity associated with the last term; here

$$\Lambda_{\text{QCD}}^2 = M^2 e^{-\frac{4\pi}{\beta_0 \alpha_s(M)}}, \quad \Lambda_V^2 = e^{\frac{5}{3}} \Lambda_{\text{QCD}}^2 = M^2 e^{-\frac{4\pi}{\beta_0 \alpha_s(M)} + \frac{5}{3}}. \quad (\text{A.3})$$

B One-loop perturbative calculation with a Wilsonian cutoff

In this Appendix we discuss aspects of the one-loop calculation of the leading Wilson coefficient ξ_A . The reasoning is quite general and is applicable to other observables as well.

As in Sect. 3, we need to distinguish between ε_M and Wilsonian μ , therefore we will deal explicitly with $\xi_A^{\text{pert}}(\varepsilon_M, \mu)$ as it appears in Eq. (6). The dependence of $\xi_A^{\text{pert}}(\varepsilon_M, \mu)$ on ε_M is given by Eq. (8). Since the right-hand side of Eq. (6) must be μ -independent, and ξ_A^{pert} must satisfy the ‘boundary condition’ Eq. (9), one way to determine $\xi_A^{\text{pert}}(\varepsilon_M, \mu)$ for arbitrary values of μ and (in principle) any order of perturbation theory is to use the μ -dependence of the matrix elements and masses appearing in Eq. (6).

Indeed, in perturbation theory the expectation values $\langle B|O_k|B\rangle_\mu$ in Eq. (6) typically depend on μ in a powerlike way,

$$\frac{d\langle B|O_k|B\rangle_\mu}{d\mu} \propto \alpha_s \mu^{d_k-4}, \quad (\text{A.4})$$

where d_k is the dimension of O_k ; the same applies to the heavy quark masses on which the Wilson coefficients generally depend. In this way the ε_M -dependence of $\xi_A^{\text{pert}}(\varepsilon_M, \mu)$ is calculated explicitly while its μ -dependence emerges as an expansion in μ/m_Q which is necessarily truncated after a few terms. This is not a serious limitation if the hard OPE scale is $O(m_b)$, but in our case the charm mass sets the lower hard scale in the problem and the expansion in μ/m_Q shows poor convergence.

To overcome this drawback we have devised a method allowing to directly compute the leading Wilson coefficient $\xi_A^{\text{pert}}(\varepsilon_M, \mu)$ as a function of μ/m_Q , without an expansion, in the one-loop approximation. The method is readily generalized to higher-order BLM corrections. We have described its main points in Sect. 3; below we provide additional explanations.

The idea behind the approach is that in one-loop calculations there is a simple connection between the normalization point of the heavy quark operators in the kinetic scheme and the hard cutoff on the gluon momentum k in the diagram. In order to preserve the analyticity and the unitarity of the Feynman integrals no limit on integrations over k_0 of the gluon is imposed in the kinetic scheme: the separation of scales is performed based on $|\vec{k}|$. In this way one computes the one-loop ξ_A^{pert} introducing an infrared cutoff on $|\vec{k}|$, instead of taking the full integral d^4k . In the b -quark static limit the step-function cutoff factor

$$\theta(|\vec{k}| - \mu) \quad (\text{A.5})$$

in the Feynman integrand yields precisely the normalization at the scale μ . The remaining part, the integral with $\theta(\mu - |\vec{k}|)$ constitutes the power-suppressed terms described by higher-dimension matrix elements in the OPE. In order to go beyond the static approximation certain modifications of the cutoff in Eq. (A.5) are required.

Let us remind why ξ_A is related to η_A^2 calculated with a cutoff. The reasoning is based on considering the OPE relations in an ensemble of gluons with the spatial momentum limited by μ in the b rest frame; the non-Abelian nature does not play a role at one-loop level. All these gluons can be considered soft, and they satisfy the OPE sum rule where the coefficients assume the tree level values. Having in mind how the sum rules are derived (for pedagogical reviews see Refs. [11, 24]), the integration in the sum rule must run over all excitation energies, from 0 to ∞ . However, in the soft gluon ensemble with $|\vec{k}| < \mu$ the

spectral density vanishes above the excitation energy

$$\varepsilon_M(\mu) = \mu + \sqrt{m_c^2 + \mu^2} - m_c; \quad (\text{A.6})$$

below $\varepsilon_M(\mu)$ it is the usual one-loop spectral density of QCD. At the same time, the operator expectation values in such an ensemble are just the one-loop QCD expectation values in the kinetic scheme normalized at μ .

We now turn to the subtleties beyond the static limit, and focus on the soft contribution $\delta\eta_A^{\text{soft}}$ to be subtracted from the one-loop η_A :

$$\eta_A \longrightarrow \eta_A - \delta\eta_A^{\text{soft}} = \eta_A - C_F g_s^2 \int \frac{d^4 k}{(2\pi)^4 i} \theta(\mu - |\vec{k}|) \dots \quad (\text{A.7})$$

Here the ellipses denote the same propagators and vertices encountered in the calculation of η_A itself; k is the gluon momentum in the diagram. There are three one-loop diagrams – the vertex correction and the wavefunction renormalization for both b and c quark.

Let us consider the vertex diagram of Fig. 2a as an example. The integrand has a general structure

$$\int \frac{d^4 k}{(2\pi)^4 i} \frac{\text{numerator}}{(k_0^2 - \vec{k}^2 + i0)(m_b^2 - (m_b - k_0)^2 + \vec{k}^2 - i0)(m_c^2 - (m_c - k_0)^2 + \vec{k}^2 - i0)}. \quad (\text{A.8})$$

At given \vec{k} the integral over k_0 is convergent and is saturated at $|k_0| \sim |\vec{k}|$; the tails at large $|k_0| \gtrsim m_Q$ contribute a power-suppressed piece. Since no cut on k_0 is allowed, the integration over k_0 can be performed by closing the integration contour in the lower half-plane, see Fig. 2b. There are three pairs of poles in the k_0 plane,

$$k_0 = \pm |\vec{k}|, \quad k_0 = m_b \pm \sqrt{m_b^2 + \vec{k}^2}, \quad k_0 = m_c \pm \sqrt{m_c^2 + \vec{k}^2}. \quad (\text{A.9})$$

With the standard Feynman prescription, blue contour α , the integration over k_0 results in the sum of the three residues corresponding to the above poles. For the first pole we have $k_0 < \mu$; however for the two other, distant, poles we have $k_0 \gtrsim m_Q \gg \mu$, regardless of the cutoff. Since the OPE generally corresponds to an expansion in all components of the gluon four-momentum, it is clear that the contributions to the integral associated with the distant (black) poles may not correctly describe the OPE power-suppressed terms. We recall that our goal is just to subtract the piece of the one-gluon loop correction to η_A associated with the terms which have already been included in the power-suppressed OPE.

Indeed, it turns out that the OPE series for the soft piece correspond to the residue of only the ‘near’ pole at $k_0 = |\vec{k}|$, while the two other residues should be discarded. This means changing the bypass prescription for the two distant poles, $-i0 \rightarrow +i0$, which moves the k_0 integration contour as shown by the green dashed line in Fig. 2b.

The $1/m_Q$ expansion in the Feynman diagrams leading to the OPE series is essentially the Taylor expansion of the heavy quark propagators in the integrand for small gluon four-momentum k . Eq. (A.8) then becomes

$$\int \frac{d^4 k}{(2\pi)^4 i} \frac{\text{numerator}}{(k_0^2 - \vec{k}^2 + i0)} \sum_{n=0} \frac{(k^2)^n}{(2m_b k_0 - i0)^{n+1}} \sum_{m=0} \frac{(k^2)^m}{(2m_c k_0 - i0)^{m+1}}; \quad (\text{A.10})$$

the poles at $k_0 = 0 + i0$ are descendants of the nonrelativistic poles located on the left of $k_0 = 0$. To reproduce the nonrelativistic expansion we calculate the integral for each term closing the contour in the lower k_0 half-plane and picking up only the gluon pole $k_0 = |\vec{k}|$. This cannot be done for the original integral in Eq. (A.8): its value is not equal to the sum of the series, because large k_0 beyond the convergence radius of expansion (A.10) contribute. However, with the modified bypass prescription for the distant poles the integration contour β in Fig. 2b can be shrunk to a contour γ (maroon) on which $|k_0| < 2m_c$ holds everywhere. For the integral over contour γ the series converges absolutely and uniformly, still embracing only the $k_0 = |\vec{k}|$ pole. This proves that the sum of the series obtained integrating term by term Eq. (A.10) gives the integral over k_0 of the original expression in Eq. (A.8) yet with the modified bypass for the distant poles along contour β .

Let us make the following general remark. At first glance, the terms in the expansion of the Feynman diagrams and in the OPE series assume a somewhat different form: the expectation values of the operators in the kinetic scheme are given by three-dimensional integrals over spatial momentum of an on-shell gluon, $k_0 = |\vec{k}|$, being defined through the heavy quark structure functions:

$$\int \frac{d^3\vec{k}}{(2\pi)^3 2|\vec{k}|} \mathcal{P}(\vec{k}) \quad (\text{A.11})$$

with $\mathcal{P}(\vec{k})$ a polynomial. It is clear, however, that the two representations have the same form once the k_0 integration is performed closing the contour in the lower half-plane. That is why integration over k_0 plays an important role in our reasoning.

At this point it becomes transparent why the OPE series yield the expansion of the sole contribution of the near pole with the on-shell gluon: the heavy quark propagators appearing in the definition of the heavy quark expectation values in the effective theory are nonrelativistic (static) propagators which have a single pole. The second, distant, pole peculiar to relativistic particles is absent from them. Therefore, at any finite order in the OPE power expansion there is no contributions associated with the distant poles, $k_0 \approx 2m_Q$ in Eq. (A.9). In this sense the distant singularities are related to the divergence of the expansion in k/m_Q rather than to the discontinuity of the individual terms.

So far we have considered the vertex diagram. The other two Feynman diagrams with the wavefunction renormalization for external quark legs have the same structure; they only depend on a single quark mass $m_Q = m_b$ or m_c , and the two pairs of the fermion propagator poles are degenerate. Consequently all the above reasoning applies to them as well.

Let us note that taking $\mu = \varepsilon_M$ the difference between μ' and ε_M becomes power-suppressed, the last term of Eq. (10) becomes of order $1/m_Q^3$ and can be neglected to the leading order μ^2/m_Q^2 . Therefore, it accounts for the recoil correction in the relation between μ and ε_M and becomes relevant where the terms $O(\alpha_s \mu^3/m_Q^3)$ are included. Its form must already be clear from the preceding derivation: in the soft gluon ensemble the emission of a gluon with energy ω yields an excitation energy $\varepsilon = \omega + \sqrt{m_c^2 + \omega^2} - m_c$ in the final state, and the spectral density is

$$w^{\text{soft}}(\varepsilon) = w^{\text{pert}}(\varepsilon) \theta(\mu' - \varepsilon), \quad \mu' = \mu + \sqrt{m_c^2 + \mu^2} - m_c. \quad (\text{A.12})$$

This explains the integration limit in the last term in Eq.(10).

The above discussion of the one-loop corrections is directly extended to incorporate any higher-order BLM corrections as well, or even to perform the complete BLM-summation. As detailed in Appendix A, the same analysis must be repeated for the diagrams with an arbitrary gluon mass λ . This has been stated already in Sect. 3 where the related technical modifications were listed. The necessary one-loop expressions at non-zero λ^2 are given in Appendix C.

C Details of the perturbative calculation

In this Appendix we provide details omitted from the main text in Sect. 3. In the case of a massive gluon the one-loop inelastic perturbative spectral density determining the recoil correction is given by

$$\begin{aligned}
w^{\text{pert}}(\varepsilon) = & C_F \frac{\alpha_s}{\pi} \frac{((M - m_c)^2 - \lambda^2) \sqrt{(M^2 - (m_c + \lambda)^2)(M^2 - (m_c - \lambda)^2)}}{12 M^3 (M - m_c)^2 (m_b M^2 - M \lambda^2 + m_b (\lambda^2 - m_c^2))^2} \theta(\varepsilon - \lambda) \times \\
& \left[2M^6 - 4M^3(4m_b + m_c)\lambda^2 + 4M\lambda^2(2m_b + m_c)(m_c^2 - \lambda^2) \right. \\
& + (3m_b^2 + 2m_b m_c + m_c^2)(m_c^2 - \lambda^2)^2 + M^4(3m_b^2 + 2m_b m_c - 3m_c^2 + 4\lambda^2) \\
& \left. + M^2(4m_c^2 \lambda^2 - 4m_b m_c^3 + 6\lambda^4 - 6m_b^2(m_c^2 - 2\lambda^2)) \right]. \tag{A.13}
\end{aligned}$$

Here $M = m_c + \varepsilon$ is the invariant mass of the final state. The one-loop zero-recoil axial current renormalization without a cutoff $\eta_A = 1 + C_F \frac{\alpha_s}{\pi} \eta_A^{(1)}(\lambda^2) + O(\alpha_s^2)$ is given by

$$\begin{aligned}
\eta_A^{(1)}(\lambda^2) = & -\frac{9y + 2yz + 24 + 9yz^2}{24} - \frac{9y^2 - 7y^2 z - 6y - 6yz + 18 + 18z}{24(1 - z)} \ln z \\
& + \frac{y(9y + 2yz - 6 + 2yz^2 - 12z + 2yz^3 - 6z^2 + 9yz^4)}{48} (\ln y + 2 \ln z) \\
& - \frac{9y^3 - 7y^3 z - 24y^2 + 8y^2 z + 12y + 44yz - 96}{48y(1 - z)\sqrt{1 - 4/y}} \ln \frac{1 + \sqrt{1 - 4/y}}{1 - \sqrt{1 - 4/y}} \\
& - \frac{-44y - 8y^2 z^2 + 7y^3 z^4 + 96/z - 12yz + 24y^2 z^3 - 9y^3 z^5}{48y(1 - z)\sqrt{1 - 4/yz^2}} \ln \frac{1 + \sqrt{1 - 4/yz^2}}{1 - \sqrt{1 - 4/yz^2}}. \tag{A.14}
\end{aligned}$$

Here we have used $y = \lambda^2/m_c^2$ and $z = m_c/m_b$. This expression coincides with the one in Eq. (B3) of Ref. [44], where it was derived by a dispersion integral starting from the Euclidean calculation of Ref. [45].

The check of the μ -independence of the OPE sum rule, Eq. (6), with the perturbative factor calculated according to Eq. (10) can be accomplished to an arbitrary BLM order at once: it suffices to establish it at a given value of the gluon mass. We demonstrate it here assuming $\varepsilon_M = \mu$. The right-hand side of the sum rule depends on μ through $\xi_A^{\text{pert}}(\mu)$ and through the heavy quark expectation values. Moreover, since all the μ -dependent components of the perturbative calculation, including the expectation values and the inelastic

integral, can be written as three-dimension integrals

$$\int \frac{d^3k}{(2\pi)^3 2k_0} \theta(\mu - k_0) \dots, \quad k_0 \equiv \sqrt{\vec{k}^2 + \lambda^2} \quad (\text{A.15})$$

with the same cutoff provided $\varepsilon_M = \mu$, we may simply check the cancellation at the integrand level at a given value of \vec{k}^2 and λ^2 .

As the μ -dependence of the individual contributions starts at $\mathcal{O}(1/m_Q^2)$, the first check is provided by the terms $\alpha_s \mu^2/m_Q^2$ [46]. At this order the power-suppressed component of the OPE part of the sum rule (6) includes only the expectation values μ_π^2 and μ_G^2 which should be considered in the static limit; the latter then vanishes. The required expressions have been given in Refs. [8, 7]. In units of

$$C_F g_s^2 \int \frac{d^3\vec{k}}{(2\pi)^3 2k_0} \quad (\text{A.16})$$

we get

$$2 + \frac{\lambda^2}{k_0^2}, \quad \left(\frac{1}{m_c^2} + \frac{2}{3m_c m_b} + \frac{1}{m_b^2} \right) \frac{\vec{k}^2}{2k_0^2} + \left(\frac{1}{m_c} - \frac{1}{m_b} \right)^2 \frac{\lambda^2 \vec{k}^2}{4k_0^4} \quad (\text{A.17})$$

for μ_π^2 and w^{pert} , respectively.

Finally, the subtracted soft piece of η_A depends on μ . The expression for $\delta\eta_A^{\text{soft}}(\mu)$ given in Eq. (18) must be expanded in \vec{k} and λ^2 :

$$\begin{aligned} \delta\eta_A^{\text{soft}} = C_F g_s^2 \int \frac{d^3k}{(2\pi)^3 2k_0} & \left\{ -\frac{1}{2} \left[\left(\frac{1}{m_c^2} + \frac{2}{3m_c m_b} + \frac{1}{m_b^2} \right) - \frac{\lambda^2}{k_0^2} \frac{2}{3m_c m_b} - \frac{\lambda^4}{4k_0^4} \left(\frac{1}{m_c} - \frac{1}{m_b} \right)^2 \right] \right. \\ & \left. - \frac{\lambda^2}{2k_0} \left(\frac{1}{m_c} + \frac{1}{m_b} \right) \left[\left(\frac{1}{m_c^2} - \frac{2}{3m_c m_b} + \frac{1}{m_b^2} \right) - \frac{\lambda^2}{k_0^2} \frac{1}{3m_c m_b} - \frac{\lambda^4}{4k_0^4} \left(\frac{1}{m_c} - \frac{1}{m_b} \right)^2 \right] + \dots \right\}, \quad (\text{A.18}) \end{aligned}$$

where the first square bracket upon integration gives the leading μ^2/m_Q^2 terms and the second line yields μ^3/m_Q^3 . Combining the above coefficients the μ -independence of the sum rule is verified at order μ^2/m_Q^2 .

A far deeper check is encountered at the level of μ^3/m_Q^3 terms. At this order the proper prescription to calculate the soft virtual correction $\delta\eta_A^{\text{pert}}$ discussed in Appendix B becomes essential. At this level one also needs to include the higher-dimension Darwin expectation value as well as the $1/m_b$ effects in the kinetic and chromomagnetic expectation values. The latter are expressed in terms of the local ρ_D^3 and ρ_{LS}^3 and of the nonlocal expectation values. Perturbatively ρ_{LS}^3 vanishes as do $\rho_{\pi G}^3$ and ρ_A^3 . The subleading term in the continuum spectral density is also required and can be obtained directly expanding Eq. (A.13).

By virtue of the SV sum rules the perturbative component of the Darwin expectation value amounts to an integral of the same form (A.15), with the integrand given by the product of the integrand for μ_π^2 and k_0 , the excitation energy for a static quark:

$$k_0 \left(2 + \frac{\lambda^2}{k_0^2} \right). \quad (\text{A.19})$$

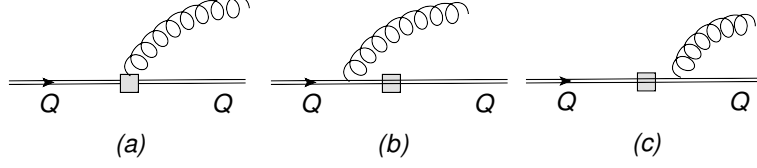


Figure 13: One-gluon amplitude diagrams involved in the calculation of the $\mathcal{O}(\alpha_s)$ perturbative spectral densities in the static limit. The square block denotes the operator in question.

Since μ_G^2 was defined in Eq. (20) to include only the magnetic field piece $-\vec{\sigma} \cdot \vec{B}$ but not the lower-component term in the complete chromomagnetic operator, to order μ^3/m_Q it acquires a contribution only from the nonlocal correlator ρ_S^3 ,

$$\delta_{\alpha_s} \mu_G^2 = \frac{1}{m_b} \delta_{\alpha_s} \rho_S^3. \quad (\text{A.20})$$

The value of μ_π^2 is perturbatively corrected, instead, by the correlator $\rho_{\pi\pi}^3$:

$$\delta_{\alpha_s} \mu_\pi^2 = 2 + \frac{\lambda^2}{k_0^2} - \frac{1}{m_b} \delta_{\alpha_s} \rho_{\pi\pi}^3, \quad (\text{A.21})$$

where overall integration (A.16) is understood.

To find one-loop $\delta_{\alpha_s} \rho_{\pi\pi,S}^3$ or, more generally, all the perturbative spectral densities in Eqs. (66), (67) one needs to square the sum of the diagrams shown in Fig. 13. The answer is obtained immediately, in particular if a little trick [46] is used, which eliminates two of the three diagrams, *b* and *c*, for the transition amplitude:

$$\rho_0(\omega) = C_F \frac{\alpha_s}{\pi} \lambda^2 \frac{(\omega^2 - \lambda^2)^{\frac{3}{2}}}{\omega^2}, \quad \rho_1(\omega) = C_F \frac{8\alpha_s}{3\pi} (\omega^2 - \lambda^2)^{\frac{3}{2}}, \quad \rho_2(\omega) = C_F \frac{\alpha_s}{\pi} \frac{(\omega^2 - \lambda^2)^{\frac{5}{2}}}{\omega^2}. \quad (\text{A.22})$$

The trick uses gauge invariance to say that one can use the simple gluon propagator

$$\frac{\delta_{ij} - \frac{k_i k_j}{k_0^2}}{\lambda^2 - k^2} \quad (\text{A.23})$$

requiring to calculate only the spatial vertices; they come from the vertex emission but not from the heavy quark lines. Using Eqs. (66), (67) and (51) we obtain at once, for instance,

$$\delta_{\alpha_s} \rho_{\pi\pi}^3 = \frac{\lambda^2 \vec{k}^2}{k_0^3}, \quad \delta_{\alpha_s} \rho_S^3 = 2 \frac{\vec{k}^2}{k_0}, \quad (\text{A.24})$$

in the same units of Eq. (A.16).

Finally, one needs the $\mathcal{O}(\mu^3/m_Q^3)$ term in the expansion of $\delta\eta_A^{\text{soft}}$; it is given in the second line of Eq. (A.18). Expanding Eq. (A.13) through the next-to-leading order, on one hand, and collecting all relevant terms from Eqs. (A.18), (A.19) and (A.24) with the explicit coefficients appearing in the sum rule, on the other hand, we arrive at the same integrand in the both sides of the sum rule (6) at $O(1/m_Q^3)$, for arbitrary value of λ^2 .

For bookkeeping purposes we quote here the perturbatively calculated moments of the spectral densities $\rho_0(\omega)$, $\rho_1(\omega)$ and $\rho_2(\omega)$, as well as those of the P -wave spectral density $\rho^P(\omega)$, defined in analogy to Eq. (67) by the perturbative relation

$$\mathcal{T}^{\frac{1}{2}-}(\omega) = \mathcal{T}^{\frac{3}{2}-}(\omega) = \frac{1}{9} \rho^P(\omega),$$

see Eq.(44). Their expressions to order α_s and $\beta_0 \alpha_s^2$ are:

$$\begin{aligned} \int_0^\mu \omega^k d\omega \rho_0(\omega) &= -\frac{1}{5} C_F \frac{\beta_0}{2} \left(\frac{\alpha_s}{\pi} \right)^2 \frac{\mu^{4+k}}{4+k} \\ \int_0^\mu \omega^k d\omega \rho_1(\omega) &= \frac{8}{3} C_F \frac{\alpha_s(M)}{\pi} \frac{\mu^{4+k}}{4+k} \left[1 + \frac{\beta_0}{2} \frac{\alpha_s}{\pi} \left(\ln \frac{M}{2\mu} + \frac{13}{6} + \frac{1}{4+k} \right) \right] \\ \int_0^\mu \omega^k d\omega \rho_2(\omega) &= C_F \frac{\alpha_s(M)}{\pi} \frac{\mu^{4+k}}{4+k} \left[1 + \frac{\beta_0}{2} \frac{\alpha_s}{\pi} \left(\ln \frac{M}{2\mu} + \frac{71}{30} + \frac{1}{4+k} \right) \right] \\ \int_0^\mu \omega^k d\omega \rho^P(\omega) &= 2 C_F \frac{\alpha_s(M)}{\pi} \frac{\mu^{2+k}}{2+k} \left[1 + \frac{\beta_0}{2} \frac{\alpha_s}{\pi} \left(\ln \frac{M}{2\mu} + \frac{5}{3} + \frac{1}{2+k} \right) \right]. \end{aligned} \quad (\text{A.25})$$

The moments of $\rho^P(\omega)$ determine, beyond the IW slope, $\bar{\Lambda}$, the kinetic and the Darwin expectation values, the higher expectation values m_2 and r_1 .

For completeness, we give here also the perturbative dependence on μ of ρ_{LS}^3 associated with power mixing:

$$\frac{d}{d\mu}(-\rho_{LS}^3) = C_A \frac{\alpha_s}{\pi} \mu_G^2 + C_A \frac{\alpha_s}{2\pi} \frac{1}{\mu} \rho_{LS}^3 + \mathcal{O}(\alpha_s^2) \quad (\text{A.26})$$

(the anomalous dimension of the spin-orbit operator coincides with that of the full chromomagnetic one). This implies the relation between the extrapolated ‘pole-scheme’ value $-\tilde{\rho}_{LS}^3$ and the Wilsonian $-\rho_{LS}^3(\mu)$:

$$-\tilde{\rho}_{LS}^3 = -\rho_{LS}^3(\mu) - C_A \frac{\alpha_s}{\pi} \mu \mu_G^2 + \mathcal{O}(\alpha_s^2). \quad (\text{A.27})$$

D Transitions to the ‘radial’ states and the inclusive yield

The inelastic zero-recoil spectral density for the *vector* $\bar{c}\gamma_0 b$ current paralleling Eq. (52) is

$$\frac{1}{2\pi i} \text{disc } T_{\text{zr}}^{(V)}(\omega) \equiv w_{\text{inel}}^{(V)}(\omega) = \left(\frac{1}{2m_c} - \frac{1}{2m_b} \right)^2 \frac{\rho_p^{(\frac{1}{2}+)}(\omega) - 2\rho_{pg}^{(\frac{1}{2}+)}(\omega) + \rho_g^{(\frac{1}{2}+)}(\omega)}{\omega^2}; \quad (\text{A.28})$$

no transitions into $\frac{3}{2}^+$ occur. It is manifestly BPS-suppressed to the second order.

As stated in Section 6.3.2, we evaluate the rate for a decay of the Ω_0 spin- $\frac{1}{2}$ heavy state into the corresponding excited half-integer-spin multiplets. The weak current coupling of these fictitious hadrons is fixed by the corresponding transition probabilities near zero recoil. Namely, the (unpolarized) zero-recoil structure functions are expressed through the

effective transition amplitudes; on the other hand, they are given by the $1/m_Q$ expansion, in our case to the second order, of the actual B -meson zero-recoil semileptonic structure functions, cf. Eqs. (52), (A.28).

There are more structure functions for a particle with spin than for actual B mesons. However, considering the unpolarized states (for instance, averaging over spin) they are reduced to the standard ones, and we use the same notations for them for decays of Ω_0 as for B mesons in QCD. V - A interference (which is not relevant here) would require a nonvanishing recoil kinematics.

The unpolarized structure functions for the transitions into the $\frac{1}{2}^+$ states are the same as the tree-level ones for B decays [47]:

$$w_1 = g_A^2 \frac{(m_1 + m_2)^2 - q^2}{2} + g_V^2 \frac{(m_1 - m_2)^2 - q^2}{2}, \quad w_2 = 2(g_A^2 + g_V^2)m_1^2, \quad w_3 = 2g_A g_V m_1, \quad (\text{A.29})$$

with the overall factor $\frac{\pi}{m_1^2} \delta(q_0 - \frac{m_1^2 - m_2^2 + q^2}{2m_1})$, where we have used the notation of Eq. (86), namely

$$\langle \frac{1}{2}^+ | \bar{c} \gamma_\mu \gamma_5 b | \Omega_0 \rangle = g_A \bar{\chi} \gamma_\mu \gamma_5 \Psi_0, \quad \langle \frac{1}{2}^+ | \bar{c} \gamma_\mu b | \Omega_0 \rangle = g_V \bar{\chi} \gamma_\mu \Psi_0. \quad (\text{A.30})$$

Note that here we use the full bispinors and assume their relativistic normalization. In this context the mass m_1 refers to the ground state in the beauty sector, $m_1 \simeq m_b + \bar{\Lambda}$ while m_2 to the excited state for charm, $m_2 \simeq m_c + \bar{\Lambda} + \varepsilon_{\text{rad}}$. Only $w_{1,2}$ contribute to the total width; it is given in Eqs. (87), (88).

For transitions into $\frac{3}{2}^+$ radial excitations we employ

$$\langle \frac{3}{2}^+ | \bar{c} \gamma_\mu \gamma_5 b | \Omega_0 \rangle = g_A \bar{\chi}_\mu \Psi_0, \quad \langle \frac{3}{2}^+ | \bar{c} \gamma_\mu b | \Omega_0 \rangle = g_V \bar{\chi}_\mu i \gamma_5 \Psi_0, \quad (\text{A.31})$$

where χ_μ are likewise fully relativistic Rarita-Schwinger wavefunctions. (The vector matrix element is considered only for completeness; its transition amplitudes into $\frac{3}{2}^+$ states involve further suppression: either more powers of velocity, or extra $1/m_Q$ or an additional overall α_s .) With this convention we have

$$w_1 = \left(g_A^2 \frac{(m_1 + m_2)^2 - q^2}{3m_1^2} + g_V^2 \frac{(m_1 - m_2)^2 - q^2}{3m_1^2} \right) \pi \delta(q_0 - \frac{m_1^2 - m_2^2 + q^2}{2m_1}), \quad w_2 = \frac{m_1^2}{m_2^2} w_1, \\ w_3 = 0, \quad w_4 = m_1^2 w_1, \quad w_5 = -\frac{m_1}{m_2^2} w_1. \quad (\text{A.32})$$

Integrating over the full phase space we obtain the corresponding width

$$\Gamma_{A,V}^{(\frac{3}{2})} = \frac{G_F^2 M_0^5 |V_{cb}|^2}{192\pi^3} g_{A,V}^2 z_{A,V}^{(\frac{3}{2})}(r), \quad r = \frac{M_{\frac{3}{2}}^2}{M_0^2}, \quad (\text{A.33})$$

with the phase space factors

$$z_{A,V}^{(\frac{3}{2})}(r) = \frac{1}{2} \left(z_0^{(\frac{3}{2})}(r) \pm \tilde{z}_0^{(\frac{3}{2})}(r) \right), \quad z_0^{(\frac{3}{2})}(r) = \frac{1}{15r} - 2r - \frac{2}{3}r^2 + 3r^3 - \frac{2}{5}r^4 - 4r^2 \ln r, \\ \tilde{z}_0^{(\frac{3}{2})}(r) = \frac{1}{6\sqrt{r}} + r^{3/2} \left(12 - \frac{32}{3}r - \frac{3}{2}r^2 + (6+8r) \ln r \right) \quad (\text{A.34})$$

The singularity at $r \rightarrow 0$ reflects here the ultraviolet problems of point-like higher-spin particles. Note that all the components of the vector transition amplitude vanish at zero recoil; the zero-recoil analysis does not constrain g_V for $\frac{3}{2}^+$. However, for this very reason it is generally suppressed by a higher power of the SV parameter Δ/M :

$$\frac{M_0^5}{192\pi^3} z_A^{(\frac{3}{2})}(r) \simeq \frac{\Delta^5}{30\pi^3}, \quad \frac{M_0^5}{192\pi^3} z_V^{(\frac{3}{2})}(r) \simeq \frac{11}{84} \frac{\Delta^2}{M_0^2} \frac{\Delta^5}{30\pi^3} \quad \text{at } \Delta \ll M_0.$$

Numerically, the yield in the vector channel is negligible for any relevant ratio $M_{\frac{3}{2}}/M_0$; the vector current does not contribute to the production of $\frac{3}{2}^+$ in our approximation.

The effective formfactors at zero recoil are obtained comparing the structure functions in Eqs. (A.29) or (A.32) in the zero-recoil kinematics (which is $q^2 = q_0^2 = (m_1 - m_2)^2$) with those in Eqs. (52), (A.28). In this way the constants g_A , g_V for $\frac{1}{2}^+$ and g_A for $\frac{3}{2}^+$ above are expressed through the amplitudes introduced in Sec. 6.1:

$$\varepsilon g_A^{(\frac{1}{2})} = \left(\frac{1}{m_c} - \frac{1}{m_b} \right) \frac{P-G}{2} + \frac{2G}{3m_c}, \quad \varepsilon g_V^{(\frac{1}{2})} = \left(\frac{1}{m_c} - \frac{1}{m_b} \right) \frac{P-G}{2}, \quad \varepsilon g_A^{(\frac{3}{2})} = \frac{1}{\sqrt{6}m_c} g, \quad (\text{A.35})$$

where ε is the mass gap for a particular state.

References

- [1] P. Gambino, T. Mannel and N. Uraltsev, *Phys. Rev.* **D81** 113002 (2010).
- [2] I.I. Bigi, M. Shifman, N. Uraltsev and A. Vainshtein, *Phys. Rev. D* **52** (1995) 196.
- [3] T. Mannel, S. Turczyk and N. Uraltsev, *JHEP* **1007** (2010) 109.
- [4] I.I. Bigi, M. Shifman, N. Uraltsev and A. Vainshtein, *Phys. Rev. D* **56** (1997) 4017.
- [5] A. Czarnecki, K. Melnikov and N. Uraltsev, *Phys. Rev. Lett.* **80** (1998) 3189.
- [6] N. Uraltsev, *Phys. Lett. B* **545** (2002) 337.
- [7] D. Benson, I. Bigi, Th. Mannel and N. Uraltsev, *Nucl. Phys.* **B665** (2003) 367.
- [8] N. Uraltsev, *Mod. Phys. Lett.* **A17** (2002) 2317.
- [9] A. Czarnecki, K. Melnikov and N. Uraltsev, *Phys. Rev. D* **57** (1998) 1769.
- [10] M.A. Shifman, N.G. Uraltsev and A.I. Vainshtein, *Phys. Rev. D* **51** (1995) 2217.
- [11] I. Bigi, M. Shifman, N.G. Uraltsev, *Ann. Rev. Nucl. Part. Sci.* **47** (1997) 591.
- [12] Heavy Flavour Averaging Group, update for the Winter 2009 conferences, see <http://www.slac.stanford.edu/>.
- [13] P. Gambino and C. Schwanda, arXiv:1102.0210 [hep-ex].

- [14] A. Pak and A. Czarnecki, *Phys. Rev. D* **78** (2008) 114015;
S. Biswas and K. Melnikov, *JHEP* **1002** (2010) 089;
P. Gambino, *JHEP* **9** (2011) 055.
- [15] P. Gambino and C. Schwanda, to appear.
- [16] K.G. Chetyrkin *et al.*, *Phys. Rev. D* **80** (2009) 074010 [arXiv:0907.2110 [hep-ph]] and arXiv:1010.6157 [hep-ph].
- [17] I. Bigi, T. Mannel, S. Turczyk and N. Uraltsev, arXiv:0911.3322; *JHEP* **1004** (2010) 073.
- [18] D. Becirevic *et al.*, *Phys. Lett. B* **609** (2005) 298.
- [19] A. Kuzmin *et al.* [Belle Collaboration], *Phys. Rev. D* **76** (2007) 012006; *Nucl. Phys. Proc. Suppl.* **162** (2006) 228.
- [20] N. Uraltsev, *Phys. Lett. B* **585** (2004) 253.
- [21] R. Casalbuoni, A. Deandrea, N. Di Bartolomeo, R. Gatto, F. Feruglio and G. Nardulli, *Phys. Rept.* **281** (1997) 145 [hep-ph/9605342].
- [22] V.M. Belyaev, V.M. Braun, A. Khodjamirian and R. Ruckl, *Phys. Rev. D* **51** (1995) 6177.
- [23] D. Becirevic, B. Blossier, E. Chang and B. Haas, *Phys. Lett. B* **679** (2009) 231 [arXiv:0905.3355 [hep-ph]].
- [24] N. Uraltsev, arXiv:hep-ph/0010328. Published in the Boris Ioffe Festschrift ‘At the Frontier of Particle Physics / Handbook of QCD’, eds. by M. Shifman (World Scientific, Singapore, 2001), vol. 3 p. 1577.
- [25] N. Uraltsev, *Phys. Lett. B* **501** (2001) 86.
- [26] A. Czarnecki and A.G. Grozin, *Phys. Lett. B* **405**, 142 (1997) [Erratum-ibid. **B 650**, 447 (2007)].
- [27] A. K. Leibovich, Z. Ligeti, I. W. Stewart and M. B. Wise, *Phys. Rev. Lett.* **78** (1997) 3995; *Phys. Rev. D* **57** (1998) 308.
- [28] F. U. Bernlochner, Z. Ligeti and S. Turczyk, arXiv:1202.1834 [hep-ph].
- [29] I. I. Bigi, B. Blossier, A. Le Yaouanc, L. Oliver, O. Pene, J. -C. Raynal, A. Oyanguren and P. Roudeau, *Eur. Phys. J. C* **52** (2007) 975 [arXiv:0708.1621 [hep-ph]].
- [30] P. Colangelo, F. De Fazio, S. Nicotri and M. Rizzi, *Phys. Rev. D* **77**, 014012 (2008).
- [31] P. del Amo Sanchez *et al.* [BABAR Collaboration], *Phys. Rev. D* **82**, 111101 (2010). [arXiv:1009.2076 [hep-ex]].

- [32] N. Uraltsev, “Dynamic Heavy Quark Theory in Quantum Chromodynamics”, Habilitation Thesis; St. Petersburg, 2007, 221p.
- [33] L. Randall and M. B. Wise, *Phys. Lett. B* **303** (1993) 135.
- [34] M. Ademollo and R. Gatto, *Phys. Rev. Lett.* **13** (1964) 264.
- [35] J. Laiho [Fermilab Lattice and MILC and MILC Collaborations], *PoS LAT* **2007** (2007) 358 [arXiv:0710.1111 [hep-lat]]; C. Bernard *et al.*, *Phys. Rev. D* **79** (2009) 014506 [arXiv:0808.2519 [hep-lat]].
- [36] J. A. Bailey *et al.* [Fermilab Lattice and MILC Collaboration], *PoS LATTICE* **2010** (2010) 311 [arXiv:1011.2166 [hep-lat]].
- [37] G. M. de Divitiis, R. Petronzio and N. Tantalo, *Nucl. Phys. B* **807** (2009) 373 [arXiv:0807.2944 [hep-lat]].
- [38] S. Hashimoto *et al.*, *Phys. Rev. D* **66** (2002) 014503 [hep-ph/0110253].
- [39] A. S. Kronfeld, *Phys. Rev. D* **62** (2000) 014505 [hep-lat/0002008].
- [40] S. Hashimoto, A. S. Kronfeld, P. B. Mackenzie, S. M. Ryan and J. N. Simone, *Phys. Rev. D* **66**, 014503 (2002).
- [41] M. Okamoto *et al.*, *Nucl. Phys. Proc. Suppl.* **140** (2005) 461 [hep-lat/0409116].
- [42] G. M. de Divitiis, E. Molinaro, R. Petronzio and N. Tantalo, *Phys. Lett. B* **655** (2007) 45 [arXiv:0707.0582 [hep-lat]].
- [43] J. A. Bailey *et al.*, arXiv:1202.6346 [hep-lat].
- [44] P. Ball, M. Beneke and V. M. Braun, *Phys. Rev. D* **52** (1995) p. 3929-3948.
- [45] M. Neubert, *Phys. Rev. D* **51** (1995) 5924.
- [46] N.G. Uraltsev, *Nucl. Phys.* **B491** (1997) 303.
- [47] B. Blok, L. Koyrakh, M. A. Shifman and A. I. Vainshtein, *Phys. Rev. D* **49** (1994) 3356 [Erratum-ibid. *D* **50** (1994) 3572].